Downloaded from orbit.dtu.dk on: May 05, 2023

DTU Library

Suspension-firing of wood with coal ash addition: Probe measurements of ash deposit build-up at Avedøre Power Plant (AVV2)

Shafique Bashir, Muhammad; Jensen, Peter Arendt; Jappe Frandsen, Flemming; Wedel, Stig; Dam-Johansen, Kim

Publication date:
2012

Document Version
Publisher's PDF, also known as Version of record

Link back to DTU Orbit

Citation (APA):
Shafique Bashir, M., Jensen, P. A., Jappe Frandsen, F., Wedel, S., & Dam-Johansen, K. (2012). *Suspension-firing of wood with coal ash addition: Probe measurements of ash deposit build-up at Avedøre Power Plant (AVV2)*. DTU Chemical Engineering.

General rights
Copyright and moral rights for the publications made accessible in the public portal are retained by the authors and/or other copyright owners and it is a condition of accessing publications that users recognise and abide by the legal requirements associated with these rights.

- Users may download and print one copy of any publication from the public portal for the purpose of private study or research.
- You may not further distribute the material or use it for any profit-making activity or commercial gain
- You may freely distribute the URL identifying the publication in the public portal

If you believe that this document breaches copyright please contact us providing details, and we will remove access to the work immediately and investigate your claim.

June 11, 2012

Suspension-firing of wood with coal ash addition: Probe measurements of ash deposit build-up at Avedøre Power Plant (AVV2)

(Revised Version)

Muhammad Shafique Bashir, Peter Arendt Jensen, Flemming Frandsen,

Stig Wedel, Kim Dam-Johansen

CHEC Research Centre

Department of Chemical and Biochemical Engineering

Technical University of Denmark,

Søltofts Plads, Building 229, DK-2800, Lyngby, Denmark

http://www.chec.kt.dtu.dk

CHEC Report No.: R1203 (confidential)

Contents

Abstract

This report is about full-scale probe measurements of deposit build-up and removal conducted at the Avedøreværket Unit 2, a 800 MW_{th} suspension boiler, firing wood and natural gas with the addition of coal ash. Coal ash was used as an additive to capture potassium (K) from wood-firing. Investigations of deposit formation rate were made by use of an advanced online ash deposition/shedding probe. Quantification of ash deposition and shedding was made via deposit mass uptake signals obtained from the deposit probe. The influence of coal ash, flue gas temperature, probe surface temperature and boiler load on ash deposition propensity was investigated. Results of ash deposition propensity showed increasing trend with increasing flue gas temperature. Video monitoring revealed that the deposits formed were not sticky and could be easily removed, and even at very high flue gas temperatures (> 1350 ^{o}C), deposit removal through surface melting was not identified. SEM-EDS analysis of the deposits showed significant presence of Ca, Al and Si, indicating that a significant amount of K has been captured by coal ash to form deposits rich in calcium-aluminum-silicates, and possible release of Cl to the gas phase as HCl(g). Effect of boiler operational parameters on gas emissions has also been investigated.

Keywords: *Dust-firing, coal ash as additive, deposits, deposit formation rate, deposit removal (shedding).*

1 INTRODUCTION

The focus on substituting fossil resources by biomass has significantly increased the interest in efficient use of biomass for heat and electricity production, and this includes the use of wood in suspension-fired boilers. In the recent decades, the focus to substitute fossil fuels by wood has significantly increased the interest in efficient use of wood in large suspension-fired boilers. However, the presence of alkali metals (K) and chlorine (Cl) in wood – even in small amount – may induce operational problems due to ash deposit formation, corrosion and deactivation of SCR catalyst [1-4]. Strategies to handle ash deposit related problems include use of additive to chemically capture potassium (K), leaching of potassium (K) from fuel, inhibition of sintering and effective deposit shedding techniques [5-12].

Some full-scale experimental studies on deposit build-up have been reported on measurements in biomass grate and fluidized-bed boilers [13-16]. Only limited data is available from wood suspension-firing where improved knowledge on the transient deposit formation and removal is needed to optimize design and operation [17-19]. Fewer full-scale pulverized wood-firing investigations are reported in the literature and the most recent ones are by Jensen et al. [5], Skrifvars et al. [19] and Bashir et al. [17, 20]. In addition, most of these studies have been based on short testing time (up to couple of hours) [5,19], while more extensive full-scale measurements are rare to find [17, 20]. Therefore, more detailed and extensive full-scale studies on transient deposit formation rate when firing wood with coal ash addition will improve our understanding of deposit formation and shedding processes.

This report aims to provide long time, full-scale data on ash deposit formation at the Avedøreværket Unit 2, a 800 MW_{th} suspension boiler, firing wood and natural gas with the addition of coal ash. The boiler was operated with coal fly ash addition to minimize problems of deposit formation, corrosion and deactivation of SCR catalyst. Possibly the alumina silicates present in the coal ash may react with potassium chloride, where HCl is released, and potassium (K) is bound in alumina silicates with relatively high melting temperatures. Furthermore, quantitative information on ash deposition propensity as functions of operating conditions is provided. The influence of coal ash to wood ash ratio, probe exposure time, probe surface temperature (500 ^{o}C, 550 ^{o}C), boiler load and flue gas temperature (750-1450 ^{o}C) on ash deposition propensity have been investigated. Effect of boiler operational parameters on gas emissions has also been investigated.

2 EUIPMENTS, MATERIALS AND METHODS

2.1 Boiler

The probe measurements were conducted at Avedøre Power Station, unit 2 (AVV2), firing wood and natural gas in suspension. The AVV2 boiler, located in the Copenhagen area, is a multi-fuel suspension-fired boiler that can apply wood, natural gas and heavy fuel oil as fuel. The boiler drawing is shown in Figure 1. The AVV2 boiler is a 80 meter high Benson type boiler with a thermal capacity of 800 MW_{th}. Overall, there are three sub-units, a straw-

fired grate boiler, a suspension-fired boiler and lastly two gas turbines [5]. In the lower part of the boiler tower is the combustion chamber, which has 16 burners in four levels (see Figure 1). There are three mills used to grind wood pellets, and the pulverized wood after being ground in the mills is blown into the burners, where the fuel particles are burned in suspension. Above the combustion chamber is a radiation shield, followed by the superheaters and economizers. The probe measuring position was situated at a level of ~48.9 m, meaning that the probe was inserted below the radiation shield (Appendix A). The AVV2 boiler is being able to operate in a pure condensing mode, a pure back pressure mode or any combination. Operating in pure condensing mode, an electrical efficiency of 48 % is obtainable. If operated in pure back pressure mode, using the thermal energy of the condensed steam for district heating, the total efficiency can be as high as 94 % [5].

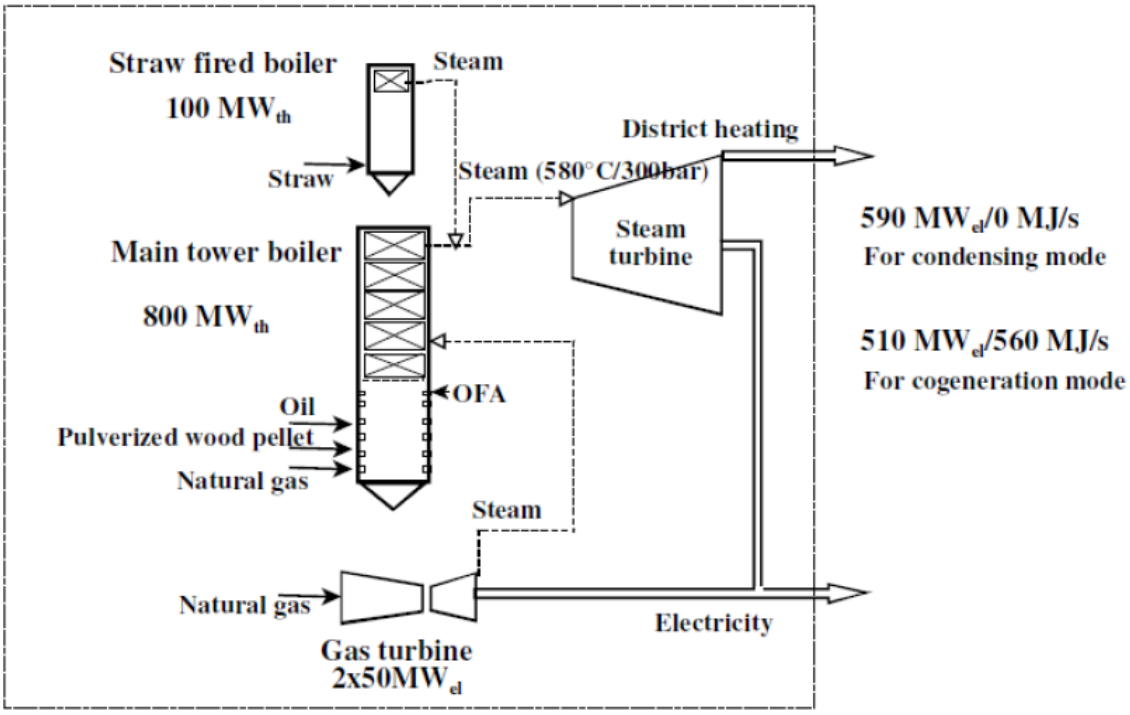

Figure 1: Flow chart of the Avedøre Power Station, unit 2. [5]

2.2 Ash deposition probe

The deposit probe system used for the measurements is shown schematically in Figure 2. The probe was made of stainless steel, about 3 m long and having an outer diameter of 40.5 mm. The deposit probe was cooled by water and air, whereby it was possible to determine heat uptake by the probe and keep a stable surface temperature. The probe was placed in an acoustic pyrometer port on the boiler wall. In the start of the current measurements, due to higher flue gas temperature (>1250 ^{o}C), it was not possible to keep the probe surface temperature between 500 and 600 ^{o}C. A possible reason was that the boiler was running with a high wood-fuel input leading to high flue gas temperatures at the probe measuring position. The problem of keeping the probe surface temperature at the desired levels was then solved by mounting the probe somewhat retracted. A special port extension pipe was installed to keep the probe only 772 mm inside the boiler (Figure 2 (a, b)). This solution believed to work satisfactory if the probe is inserted slowly in the boiler because with the formation of a small layer of deposits on the probe, the probe surface temperature fluctuations were considerably reduced.

(a)

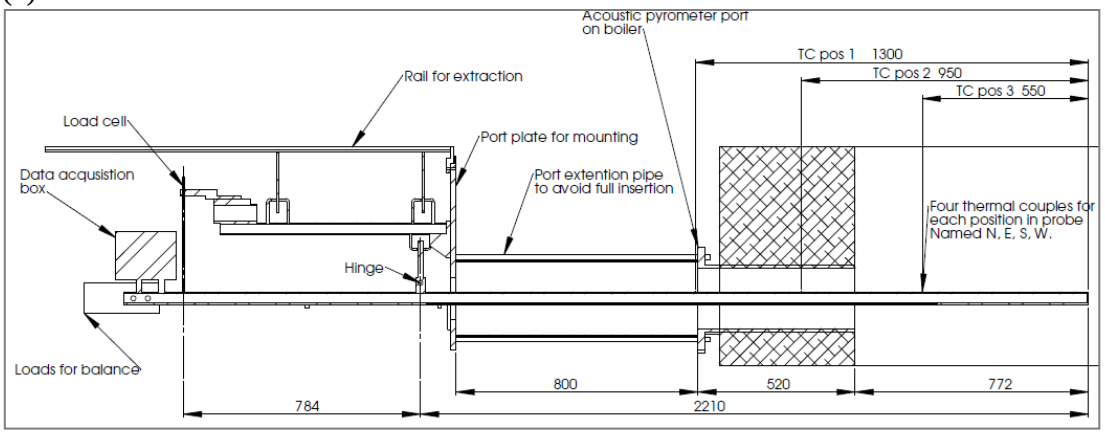

(b)

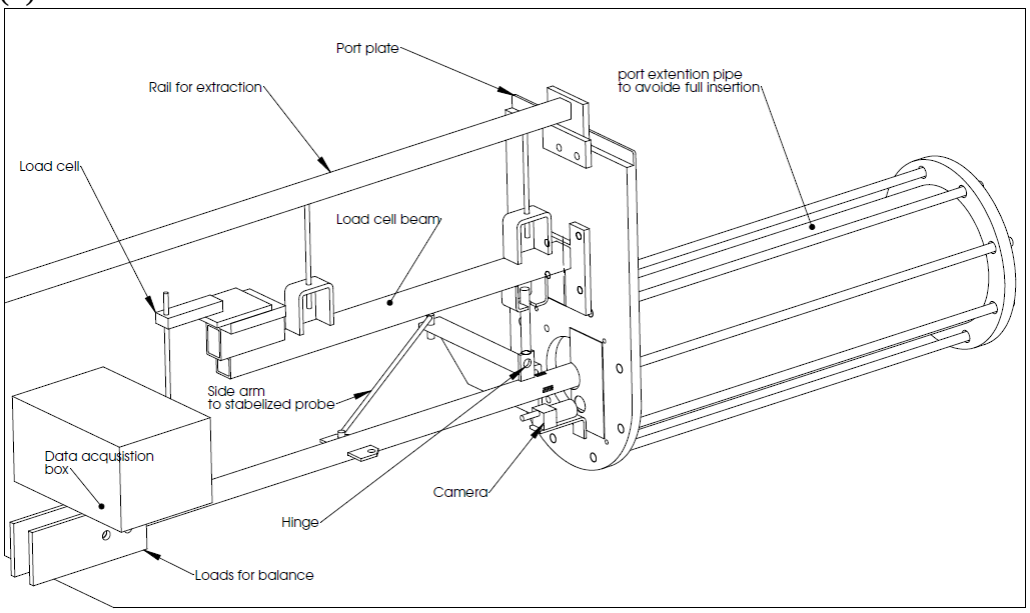

(c)

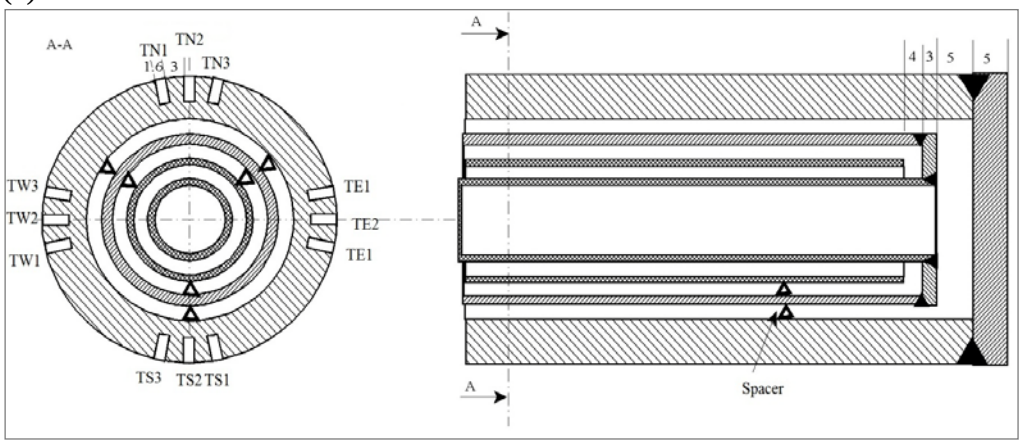

Figure 2: a) Schematic drawing of the probe with identified positions of temperature measurements, deposition area, port extension pipe, port plate for mounting, hinge, load cell and rail for pulling out the probe, b) layout of the complete probe set up, c) cross-sectional view perpendicular to the probe axis and cross-sectional view along the axis of annuli.

In total, 12 thermocouples were placed inside the outer probe metal tube with four thermo-elements at three different horizontal positions (Figure 2 (c)). In each horizontal position, the thermocouple provided temperature information at the N, S, E and W position of the probe. However, due to the modifications with the extension pipe, probe temperature measurements only at horizontal position 3 were possible.

The flue gas temperature near the probe was measured using a simple thermocouple in a protective shell. In addition, a suction pyrometer (International Flame Research Foundation model, IFRF [22]) was also used for some periods to find the difference between the thermocouple flue gas temperature measurements and suction pyrometer flue gas temperature measurements.

It was tried to make a special port for video monitoring functional at the right wall of the probe measuring position in order to have a better angle of view, but due to problems in maintaining the port temperature at the required levels (< 50 ^{o}C), a CCD (charge-coupled device) camera was placed below the probe to register the deposit formation and removal processes on the probe (Figure 2 (b)).

2.2.1 Probe heat uptake

The water and air flow to the probe was measured by flow meters at the inlets of the probe. The temperatures of the water and air were measured by 4 thermocouples at the inlet and outlet positions. The probe heat uptake was then calculated under steady state conditions using:

$$Q = \frac{\dot{m}_w C_{p,w}\left(T_{w,out} - T_{w,in}\right) + \dot{m}_a C_{p,a}\left(\overline{T}\right)\left(T_{a,out} - T_{a,in}\right)}{s} \qquad (1)$$

Where Q is the heat uptake (W/m^2), $\dot{m}$ is the flow rate (kg/s), C_p is the heat capacity (J/kg/K), T is the temperature (K), while in the superscripts w and a represent water and air, respectively. In the above equation (1), s represents the effective probe surface area.

2.2.2 Deposit mass uptake

The deposit mass uptake was calculated by using the following torque balance:

$$m_d g = \left(m_{to} - m_{t1}\right) g \frac{L_1}{L_2} \qquad (2)$$

Where m_d is the deposit mass (g), m_{to} is the initial signal of the load cell, m_{t1} is the final signal of the load cell, g is the gravitational acceleration (m/s^2), while L_1 and L_2 are the distances (mm) from the hinge to the balance and to the mass center of the deposit, respectively.

2.3 Fuels

The fuels fired during the measurements were wood-dust and natural gas. As it was not possible to obtain fuel samples, the composition of the applied fuels is adopted from previous measurements at AVV2 ([5], Table 1). Fuel analysis shows that the wood fuel has

small content of potassium (K) and chlorine (Cl), while calcium (Ca) and silica (Si) are present in significant amounts. The natural gas analysis shows a large content of CH_4 and C_2H_6.

The coal ash used as an additive contains significant content of aluminum (Al) and silicon (Si), indicating possible potential of the coal ash to capture potassium (K) formed during wood combustion.

Table 1: Analysis of the fuels fired and added coal ash. [5] ar: as received, db: dry basis

Parameter	Wood	Coal ash	Parameter	Units	Natural gas
Ash contents (wt% ar), assumed	1.0	--	--	--	--
Moisture (wt%)	5.80	--	--	--	--
Higher Heat Value (MJ/kg db)	17.0	--	Heating value	MJ/kg	48.07
C (wt% db)	46.84	--	CH_4	mol. %	89.06
S (wt% db)	0.009	0.26	C_2H_6	mol. %	6.08
N (wt% db)	0.094	--	C_3H_8	mol. %	2.47
H (wt% db)	5.91	--	iC_4H_{10}	mol. %	0.39
O (wt% db)	40.53	--	nC_4H_{10}	mol. %	0.54
Cl (wt% db)	0.0043	0.0	C_5H_{12}	mol. %	0.11
Al (wt% db)	0.014	14.0	nC_5	mol. %	0.08
Ca (wt% db)	0.14	5.2	C_{5+}	mol. %	0.05
Fe (wt% db)	0.013	2.3	N_2	mol. %	0.29
K (wt% db)	0.048	0.45	CO_2	mol. %	0.91
Mg (wt% db)	0.024	0.91	--	--	--
Na (wt% db)	0.005	0.11	--	--	--
P (wt% db)	0.0058	0.81	--	--	--
Si (wt% db)	0.17	20.0	--	--	--

2.4 Procedure of experiments

A series of deposit probe measurements were conducted in a region just below the radiation shield. In the measurements, varying ratio of coal ash to the wood ash was used. Each measurement lasted 1-5 days (all measurements from 04 April to 15 April, 2011). The influence of coal ash, boiler load, probe surface temperature and flue gas temperature on ash deposition propensity was investigated. The target probe surface temperatures were varied between 500 and 550 ^oC in order to investigate ash deposition at two different probe surface temperatures. The deposition probe was exposed to flue gas temperatures from 750 to 1450 ^oC. The overall experimental summary is shown in Table 2. The first three tests are at higher boiler loads with varying biomass loads, while test four is long due to the fact that the boiler was running smoothly for a longer period at lower overall boiler load and biomass load, while test 5 is based on measurements at moderate boiler load.

In each measurement, boiler operational data was collected to make it possible to analyze the influence of boiler operational parameters on ash deposition and gas emissions (CO, NO_x and SO_2). Biomass load was calculated by using equation (3),

$$Biomass\ Load\ (\%) = \frac{Wood\ fuel\ flow\ rate \cdot Heating\ value\ of\ wood}{800 MW_{th}} \cdot 100 \quad (3)$$

The sootblowers located very near to the probe measuring position (0.8 m to the right on the same wall and about 3 m to the right on the right wall) were shut down during all the tests, while the rest of the sootblowers in the probe measuring position were still in operation.

Table 2: Experimental summary. W: wood, NG: natural gas

Test no.	**1**	**2**	**3**	**4**	**5**
Start date- **End date**	**05/04-06/04**	**05/04-06/04**	**06/04-07/04**	**08/04-13/04**	**13/04-15/04**
Fuel	W and NG	W and NG	W and NG	W and NG	W and NG
Boiler load (%)	91	98	88	41	76
Biomass load (%)	44	81	72	18	59
Target probe temperature (^{o}C)	550	550	550	500	500
Exposure time (h)	26	16	28	116	52

3 RESULTS AND DISCUSSION

3.1 Probe functionality

A great deal of information was collected by using the deposition probe. However, there were some technical issues regarding control of the air flow to the probe and to keep the probe surface temperature at the required level. In the start of the measurements, due to high flue gas temperature (>1250 ^{o}C), it was not possible to keep the probe surface temperature between 500 and 600 ^{o}C. A possible reason was that the boiler was running with a high wood-fuel input leading to high flue gas temperatures at the probe measuring position. The problem of keeping the probe surface temperature at the desired levels was then solved by mounting the probe somewhat retracted. A special port extension pipe was installed to keep the probe only 772 mm inside the boiler. However, even though only 772 mm probe was inside the boiler, due to the higher flue gas temperature, there were still fluctuations in the probe surface temperature. The control parameters for the air flow to the probe added additional problems. However, by adjusting the air pressure to the controller (air) and finding appropriate PID parameters for the controller (air), the fluctuations in the probe surface temperature were reduced. The load cell worked well to quantify the deposit build-up. Due to high flue gas temperature, it was not possible to cool the camera port. Therefore, the camera was placed just below the probe instead of in a separate port. The

video quality and angle of view were therefore not the same as were planned. However, still we were able get some good images to identify the deposit formation and shedding processes.

3.2 Data treatment

A large set of data was obtained from the Power Plant and the probe measurements, and a data treatment procedure was adopted for each test. As an example, the detailed signals of flue gas temperature, deposit mass uptake, events of plant sootblowing and probe heat uptake during test 3 are shown in Figure 3, while fuel flow and boiler load are shown in Figure 4. The thick black line along with the deposit mass uptake signals (Figure 3) indicate the events when the nearby plant sootblowers were in operation. It was observed that even though the plant sootblowers located very near to the probe measuring position (0.8 m to the right on the same wall and about 3 m to the right on the right wall) were closed, the rest of the sootblowers were to some extent effective in causing smaller fluctuations to the deposit mass uptake. The information about the activeness of the surrounding plant sootblowers was provided by DONG energy.

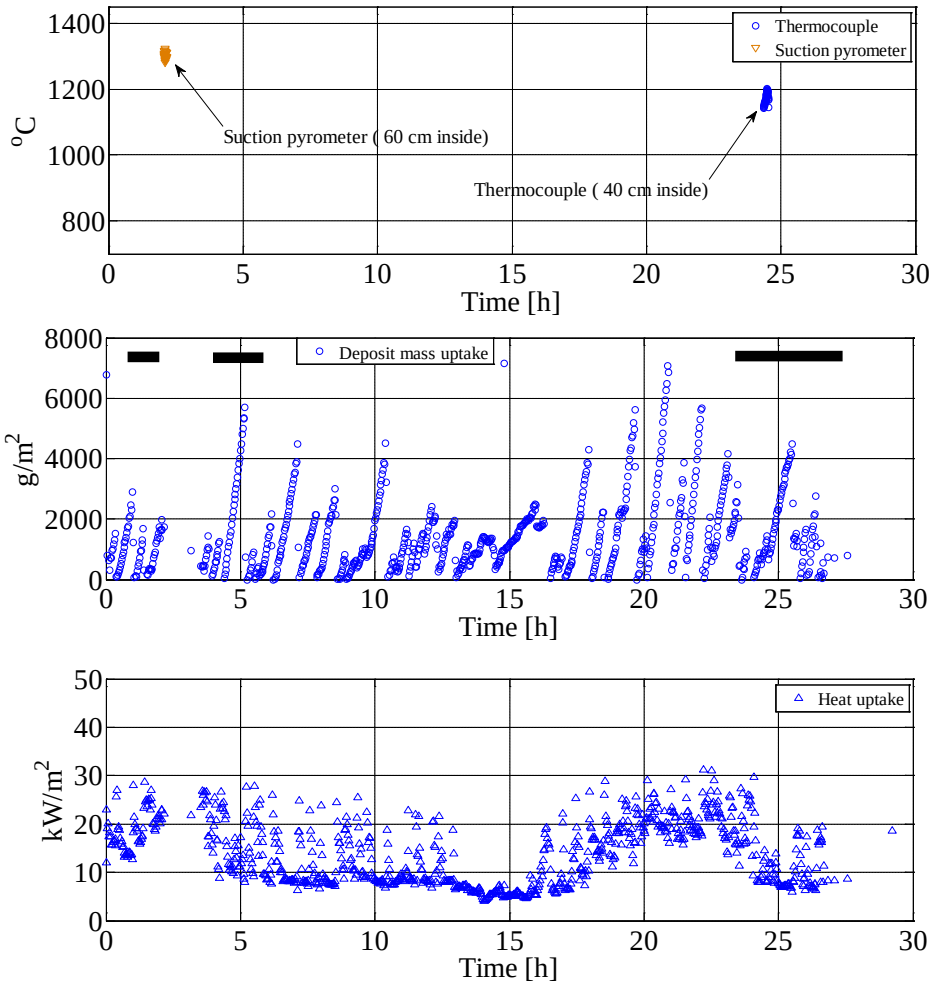

Figure 3: Flue gas temperature, deposit mass uptake, plant sootblowing and probe heat uptake during test 3. The thick black line in the middle figure shows the time when the surrounding sootblowers were in operation.

During test 3, the boiler was running at a mean load of 88.5 %. The biomass (wood) load was more than 80 % in the first 5 h and then slowly decreased to about 70 % in the next 5 h, and between 13 to 17 h, the biomass load fluctuated at approximately 50 %. The flue gas temperature measured during this test was around 1300±75 ^{o}C based on flue gas temperature measurements with suction pyrometer for a short period. The flue gas temperature for the rest of the test was estimated based on the thermocouple readings and difference between temperature measured by suction pyrometer and thermocouple, and boiler load information. The deposit mass uptake signals indicate a number of events with steep increase and then a sudden drop due to shedding of deposits (Figure 3). It can be seen that at higher biomass and boiler load, the deposit mass uptake curve is steeper during time with lower biomass and boiler load, possibly due to changes induced by flue gas temperature and biomass ash flux (Figure 4). The probe heat uptake fluctuations are also evident at higher biomass and boiler load due to larger amount of air needed to keep the probe surface temperature close to the target temperature.

The fuel (wood) flow through each mill during test 3 is shown in Figure 5. The coal ash flow and ratio of coal ash to fuel ash is also shown in the figure. It can be seen that during the 13 to 17 h period, mill 10 was not in operation, thereby causing a reduced biomass load and a slight increase in coal ash to wood ash ratio. The deposit mass uptake signals during this interval are less steeper compared to the events when mill 10 was in operation.

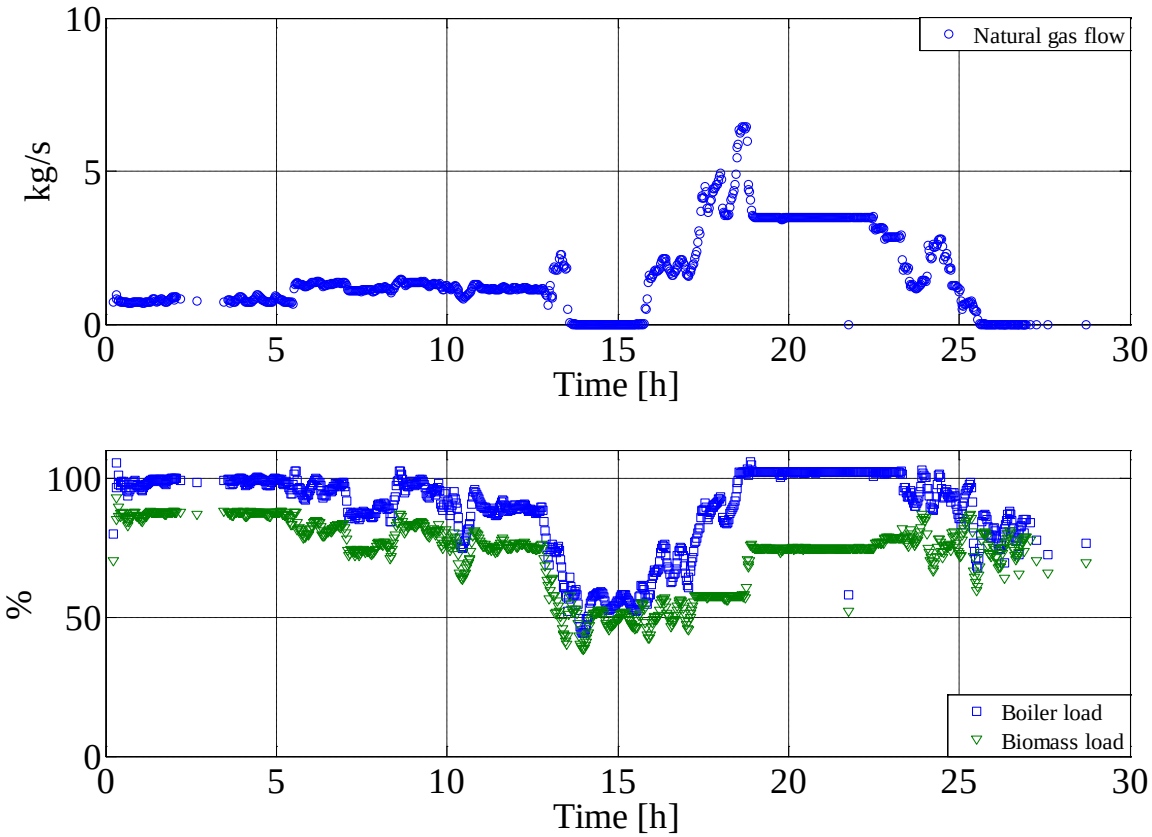

Figure 4: Natural gas flow, overall boiler load and biomass load during test 3.

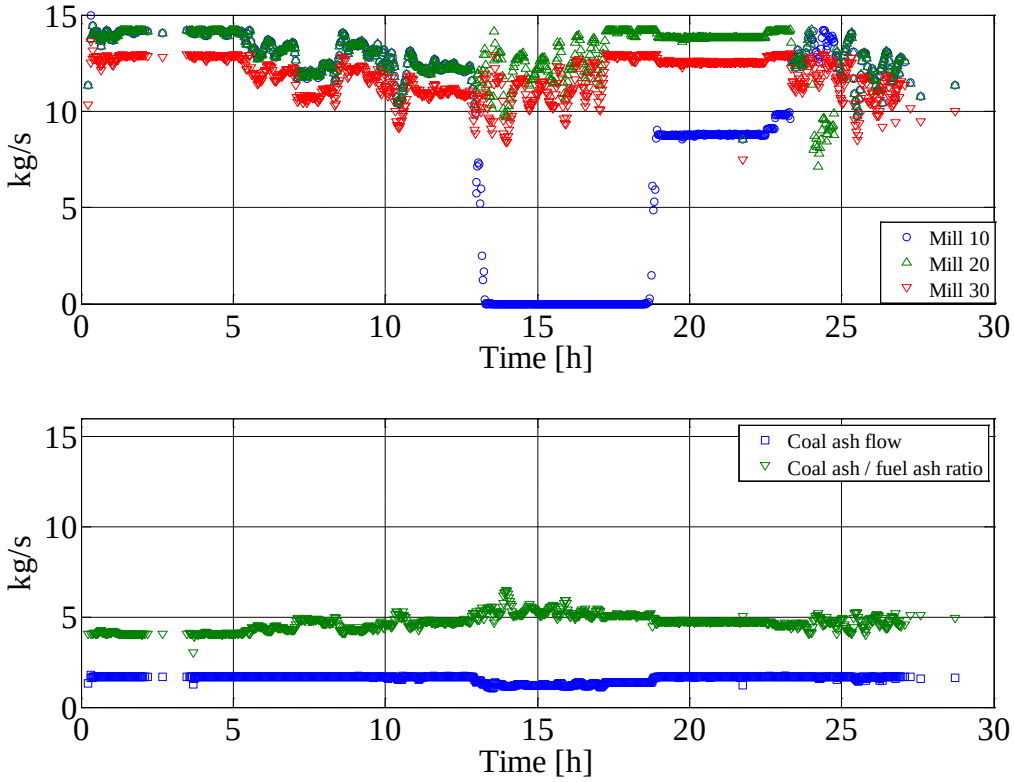

Figure 5: Fuel flow (wood) through each mill of the boiler, coal ash flow (kg/s) and ratio between coal ash and wood ash flow during test 3. It is assumed that wood fuel contains 1.0 wt. % ash.

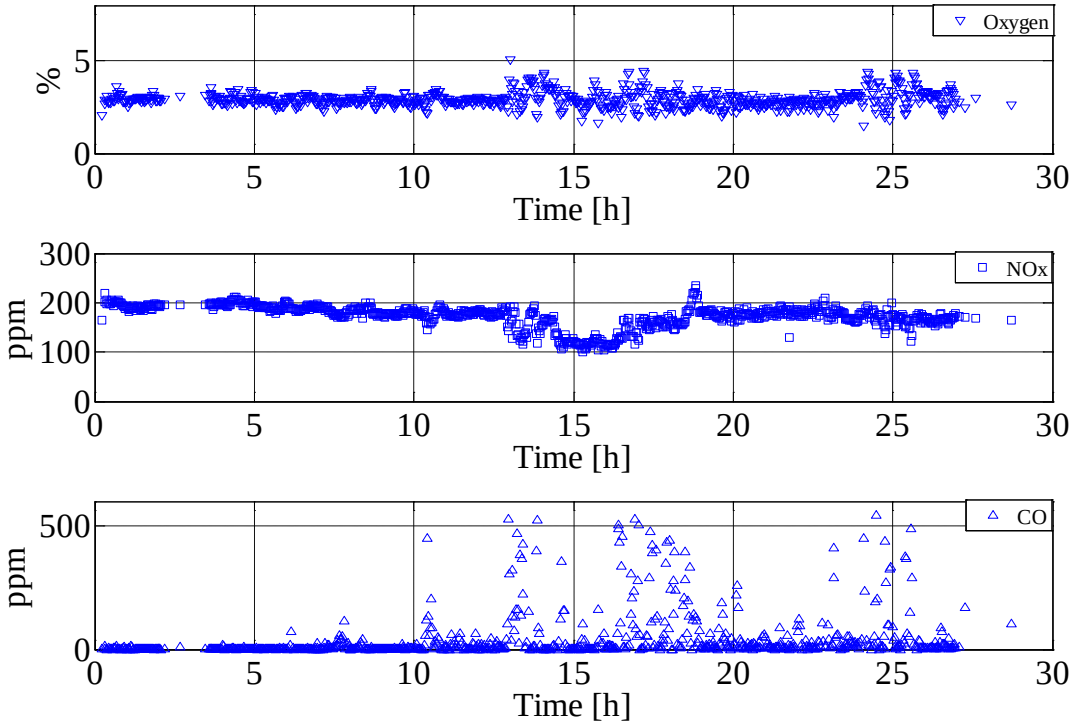

Figure 6: Oxygen level, NOx level before DeNOx and CO level during test 3.

The gas emissions (CO and NO_x) are shown in Figure 6. It is clear that NO_x emissions were reduced at lower biomass and boiler load. The CO emissions indicate fluctuations during the 13-20 h and 23-27 h period, possibly caused by fluctuations in the fuel flow through mills during these periods. CO emissions are generally low at smoother fuel flow to the boiler.

The probe temperatures were continuously monitored and the measured signals of four thermo-elements at position 3 are shown in Figure 7. The S3 position was used as target probe temperature. The water and air flow needed to keep the probe surface temperature stable and close to the target are shown in Figure 8. There is a seen significant drop in probe surface temperatures from 13 to 17 h of exposure time due to reduced boiler load. However, this trend indicates that further improvement in the air flow control is needed to keep the probe surface temperature close to the target temperature with least fluctuations, even at low and high flue gas temperatures. The detailed signals of flue gas temperature, mass uptake, heat uptake, fuel flow, boiler load, biomass load, probe surface temperatures and coolant flow to the probe for the rest of the tests can be found in Appendix B.

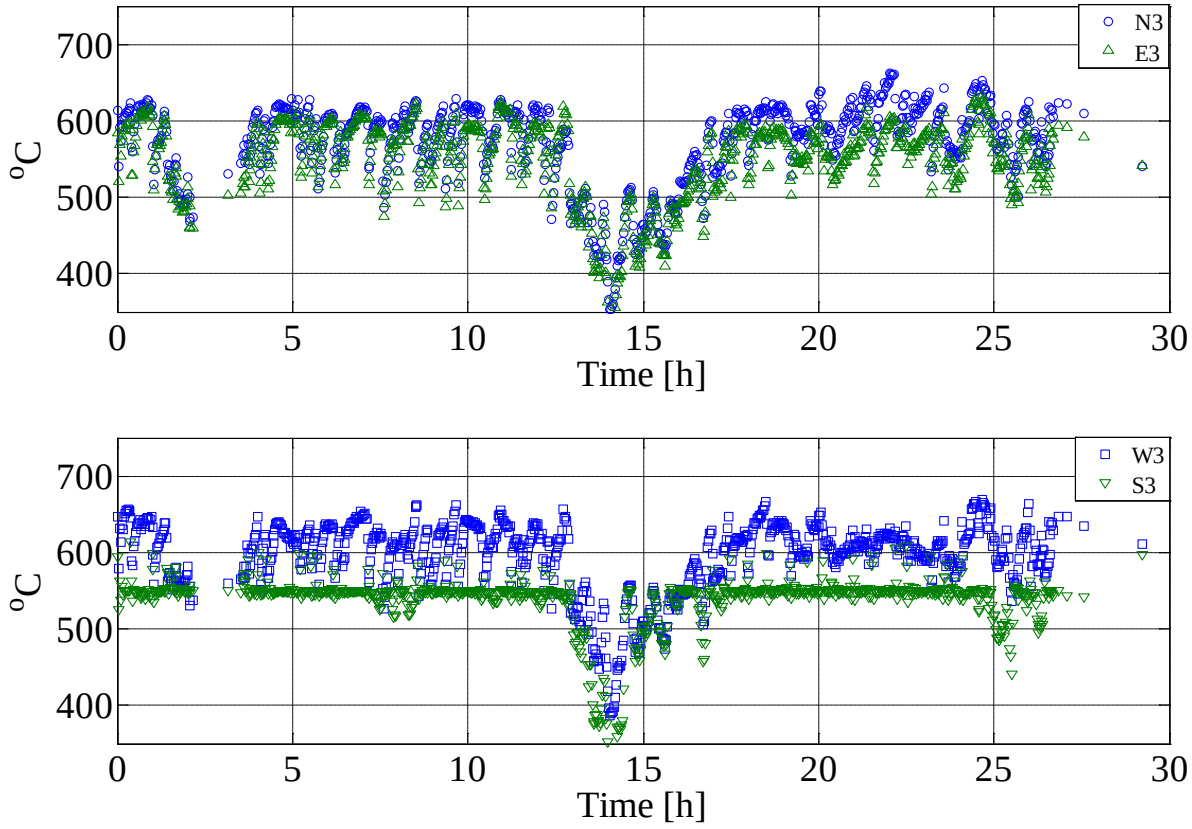

Figure 7: Measured probe surface temperatures during test 3.

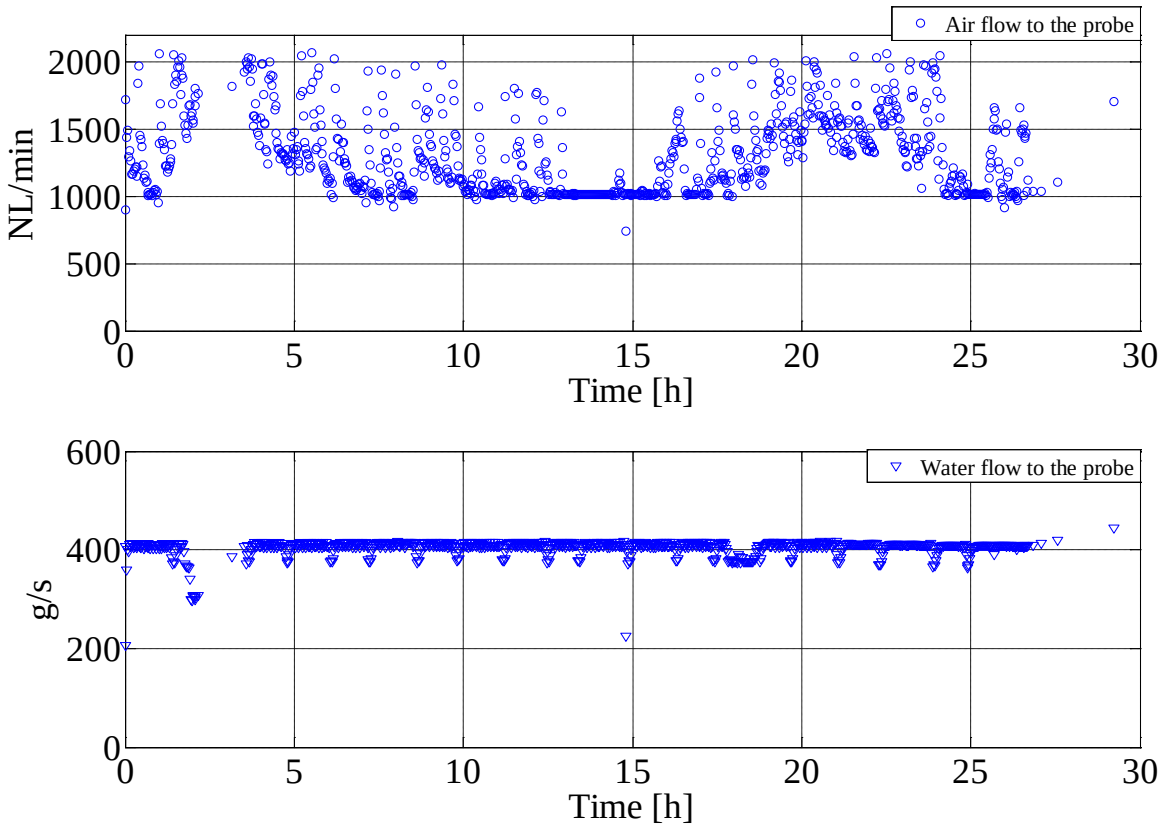

Figure 8: Water and air flow to the probe measured during test 3.

3.2.1 Ash deposition propensity

The amount of deposit collected on the probe is a function of both the deposit formation process and shedding events as shown in Figure 3. As an example, significant amount of deposits formed even after 50 minutes as is evident from Figure 9. Apart from deposit build-up, there are different kinds of deposit shedding, natural and caused by plant sootblowing. To handle this kind of data, two different measures of deposit formation rate are used in the analysis of the data. The first is the integral deposit formation rate (IDF-rate) found by dividing the integral mass change over integral time intervals (of order several hours) by the time interval. The IDF-rate is similar to deposit formation rates based on total deposit mass uptake divided by probe exposure time reported in previous full-scale investigations, but it is a relatively crude measure that includes all deposit shedding in addition to actual deposit formation. In order to remove major shedding events from the determination of deposition rates a second measure, the derivative-based deposit formation rate (DDF-rate), was devised. This was determined by averaging the deposit mass uptake signals over short time intervals (of order minutes), calculating the local values of the time derivative of the mass uptake, removing large negative values signifying major shedding events, and finally time smoothing the derivatives to remove excessive noise. The complete procedure used to calculate the DDF-rate is shown in Appendix C. Looking at the deposit mass uptake data in the different tests, following observations were made:

Test 1. A lot of build-up and fast shedding of all the deposits up to 14 h of exposure time. About 20 events in the first 14 h can be found where all of the deposits attached to the probe are removed naturally. After 15 h the deposit level is constant at 4,000 g/m^2.

Test 2. During all the measuring time (total 15 h) there were observed fast deposit build-up to maximum 6,000 g/m^2 and then sudden shedding of all deposit. A lot of shedding events were observed.

Test 3. A similar deposit build-up behavior as in test 2, but the probe was placed in the boiler for 27 h.

Test 4. A slow deposit formation process up to 10 h and then there are observed a constant amount of deposit build-up to a probe residence time of 110 h. The boiler was running at lower biomass and boiler load.

Test 5. Only small amounts of deposits are observed on the probe in most of the time (less than 200 g/m^2). Several cases of fast deposit build-up and deposit shedding appear sometimes.

The DDF-rate may be influenced by the coal ash flow rate. Therefore, ash deposition propensity provides useful information about the fraction of total ash actually depositing on the deposit probe. The ash deposition propensity in the present case was calculated by dividing the DDF-rate with the total ash flux. The DDF-rate represents the transient deposit build-up meaning that if the DDF-rate is equal to the total ash flux, all of the ash the probe will experience is going to stick to the deposit probe.

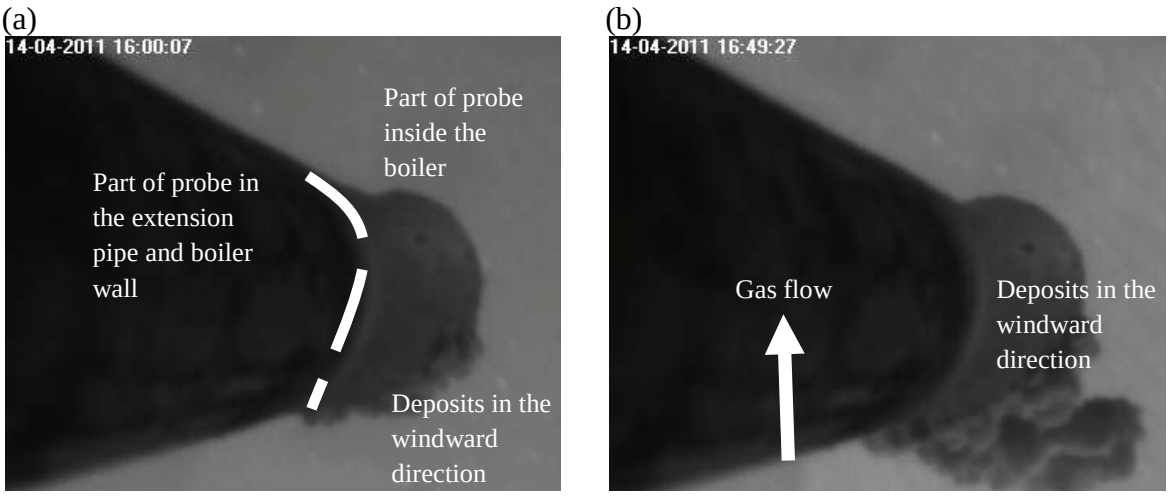

Figure 9: Deposit build-up in just 50 minutes during test 5 (total exposure time of 31.3 h).

The calculated DDF-rate was then used to determine ash deposition propensity using the following correlation [21],

$$\text{Ash deposition propensity } (\%) = \text{Impaction efficiency} \times \text{Capture efficiency} = \frac{\text{Transient deposition flux}}{\text{Ash flux}} \cdot 100 = \frac{\text{DDF-rate}}{\text{Ash flux}} \cdot 100 \quad (4)$$

$$\text{Ash flux (g/m}^2\text{/h)} = \frac{m_f X_a}{A_r} + \frac{ash_{coal}}{A_r} \quad (5)$$

In the above equation (5), m_f represents the wood fuel flow to the boiler, X_a represents fraction of ash in dry wood fuel, ash_{coal} represents the coal ash flow and A_r represents the cross-sectional area of the boiler at the probe measuring position.

The calculated DDF-rate during test 3 is shown in Figure 10. It is clear that DDF-rate decreases at decreased biomass load and boiler load (between 13 to 17 h). The DDF-rate

shows a big peak after the introduction of fuel through mill 10 after 17 h of exposure time, when the natural gas flow was relatively larger (~ 4 kg/h). The calculated ash deposition propensity almost follows the same trend as the DDF-rate (Figure 11). The calculated DDF-rates and ash deposition propensity for each test can be found in Appendix B. For test 3, it is seen that when the boiler is approximately near full load, the deposit formation rate is above 3,500 g/m^{2}h.

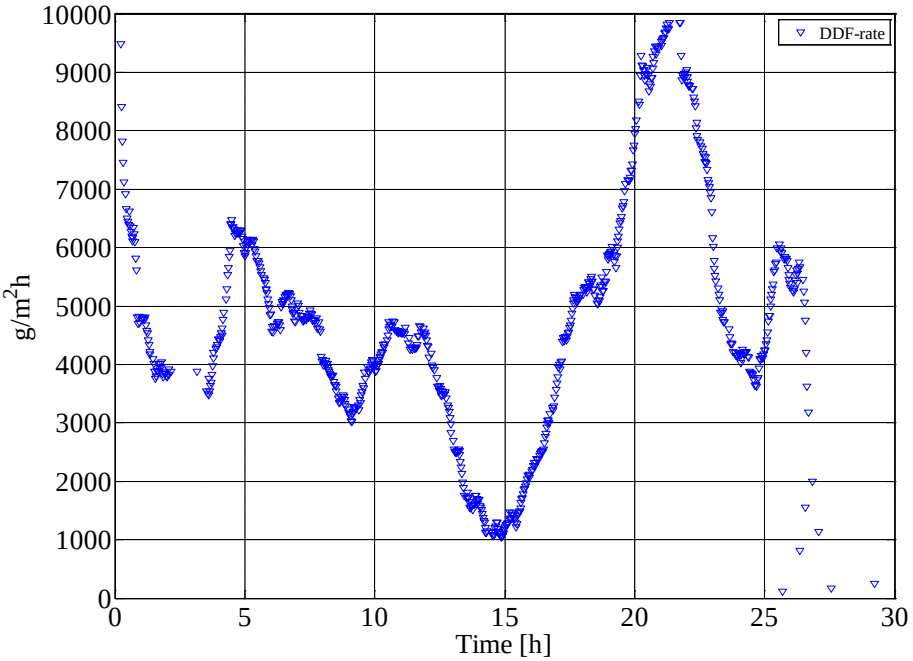

Figure 10: Calculated Derivative-based Deposit Formation (DDF) rate during test 3.

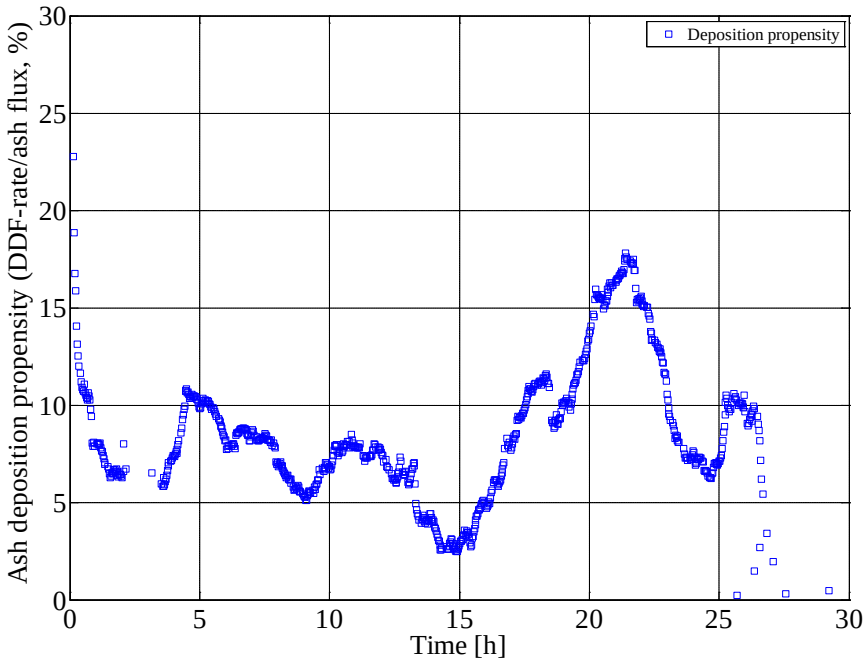

Figure 11: Calculated ash deposition propensity during test 3.

3.3 Influence of local conditions on deposition propensity

To make it possible to investigate the influence of different operational parameters on ash deposition propensity, mean values of each test were determined. Five data points were generated and it was possible to analyze the influence of probe surface temperature, local flue gas temperature and boiler operational parameters on ash deposition propensity and gas emissions. Table 3 provides an overview of the conducted measurements. The mean flue gas temperature in the range of 950 to 1350 ^{o}C can be seen, while the impact of flue gas temperature on ash deposition propensity is shown in Figure 12. It can be seen that ash deposition propensity increased with increasing flue gas temperature. The possible reason for increased ash deposition propensity at higher flue gas temperatures could be that the particles hitting the probe are partially molten, whereby a larger fraction of impacted ash particles sticks to the deposit.

Table 3: Summary of all main results of the measurements. [a] standard deviation.

	Unit	Test 1	Test 2	Test 3	Test 4	Test 5
Exposure time	h	26	16	28	116	52
Biomass load	%	44.10	81.16	72.18	18.20	59.24
Boiler load	%	91.22	97.63	88.47	41.37	76.28
Natural gas flow	kg/s	7.86	2.55	1.62	3.87	2.53
Probe surface temperature (mean of N3, E3, S3, W3)	^{o}C	577	583	561	483	525
Coal ash to wood ash ratio	--	3.63	4.35	4.69	7.35	5.79
Ash flux (wood with 1 wt. % ash + coal ash)	g/m^{2}h	28886	58782	54931	20580	45571
Flue gas temperature	^{o}C	1350 ± 75	1250 ± 75	1300 ± 75	950 ± 75	1075 ± 75
Deposit mass uptake (mean)	g/m^2	2648	1589	1370	1691	375
DDF-rate (st. dev.)[a]	g/m^{2}h	4717 (23051)	4501 (3473)	4849 (2603)	96 (647)	653 (1055)
IDF-rate (deposition rate) (initial 12 h)	g/m^{2}h	212	156	53	128	30
Ash deposition propensity ,DDF-rate/ash flux (st. dev.)[a]	%	16.33 (79.8)	7.66 (5.91)	8.83 (4.73)	0.47 (3.14)	1.43 (2.31)
Heat uptake	kW/m^2					
Mean	kW/m^2	--	20.61	13.55	8.10	18.37
Deposit mass uptake < 1500 g/m^2	kW/m^2	--	22.52	13.82	8.25	--
Deposit mass uptake > 1500 g/m^2	kW/m^2	--	18.23	13.03	6.38	--
NO_x (6% O_2)	ppm	170	191	172	99	118
CO	ppm	48	5.0	37	1	20
O_2	%	2.41	2.79	2.90	3.29	2.95
SO_2	ppm	0.33	4.82	8.23	--	4.32

The mean probe heat uptake for each measurement is shown in Table 3 along with the impact of ash deposits on probe heat uptake for two different set of deposit mass loads on the probe (less than and greater than 1,500 g/m^2). It can be seen that probe heat uptake is reduced when the deposit mass load is increased; however, the probe heat uptake reduction is different for each test possibly due to flue gas temperature and probe surface temperature differences. In addition, due to problems at the temperature measuring position of air and water inlet to the probe, the heat uptake was not accurately calculated during test 1. Also, during test 5, due to unstable probe temperature, the results of probe heat uptake are not included.

Some of the parameters in Table 3 cannot be regarded as independent. The coal ash injection flows were to some extent kept constant. However, an increase in the biomass load seems to have induced an increase flue gas temperature and decreased the coal to wood ash ratio. The impact of coal ash to fuel ash ratio on ash deposition propensity is shown in Figure 13 (a) at different probe surface temperatures. It can be seen that deposition propensity increased with decrease in coal ash to fuel ash ratio. However, as shown in Figure 13 (b), the points with high coal ash to wood ash ratio also have low biomass and boiler load. Changes in boiler load influence the flue gas temperature, and the coal ash to wood ash ratio was lowest in the tests with high flue gas temperature. With the few measuring points available and the limited variation in the ash ratio (coal ash to wood ash), it is difficult to determine the influence of this parameter.

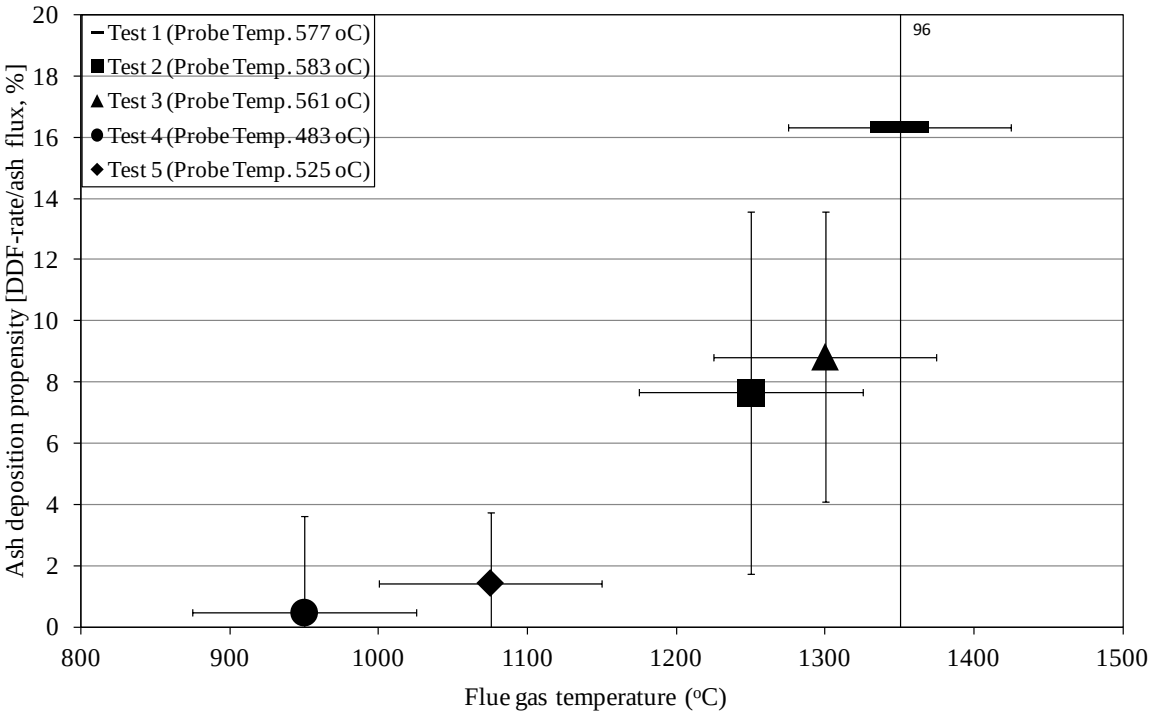

Figure 12: Impact of flue gas temperature on ash deposition propensity (deposition flux/ash flux, %). The error bars indicate possible variation of the flue gas temperature due to the fact that the suction pyrometer was used only for small periods to find the true flue gas temperature.

Based on the experiences from previous measurements, we believe that when high deposition flux to ash flux ratio is observed, the main cause is the flue gas temperature.

(a)

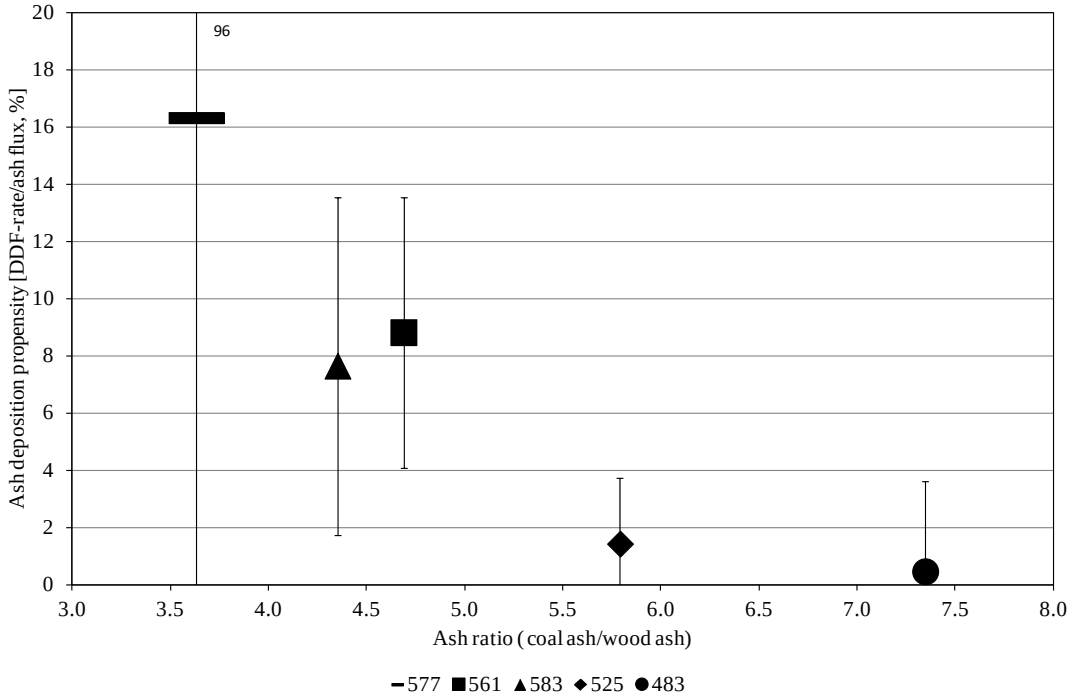

(b)

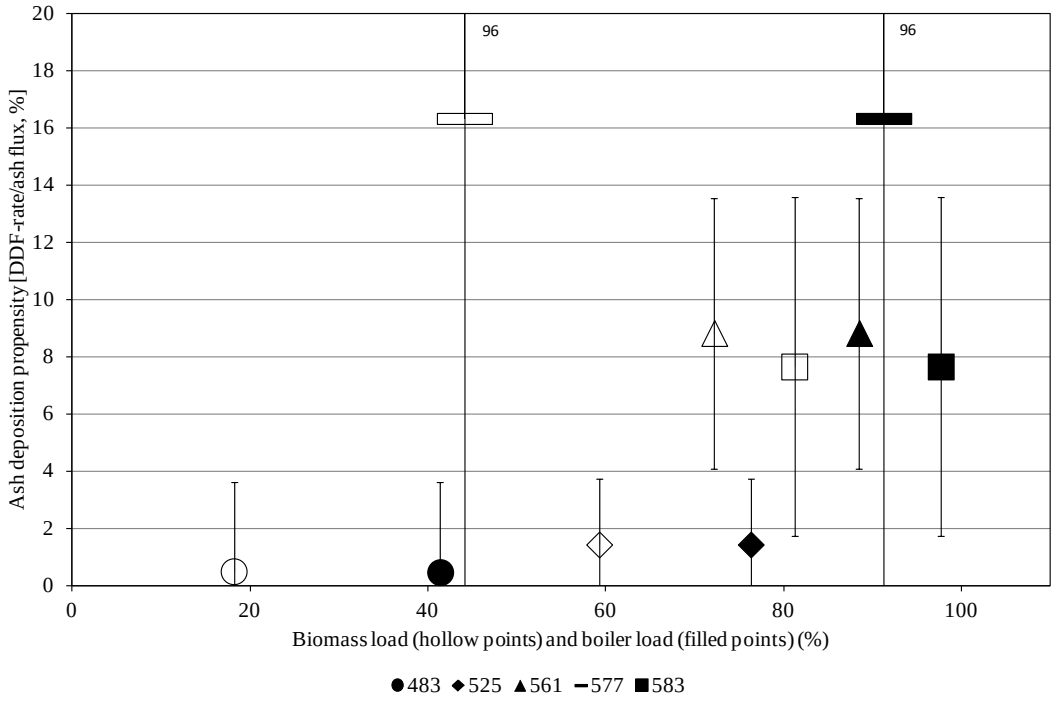

Figure 13: a) Impact of coal ash to fuel ash ratio on ash deposition propensity at different probe surface temperatures, b) impact of biomass load (hollow points) and boiler load (filled points) on ash deposition propensity at different probe surface temperatures.

3.4 Comparison of results with previously conducted probe measurements

The deposit formation rate (g/m^2/h) can also be determined based on the mass increase divided by a given probe exposure time and we have called this the integrated deposit formation rate (IDF-rate). In mathematical terms, let $m(t)$ be the continuously monitored probe mass uptake. If the probe signal was noise free and no shedding events of any kind occurred, the true deposit formation rate would be the derivative $m'(t)$. However, the signal is not noise free, and both minor and major shedding events occur, so that the derivative $m'(t)$ represents the net deposit accumulation rate at any time. We defined IDF- and DDF-rates corresponding to the mathematical expressions

$$\text{IDF-rate} = \frac{\int_{t_1}^{t_2} m'(t)\,dt}{t_2 - t_1} = \frac{m(t_2) - m(t_1)}{t_2 - t_1} \quad (6)$$

$$\text{DDF-rate} = \langle m'(t) \rangle \quad (7)$$

where $\langle m'(t) \rangle$ represents a moving average over short time intervals without major shedding events.

In previously conducted measurements at straw and/or wood-fired boilers, the deposit formation rates were calculated by inserting the probe inside the boiler for 2-12 h [11,19]. In the current measurements, the deposit mass uptake signal after 12 h was measured and then divided by 12 h to get the IDF-rate. However, the IDF-rate can be influenced by shedding events during the time interval of the deposit collection. This could also happen when people report deposit formation rate when they took the probe out and divide the deposit amount collected by the probe exposure time, but the deposit mass can be significantly lower because of shedding. The values of IDF-rate calculated for the current study are therefore just representing arbitrary numbers. The deposit build-up pattern observed in tests 1, 2, 3 and 5 makes the calculated IDF-rate quite random. The deposit mass uptake at 12 h can be anywhere between 0 and 6,000 g/m^2, which implies that in the case with a lot of fast shedding, IDF-rate data are not meaningful. However, a comparison of previous full-scale deposit probe measurements was made for different wood-fired boiler measurements and the current measurements (see Table 4 and Figure 14). The data points, even those at approximately the same conditions, have a large spread, which is a result of the difficulties of keeping all operational parameters constant during full-scale measurements. However, within the range of deposit formation rates, some systematic tendencies can be observed. Previous probe measurements at AVV2 unit 2 showed deposit formation values in the range of 5-13 g/m^2/h during wood dust and natural gas firing (may be oil firing also), with and without the addition of coal ash. Skrifvars et al. [19] measured deposit formation rate in the range of 12-74 g/m^2/h (mean 40 g/m^2/h of 4 measurements) at 920 ^{o}C and between 3 to 15 g/m^2/h (mean 7 g/m^2/h of four measurements) at 750 ^{o}C in a wood pulverized fuel boiler. Overall, it is observed that an increased flue gas temperature and straw addition in wood (increased K contents) cause an increased deposit formation rate, while a changed probe surface temperature seems not to cause any systematic change. Moreover, the present measurements indicate increased deposit formation rates compared to previous measurements at the same boiler [5], possibly due to higher flue gas temperatures. In addition, the IDF-rates may be severely influenced by uncontrolled fluctuations and shedding events in the initial 12 h period.

Table 4: Ash deposition data from the previous and current full-scale measurements. Amager Unit 2 (AMV2) and Unit 1 (AMV1) are straw and/or wood-fired suspension boilers. Jorbo, Sweden is a down-fired pulverized fuel boiler. Avedøre Unit 2 (AVV2) is a wood and natural gas fired suspension boiler.

No.	Boiler	Fuel (+ additive)	Fuel ash	Probe position	Probe surface temp.	Flue gas temp.	Exposure time	IDF-rate	Ref.
		--	% wt.	--	^{o}C	^{o}C	h	g/m^{2}h	
1	AVV2	Wood + natural gas (+ coal ash)	1.0	Just below radiation shield	577	1350	12.0	212	
2	AVV2	Wood + natural gas (+ coal ash)	1.0	Just below radiation shield	583	1250	12.0	156	
3	AVV2	Wood + natural gas (+ coal ash)	1.0	Just below radiation shield	561	1300	12.0	53	
4	AVV2	Wood + natural gas (+ coal ash)	1.0	Just below radiation shield	483	950	12.0	128	
5	AVV2	Wood + natural gas (+ coal ash)	1.0	Just below radiation shield	525	1000	12.0	30	
6	AVV2	Wood + natural gas	0.6	Near radiation shield	500	923	~4.0	5	[5]
7	AVV2	Wood + natural gas	0.6	Near radiation shield	476	930	~5.0	13	[5]
8	AVV2	Wood + natural gas	1.2	Near radiation shield	491	918	~2.4	10.5	[5]
9	AVV2	Wood + natural gas	1.2	Near radiation shield	500	929	~4.5	4.5	[5]
10	AVV2	Wood + natural gas + oil	0.67	Near radiation shield	504	885	--	6.5	[5]
11	AVV2	Wood + oil (+coal ash)	--	Near radiation shield	503	955	~3.5	10	[5]
12	AVV2	Wood (+coal ash)	--	Near radiation shield	474	938	~2.5	12.5	[5]
13	Jorbro	Wood	0.55	Superheater	520	920	~2.0	40	[19]
14	Jorbro	Wood	0.55	Superheater	520	750	~2.0	7	[19]
15	AMV1	Straw + wood	5.1	Superheater	493	910	12.0	55	[17]
16	AMV1	Straw + wood	5.0	Superheater	593	821	13.5	57	[17]
17	AMV1	Straw + wood	1.3	Superheater	481	765	12.0	22	[17]
18	AMV1	Straw + wood	3.4	Superheater	479	847	6.0	95	[17]
19	AMV1	Straw + wood	1.6	Superheater	494	815	12.0	87	[17]
20	AMV1	Straw + wood	1.0	Superheater	563	823	12.0	1	[17]
21	AMV1	Straw + wood	0.85	Superheater	538	772	12.0	3	[17]
22	AMV1	Straw + wood	0.8	Superheater	539	745	12.0	1	[17]
23	AMV2	Straw + wood	5.4	Superheater	500	863	12.0	33	[20]
24	AMV2	Straw + wood	4.2	Superheater	500	856	12.0	33	[20]
25	AMV2	Wood	3.3	Superheater	500	586	12.0	1	[20]

(a)

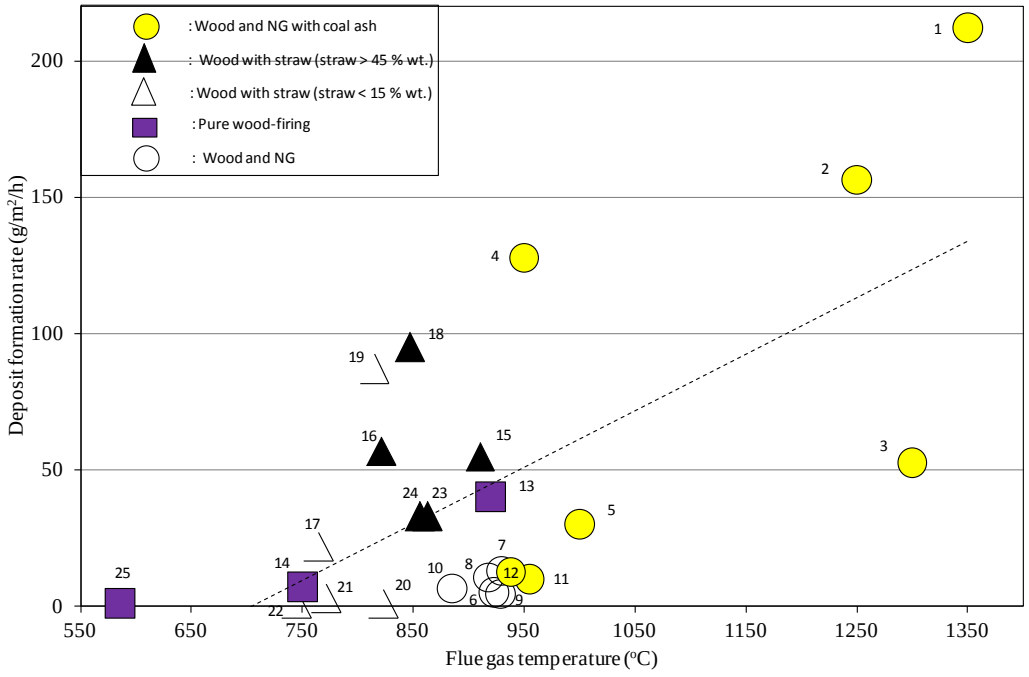

(b)

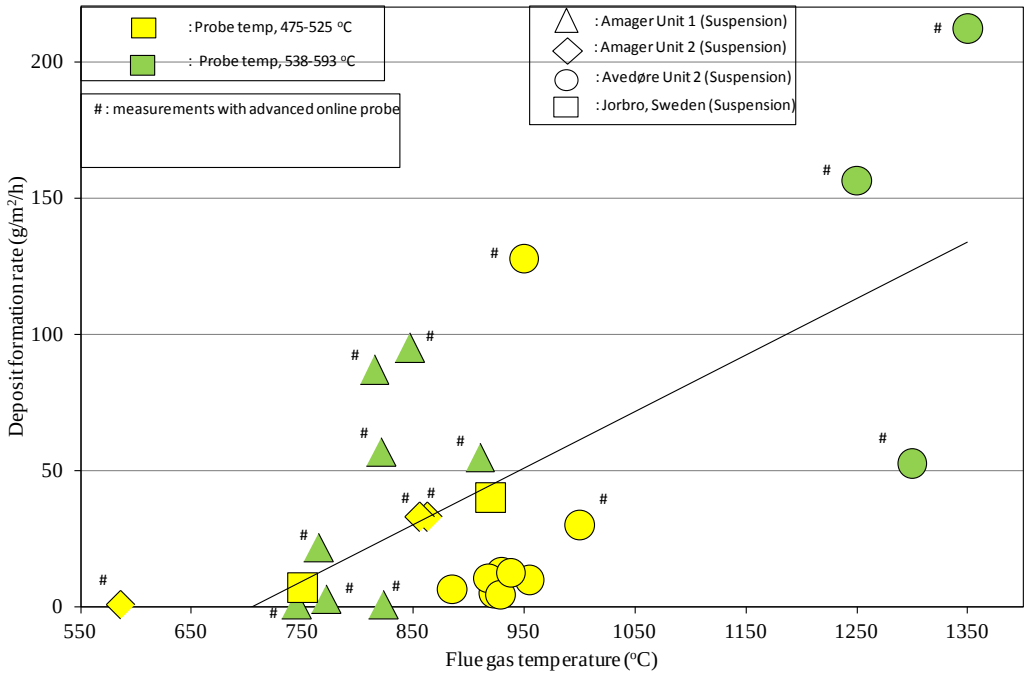

Figure 14: Impact of flue gas temperature on deposit formation rates (IDF-rates), a) comparison of deposit probe measurements data for wood-firing with and without co-firing wood in combination with other fuels, b) comparison of data set with marking of the probe surface temperature and the boilers where the measurements were preformed [5,17,19,20.] Graph details: NG is meant for natural gas, a) the number on each point represents the corresponding number in Table 4. b) the color represents the probe surface temperature, while point shape represents the boiler type. # indicates points where measurements were conducted with advanced probe. Amager Unit 2 (AMV2) and Unit 1 (AMV1) are straw and/or wood-fired suspension boilers. Jorbro is a down-fired pulverized fuel boiler. Avedøre Unit 2 (AVV2) is a wood, oil and natural gas fired suspension boiler. Furnace oil was fired in addition to wood and natural gas during points 10 and 11 mentioned in Figure 14 a).

3.5 Deposit shedding

The deposit mass uptake signals were continuously monitored along with video monitoring in order to identify shedding events. The larger shedding events appear as a sudden decrease in the deposit mass uptake signal and a corresponding increase in the probe heat uptake signal. Video monitoring during almost all the tests revealed that the deposits were not sticky and were easy to remove (see Figure 15), even at very high flue gas temperatures (> 1350 ^{o}C). Deposit removal through surface melting was not identified. This indicates that potassium (K) has been captured by coal ash rich in aluminum-silicates whereby an ash with a high melting temperature is formed. A typical example of a deposit shedding event is shown in Figure 15. It can be seen that the deposits are not strongly attached to the probe and were removed naturally. The deposits are loosely attached as shown in Figure 15 (a), and after just 2 minutes, a significant amount of deposit was removed from the upstream side of the probe (see Figure 15 (d)). It was seen that deposit were removed through debonding when a complete/partial deposit layer is detached from the probe. Similar results were seen after finishing the new measurements at AVV2, where two cameras were used. The deposit removal was caused by both naturally occurring shedding events and shedding events caused by plant sootblowing (see Figure 3).

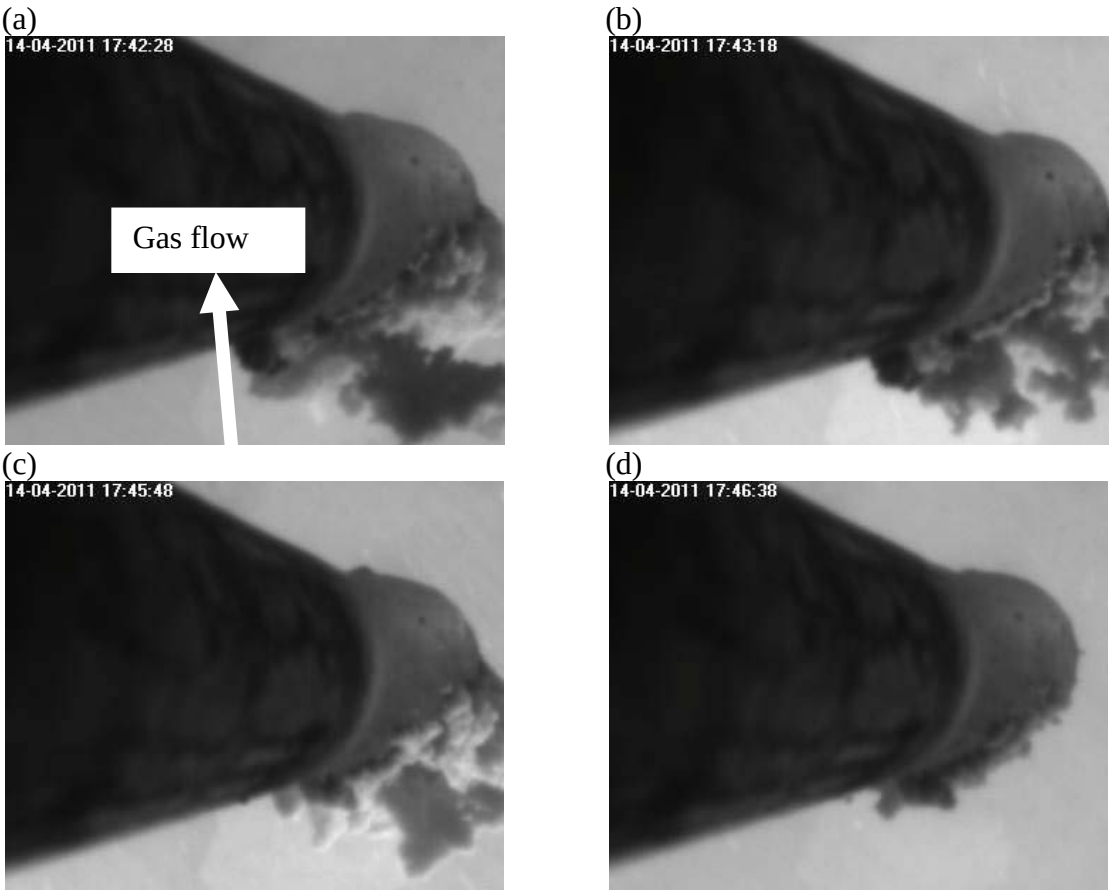

Figure 15: Images of probe before and after deposit shedding during test 5 (30.3 h exposure time).

During the calculation of DDF-rates, a particular negative slope cut off level was selected to determine major shedding events accurately, while still giving a satisfactory prediction of apparent DDF-rates. The selected cut off level was -3,800 g/m^2/h for all the tests.[17] This cut off level strikes a balance between including larger shedding events in the analysis and preventing deposit mass signal noise from being counted on a shedding event. The selected minimum magnitude of a shedding event included in the analysis was -105 g/m^2 and this was calculated by equation (8).

$$\text{minimum shedding event magnitude} = \text{slope cut off level} \cdot \text{ sampling interval} = -3800 \frac{\text{g}}{\left(\text{m}^2\text{h}\right)} \frac{\text{h}}{\left(3600\ \text{s}\right)} \cdot 100\ \text{s} = -105 \frac{\text{g}}{\text{m}^2} \quad (8)$$

To make it possible to investigate the influence of different operational parameters on the ash deposition and shedding, each test was divided into further sub-tests based on the number of hours (usually 6 hours). A significant number of data points thus allowed us to analyze the influence of local boiler operational parameters on deposition rate and deposit shedding. The results are summarized in Table 5. For a complete test there can be seen a difference between the DDF-rate and the deposit shedding rate (mean deposit removal multiplied by deposit removal frequency) even though the deposit mass uptake signals indicate a little amount of deposits accumulated on the probe at the end of most of the tests. This difference is probably due to the fact the selected number of minimum shedding event is -105 g/m^2, and any shedding event less than that will potentially cause an error.

Table 5: Overall summary of ash deposition and deposit shedding.

Test	Exposure time (h)	Boiler load (%)	Biomass load (%)	Gas temp (^{o}C)	Probe temp (S3) (^{o}C)	Deposit mass uptake (g/m^2)	Heat uptake (kW/m^2)	DDF-rate (g/m^{2}h)	Ash flux (g/m^{2}h)	Deposition propensity (%)	St. dev. (deposition propensity)	Max deposit drop (g/m^2)	Mean deposit drop (g/m^2)	Mean deposit removed (%)	Deposit removal frequency (hr^{-1})
Test 1	1-6	89.64	77.07	--	555.32	395.44	--	14312	57608	24.84	83.92	4437	1723	--	2.00
Test 1	6-12	91.71	64.99	--	540.21	1860.64	--	4201	50141	8.38	2.21	5447	2187	75.36	1.50
Test 1	12-18	92.67	3.27	--	610.91	3948.13	--	855	7369	11.61	16.75	966	952	22.52	0.33
Test 1	18-25.10	90.74	38.90	1314	570.24	3811.31	--	1481	9558	15.50	36.91	1770	1770	39.90	0.17
Test 1	Overall test	91.22	44.10	1350 ± 75	570.39	2648.00	--	4717	28886	16.33	79.80	5447	1835	--	0.96
Test 2	1-6	94.22	79.09	--	553.90	1719.01	20.97	5343	58374	9.15	8.96	6303	2972	89.56	1.00
Test 2	6-12	99.75	80.99	--	553.00	1585.31	20.92	4194	58762	7.14	0.90	5168	2006	70.46	1.83
Test 2	12-15.15	100.38	85.71	--	550.61	1333.62	19.28	3381	59651	5.67	1.48	2683	1346	70.20	1.33
Test 2	Overall test	97.63	81.16	1250 ± 75	552.89	1589.30	20.61	4501	58782	7.66	5.91	6303	2027	74.96	1.65
Test 3	1-6	98.30	86.39	--	550.32	1034.58	17.83	5730	59583	9.62	6.27	5817	1900	98.10	1.67
Test 3	6-12	91.23	77.33	--	545.94	1198.73	10.84	4291	58291	7.36	0.99	4400	1492	70.75	2.33
Test 3	12-18	68.02	53.45	--	501.44	1195.90	8.24	2595	44757	5.80	2.80	4264	1174	63.44	2.17
Test 3	18-24	100.48	73.93	--	549.43	1960.68	19.80	7224	57179	12.63	3.25	7777	2938	83.94	2.00
Test 3	24-26.70	85.09	74.48	--	530.81	1402.54	10.49	4608	57260	8.05	1.84	2897	1310	83.86	1.50
Test 3	Overall test	88.47	72.18	1300 ± 75	535.26	1369.55	13.55	4874	54931	8.87	4.71	7777	1762	78.59	2.17

Test	Exposure time (h)	Boiler load (%)	Biomass load (%)	Gas temp (°C)	Probe temp (S3) (°C)	Deposit mass uptake (g/m^2)	Heat uptake (kW/m^2)	DDF-rate (g/m^2h)	Ash flux (g/m^2h)	Deposition propensity (%)	St. dev. (deposition propensity)	Max deposit drop (g/m^2)	Mean deposit drop (g/m^2)	Mean deposit removed (%)	Deposit removal frequency (hr^{-1})
Test 4	1-6	39.20	18.07	--	496.50	573.03	6.30	872	35861	2.43	7.25	0	0	0.00	0.00
Test 4	6-12	39.22	18.09	--	499.74	1453.85	6.66	96	24546	0.39	0.56	0	0	0.00	0.00
Test 4	12-18	38.85	18.09	--	499.64	1592.29	7.04	124	19188	0.64	1.21	0	0	0.00	0.00
Test 4	18-24	38.99	18.09	--	499.79	1642.61	7.44	9	19027	0.04	0.11	0	0	0.00	0.00
Test 4	24-30	39.03	18.09	--	499.63	1648.21	7.86	172	19357	0.89	1.30	0	0	0.00	0.00
Test 4	30-36	39.04	18.09	--	499.62	1664.08	7.42	4	19591	0.02	0.10	0	0	0.00	0.00
Test 4	36-42	38.90	18.09	--	499.75	1703.40	7.60	8	19477	0.04	0.10	0	0	0.00	0.00
Test 4	42-48	43.45	18.09	--	499.81	1771.23	9.19	158	18789	0.84	1.40	0	0	0.00	0.00
Test 4	48-54	44.11	18.09	--	499.79	1919.17	10.35	17	19408	0.09	0.16	0	0	0.00	0.00
Test 4	54-60	42.43	18.09	--	499.49	1931.84	10.16	--	19129	--	--	224	224	12.44	0.17
Test 4	60-66	43.62	18.09	--	499.53	1814.75	11.07	99	20035	0.50	0.50	0	0	0.00	0.00
Test 4	66-72	43.17	18.08	--	499.63	1685.38	6.64	61	19187	0.32	1.18	0	0	0.00	0.00
Test 4	72-78	42.08	18.09	--	499.55	1721.72	7.08	12	19343	0.06	0.14	0	0	0.00	0.00
Test 4	78-84	41.49	18.09	--	499.79	1754.44	7.19	0	19964	0.00	0.08	261	261	15.48	0.17
Test 4	84-90	42.28	18.09	--	499.59	1809.54	6.88	182	19400	0.94	1.17	0	0	0.00	0.00
Test 4	90-96	42.66	18.09	--	499.79	1891.19	7.76	--	19389	--	--	0	0	0.00	0.00
Test 4	96-102	43.02	18.83	--	499.78	1885.18	9.30	--	19702	--	--	0	0	0.00	0.00
Test 4	102-108	42.73	19.18	--	499.69	1909.02	10.06	8	19862	0.04	0.04	0	0	0.00	0.00
Test 4	108-110	42.36	19.14	--	495.58	1798.28	6.98	--	19575	--	--	232	190	10.13	0.33
Test 4	Overall test	41.37	18.20	950 ± 75	499.45	1691.41	8.10	96	20580	0.47	3.14	261	216	12.05	0.04
Test 5	1-6	43.13	19.18	970	499.57	80.27	9.57	384	19626	1.96	11.09	0	0	0.00	0.00
Test 5	6-12	57.11	23.93	--	531.70	121.34	12.18	68	22473	0.30	0.84	0	0	0.00	0.00
Test 5	12-18	84.57	70.66	--	563.47	463.79	18.19	561	53104	1.06	0.87	1687	848	75.75	0.50
Test 5	18-24	87.06	73.69	--	569.21	512.86	19.42	476	55756	0.85	0.87	1896	708	51.59	0.67
Test 5	24-30	89.35	75.11	1214	574.12	387.78	22.53	661	58071	1.14	0.66	487	338	51.71	1.67
Test 5	30-36	94.85	81.96	--	563.57	493.95	24.98	1458	58638	2.49	1.68	805	445	53.35	2.67
Test 5	36-42	68.24	59.35	--	516.34	392.48	16.06	669	45817	1.46	2.24	1017	486	55.14	1.83
Test 5	42-48	81.22	67.37	--	541.84	417.12	21.21	712	50069	1.42	1.48	889	490	48.10	1.17
Test 5	48-51.50	91.33	73.80	--	568.34	662.07	25.61	1280	53673	2.39	1.00	1352	468	50.51	1.83
Test 5	Overall test	76.28	59.24	1075 ± 75	546.09	374.87	18.37	653	45571	1.43	2.31	1896	481	53.28	1.20

All the measurements are summarized in Table 5, while in Figure 16 is shown the deposition propensity as a function of boiler load. Flue gas temperature measurements are not available for most of the six hour periods and changed deposit behavior as a function of flue gas temperature can therefore not be plotted. In Figure 17, Figure 18 and Figure 19 are shown the shedding frequency and the amount of the deposit removed in a single shedding period (6 h), as a function of boiler load. From Figure 16 is seen a weak increase in deposition propensity with increasing boiler load, probably caused by the increased local flue gas temperature. It is observed in Figure 17, Figure 18 and Figure 19 that both the shedding frequency and the amount of deposit removed in an actual event increases with increasing boiler load.

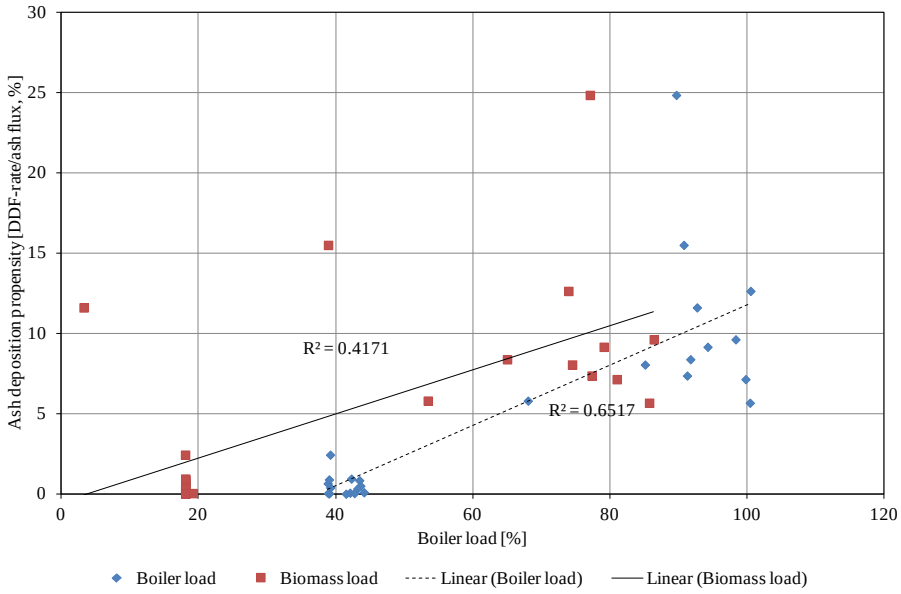

Figure 16: Impact of boiler load and biomass load on ash deposition propensity. Data of each 6 hours from test 1 to 4. Test 5 is excluded due to difficulties in keeping probe surface temperature constant.

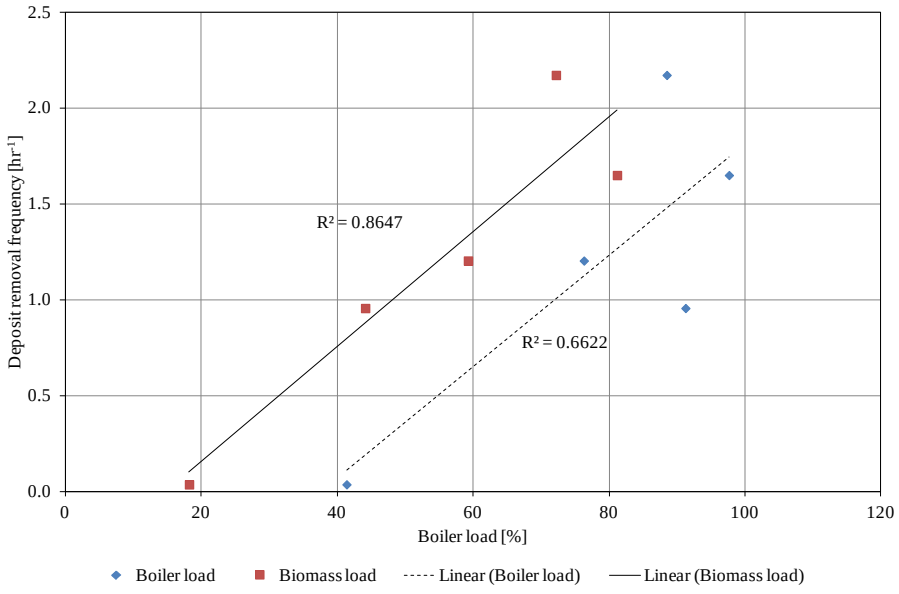

Figure 17: Impact of boiler load and biomass load on deposit removal frequency. Data of each test.

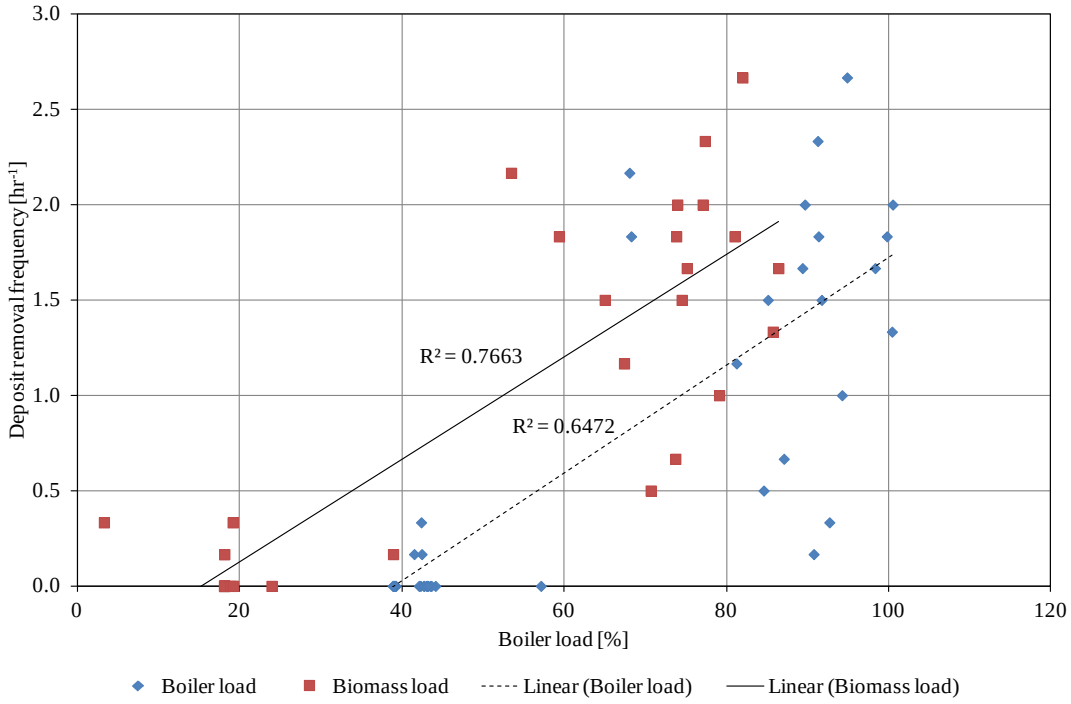

Figure 18: Impact of boiler load and biomass load on deposit removal frequency. Data of each 6 hours from test 1 to 5.

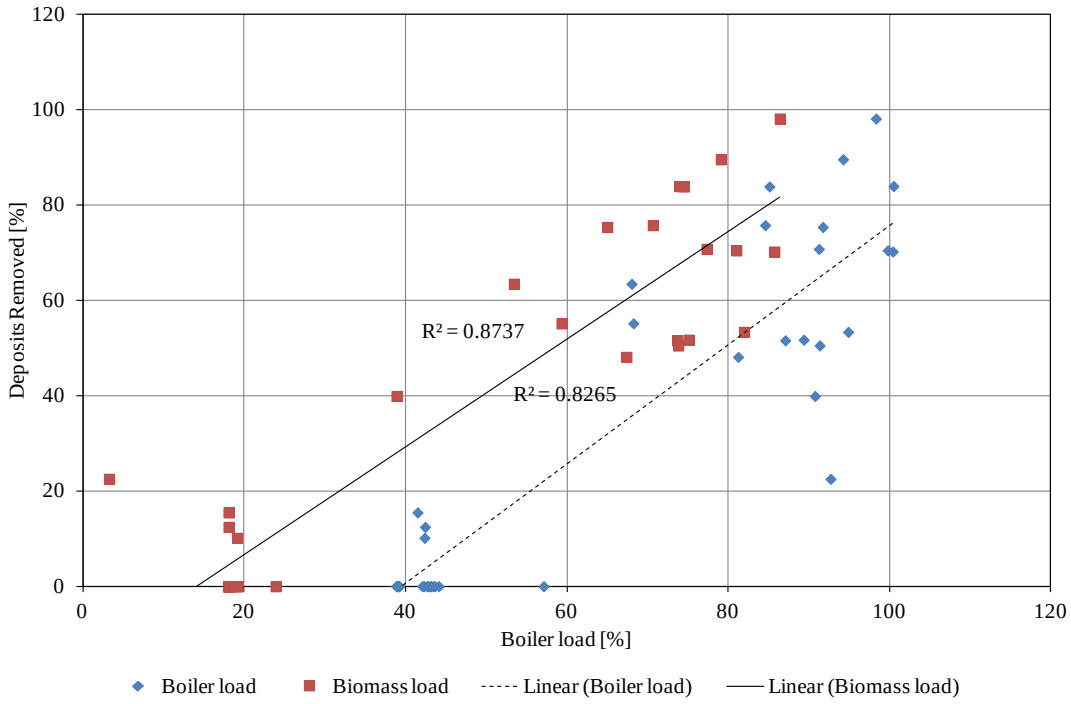

Figure 19: Impact of boiler load and biomass load on percentage of deposits removed. Data of each 6 hours from test 1 to 5.

3.6 Morphology and chemical composition of deposits

At the end of the experiment, the probe was carefully taken out of the boiler; the deposits were removed, photographed and finally an overall representative sample was selected for SEM-EDS analysis to characterize morphology and composition of deposits. Deposits from the downstream and upstream side of the probe were collected separately for later SEM-EDS analysis. The results of SEM-EDS analysis of only two tests (test 3 and test 5) are discussed based on the morphology and elemental composition of deposits on the upstream and downstream side of the probe. A typical image of upstream deposits from test 3 is shown in Figure 20, while the SEM-EDS results of upstream and downstream deposits are shown in Figure 21 and Figure 22, respectively. The chemical composition of the upstream deposits shows that the particles are primarily rich in Si, Al and Ca, while K is found in small amounts. The bigger particles contain lesser Ca, compared to small particles as observed in spot 4 and 5. The chemical composition of the downstream side deposits also shows a high content of Ca, Si and Al. In addition, Cl is not found either on the upstream side or on the downstream side of the probe. Therefore, potentially Cl has been released to the gas phase as HCl(g).

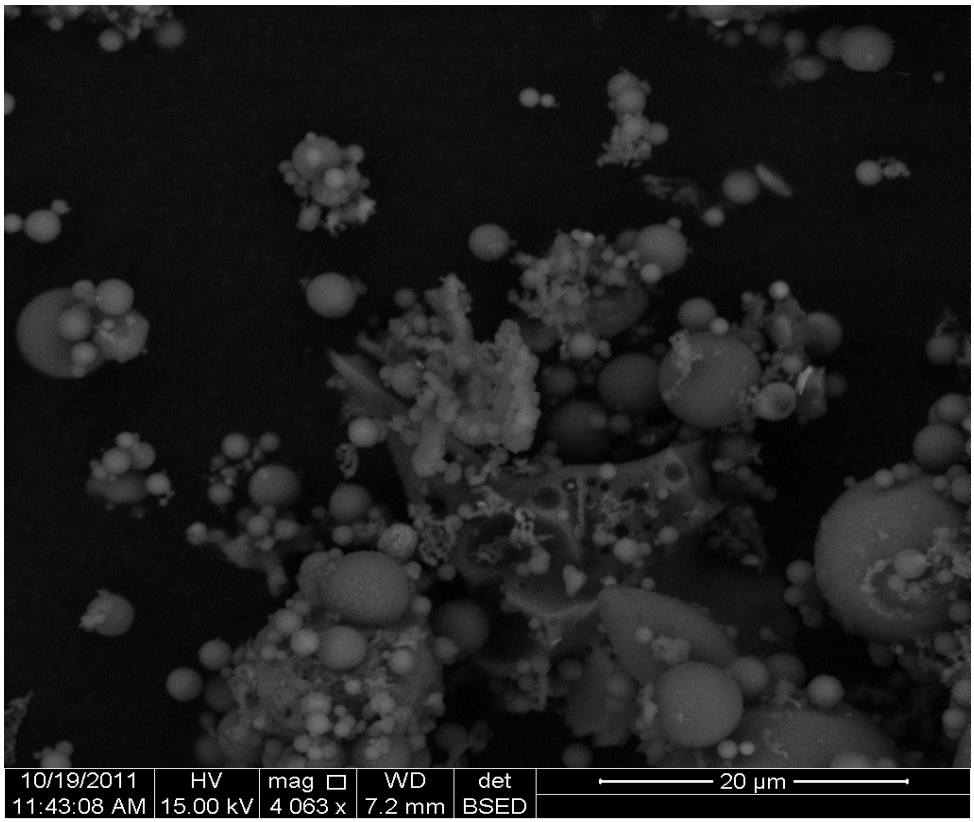

Figure 20: Morphology of upstream deposits from test 3.

(a)

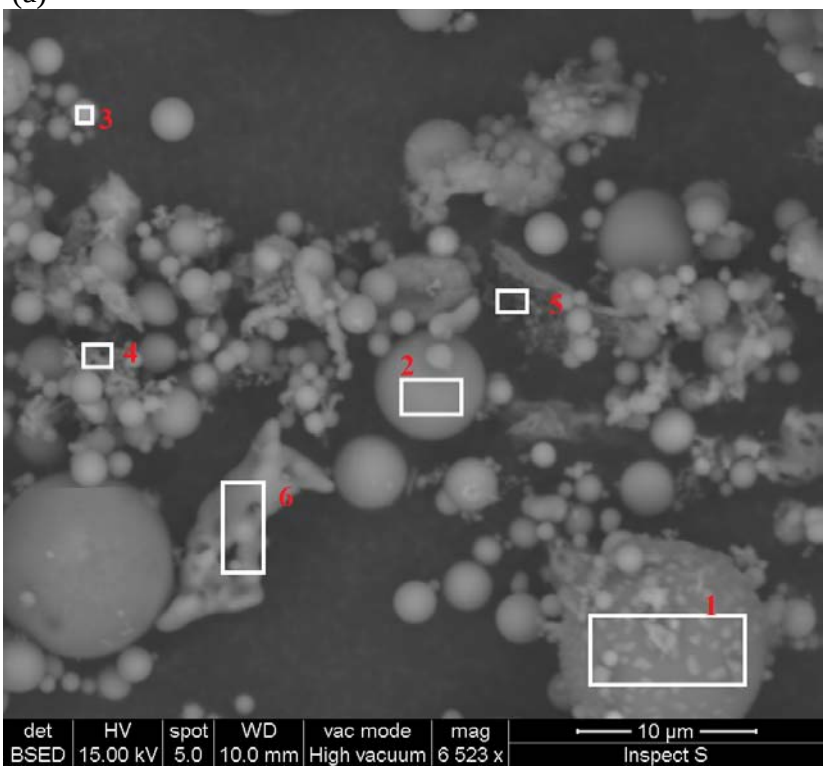

(b)

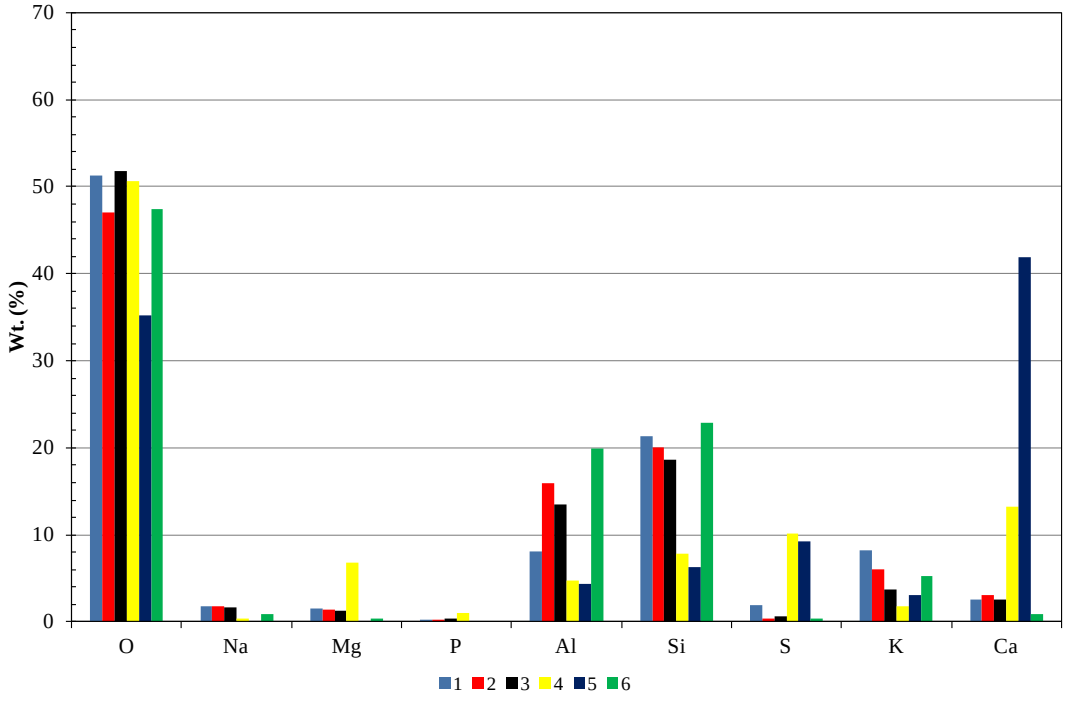

Figure 21: Morphology and composition of upstream side deposits formed during test 3.

(a)

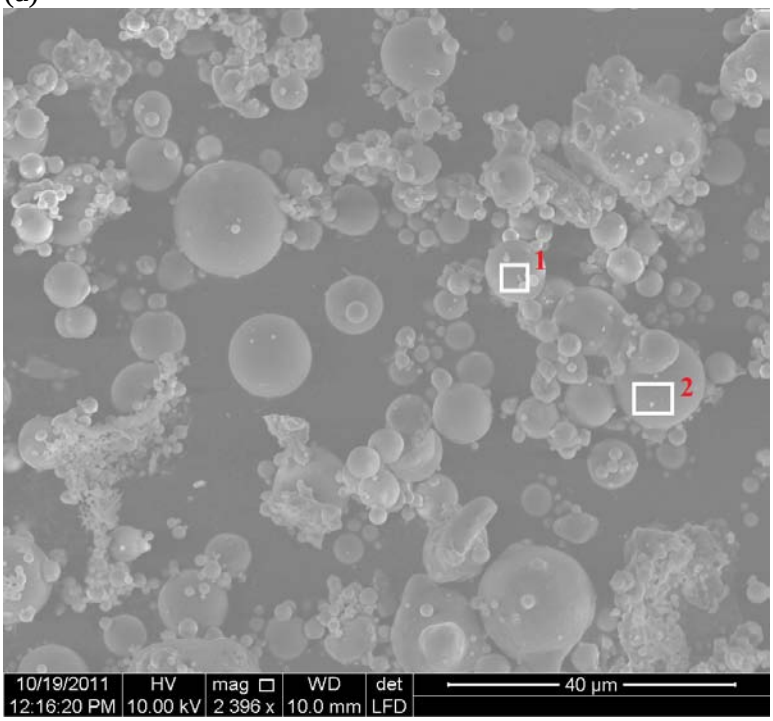

(b)

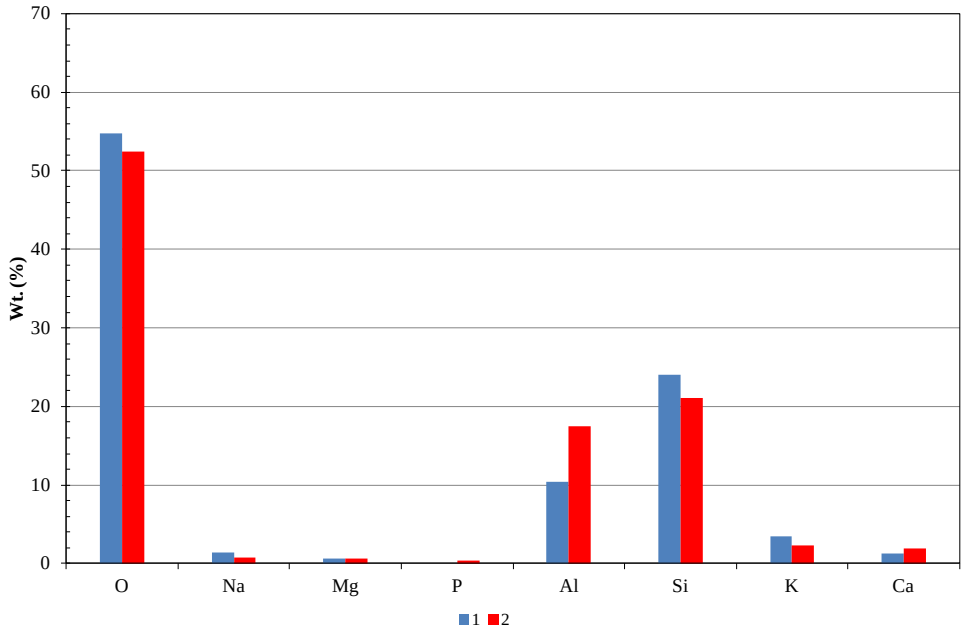

Figure 22: Morphology and composition of downstream side deposits formed during test 3.

An image and spot analysis of upstream deposits collected during test 5 is shown in Figure 23. I can be seen that most of the particles have a high content of Ca, Si and Al. Spot 5 and 6 contain more Na and K, compared to other spots possibly due to the fact that the very small particles adhered on large particles. The image and spot analysis of downstream deposits collected during test 5 is shown in Figure 24. The downstream deposits are rich in Ca, Si and Al. It is also interesting to note that spot 1, 2, 3 and 9 shows higher contents of K and Na compared to other spots, indicating that the small particles on these spots have a

high content of alkali metals. However, the composition of the deposits from both tests does not show a high concentration of K and Na. It is also worthwhile to note that Cl is not found either on the upstream or on the downstream side of the probe during test 5.

(a)

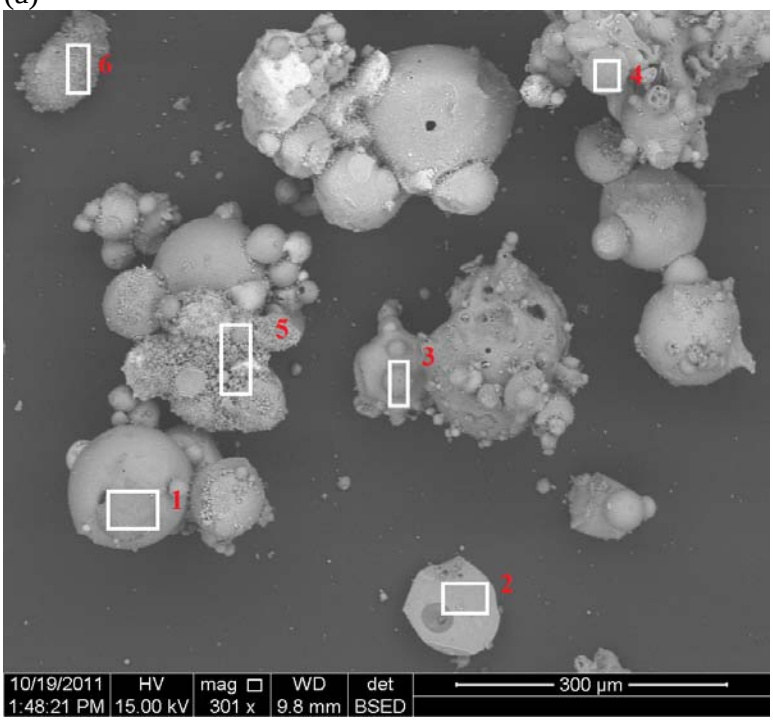

(b)

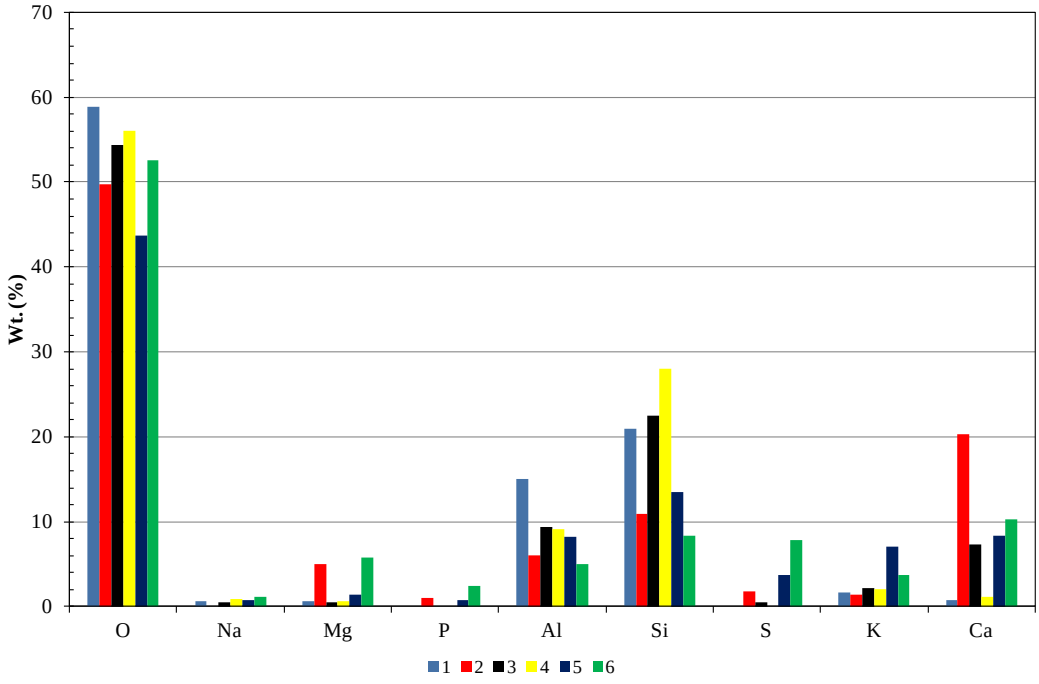

Figure 23: Morphology and composition of upstream side deposits formed during test 5.

(a)

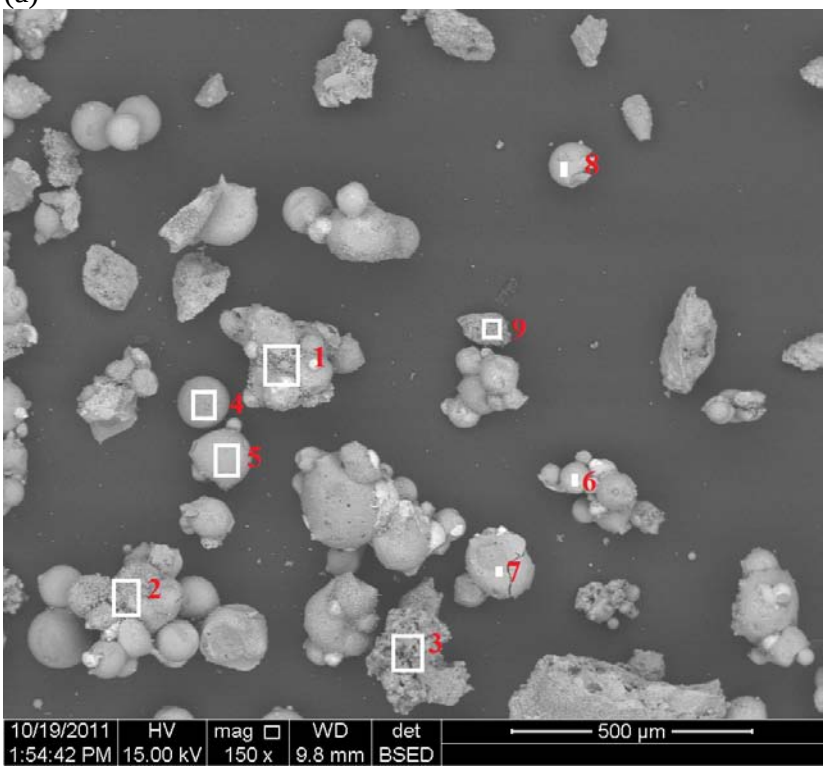

(b)

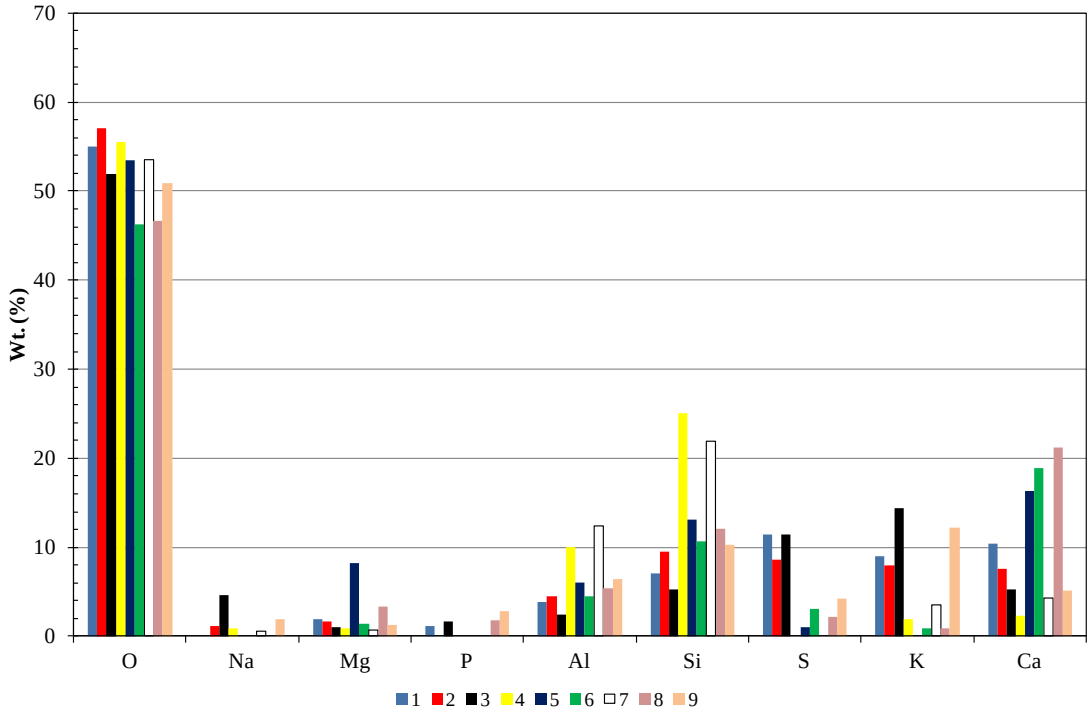

Figure 24: Morphology and composition of downstream side deposits formed during test 5.

3.7 Effect of operating parameters on the emissions of NO, SO_2 and CO

The effect of operating parameters on NO, SO_2 and CO emissions was also studied. The impact of biomass load and boiler load on NO_x emissions is shown in Figure 25, while impact of flue gas temperature on NO_x emissions is shown in Figure 26. It can be seen that NO_x emissions increased with increasing boiler load contrary to the previous full-scale measurements at the same boiler [5]. However, there is no clear tendency of increase of NO_x emissions with increase in biomass load. There is seen an increased NO_x emissions at higher flue gas temperatures, possibly due to formation of thermal NO_x.

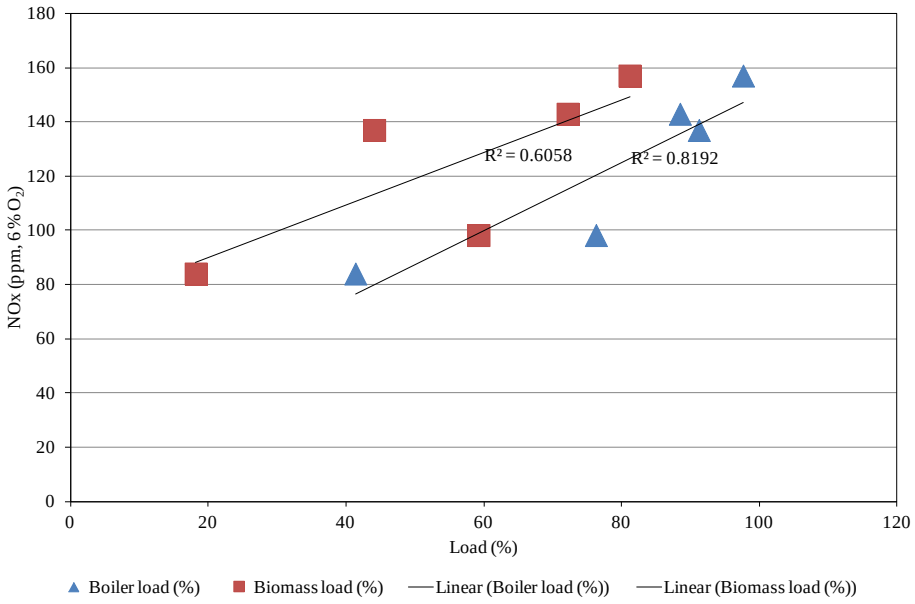

Figure 25: Impact of biomass load and boiler load on NOx emissions.

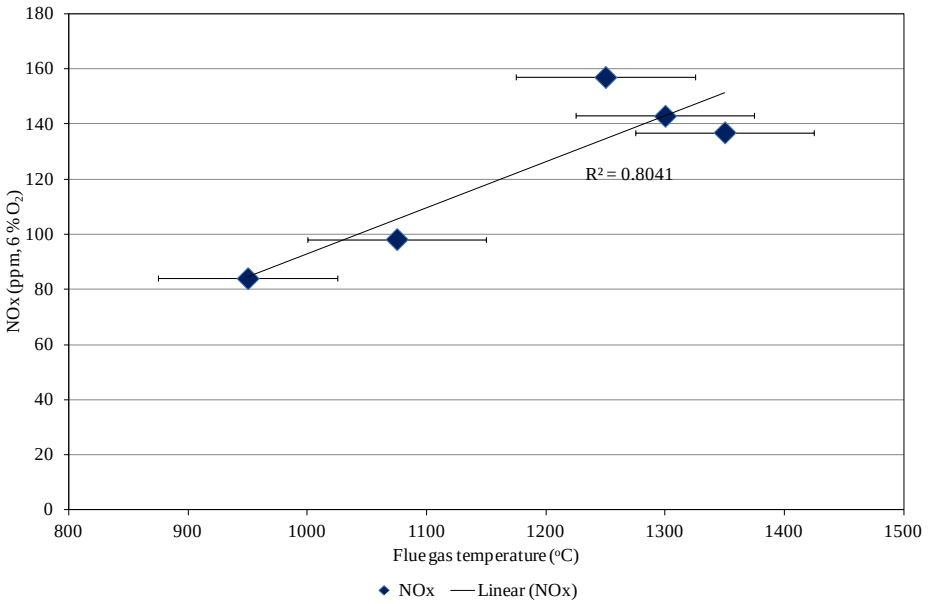

Figure 26: Impact of flue gas temperature on NOx emissions.

The impact of biomass load and boiler load on CO emissions is shown in Figure 27. There is not seen a correlation between biomass and boiler load on CO emissions. However, a relation between oxygen level and CO emissions can be seen in Figure 28. It can be seen that CO emissions increased at reduced oxygen levels, and a maximum value of 48 ppm is evident at 2.4 % O_2. The SO_2 emissions were observed to be very small in all the measurements and a maximum value of 8.2 ppm was seen during test 3.

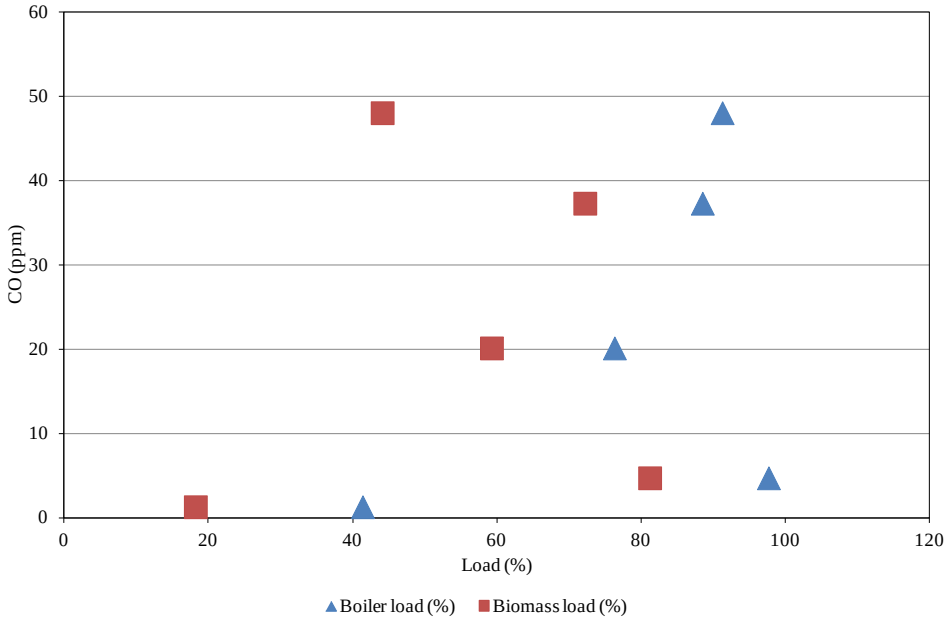

Figure 27: Impact of biomass load and boiler load on CO emissions.

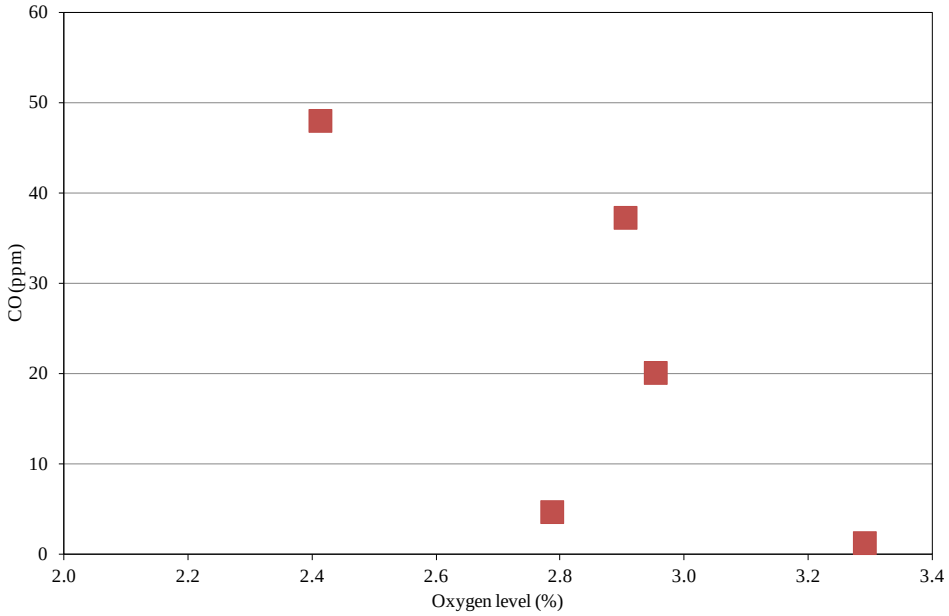

Figure 28: Relation between oxygen level and CO emissions.

4 SUMMARY AND CONCLUSIONS

A series of deposit probe boiler measurements were conducted at Avedøre Unit 2, a wood and natural gas suspension-fired boiler, to investigate ash deposition with coal ash addition. The probe was placed just below the radiation shield in the top of the boiler chamber. The measurements included deposit mass, heat uptake, flue gas temperature and video registration. The overall conclusions are summarized in the following points:

- Changes in biomass boiler load lead to some degree to changes in boiler flue gas temperature and the used coal ash to wood ash ratio. It is therefore difficult to determine which changes that causes the observed large changes in the deposit formation rate. However, a high increase in local flue gas temperature increased the deposit formation rate in this study, and this has also been observed in other previous deposit probe biomass boiler studies.
- Video monitoring revealed that the deposits formed were not sticky and could be easily removed by gravity shedding, and even at very high flue gas temperatures (> 1350 ^{o}C), deposit removal through surface melting was not identified. This indicates that potassium (K) has been captured by coal ash to form deposits with high melting temperatures.
- The percentage of deposits removed at a shedding event and deposit removal frequency increases to some extent with increasing boiler load and biomass load.
- NO_x emissions increased with increase in flue gas temperature, possibly due to formation of thermal NO_x.
- CO emissions reduced with increase in O_2 level. However, CO emissions were very small even at lower O_2 level (48 ppm at 2.4 % O_2).
- SO_2 emissions in all the measurements were very small with a maximum value of 8 ppm.
- SEM-EDS analysis of deposits shows significant presence of Ca, Al and Si, indicating that K has been captured by the coal ash to form deposits rich in calcium-aluminum-silicates. Cl was not found either on the upstream side or on the downstream side of the probe, and potentially Cl has been released to the gas phase as HCl(g).

ACKNOWLEDGEMENTS

The financial support by DONG Energy is gratefully acknowledged. We are thankful to the operational staff at the Avedøre Power Station, for their technical support during the full-scale measurements.

References

(1) Frandsen, F. J. Ash formation, deposition and corrosion when utilizing straw for heat and power production. Doctoral Thesis, Technical University of Denmark. **2011**, ISBN 978-87-92481-40-5.

(2) Baxter, L. L. Ash deposition during biomass and coal combustion: A mechanistic approach. *Biomass and Bioenergy* **1993**, 4, 85-102.

(3) Nielsen, H. P. Deposition and high temperature corrosion in biomass-fired boilers. PhD Thesis, Technical University of Denmark. **1998**, ISBN 87-90142-47-0.

(4) Montgomery, M.; Jensen, S. A.; Borg, U.; Biede, O.; Vilhelmsen, T. Experiences with high temperature corrosion at straw-firing power plants in Denmark, *Materials and Corrosion* **2011**, 62, 593-605.

(5) Jensen, P. A.; Dall'ora, M.; Lin, W.; Clausen, S.; Hansen, J.; Simonson, P.; Berg, M.; Jensen, A. D. Measurements on the 800 MW_{th} Avedøre oil, gas and wood co-fired suspension-boiler-Analysis of emission, burnout, deposit and FTIR measurements from April 2005 (Appendix E), CHEC Research Centre, Technical University of Denmark, **2008**.

(6) Jensen, P. A.; Sander, B.; Dam-Johansen, K. Removal of K and Cl by leaching of straw char. *Biomass and Bioenergy* 2001, 20, 447-457.

(7) Andersen, K. H.; Frandsen, F. J.; Hansen, P. F.; Wieck-Hansen, K.; Rasmussen, I.; Overgaard, P.; Dam-Johansen, K. Deposit formation in a 150 MWe utility PF-boiler during co-combustion of coal and straw, *Energy Fuels* **2000**, 14, 765-780.

(8) Zbogar, A.; Frandsen, F.; Jensen, P. A.; Glarborg, P. Shedding of ash deposits, *Prog. Energy Combust. Sci.* **2009**, 35, 31-55.

(9) Jensen, P. A.; Sørensen, L. H.; Hu, G.; Holm, J. K.; Frandsen, F.; Henriksen, U. B. Combustion experiments with biomass fuels and additives in a suspension fired entrained flow reactor – Test of Ca and P rich additives used to minimize deposition and corrosion. PSO Project, CHEC Research Centre, Technical University of Denmark. **2006.**

(10) Jensen, P. A.; Zhou, H.; Frandsen, F. J.; Hansen, J. Ash deposits removal in biomass power plant boilers, Proceeding of 15th European Biomass Conference and Exhibition. Berlin, Germany, 07-11 May, **2007**.

(11) Tobiasen, L.; Skytte, R.; Pedersen, L. S.; Pedersen, S. T.; Lindberg, M. A. Deposit characteristics after injection of additives to a Danish straw-fired suspension boiler. *Fuel Process Technol.* **2007**, 88, 1108-1117.

(12) Wu, H.; Glarborg, P.; Frandsen, F. J.; Dam-Johansen, K.; Jensen, P. A.; Dust-firing of straw and additives: Ash chemistry and deposition behavior, *Energy Fuels* **2011**, 25, 2862-2873.

(13) Åmand, L. E.; Leckner, B.; Eskillson, D.; Tullin, C. Ash deposition on heat transfer tubes during demolition wood, *Energy and Fuels* **2006**, 20, 1001-1007.

(14) Jensen, P. A.; Stenholm, M.; Hald, P. Deposition investigation in straw-fired boilers. *Energy Fuels* **1997**, 11, 1048-1055.

(15) Zhou, H.; Frandsen, F. J.; Jensen, P. A.; Glarborg, P. PSO Project 4106, CHEC report R0603, CHEC Research Centre, Technical University of Denmark. **2006**.

(16) Zbogar, A.; Frandsen, F. J.; Jensen, P. A.; Hansen, J.; Glarborg, P., Experimental investigation of ash deposit shedding in a straw-fired boiler. *Energy Fuels* **2006**, 20(2), 512-519.

(17) Bashir, M. S.; Jensen, P. A.; Frandsen, F.; Wedel, S.; Dam-Johansen, K.; Wadenbäck, J.; Pedersen, S. T.; Suspension-firing of biomass. Part 1: Full-scale measurements of ash deposit build-up, *Energy Fuels* **2012**, 26, 2317-2330.
(18) Nordgren, D. et al., Ash transformations in pulverised fuel co-combustion of straw and woody biomass. *Fuel Process Technol.* **2011**, doi:10.1016/j.fuproc.2011.05.027.
(19) Skrifvars, B-J.; Lauren, T.; Hupa, M.; Korbee, R.; Ljung, P. Ash behavior in a pulverized wood fired boiler - a case study. *Fuel* **2004**, 83, 1371-1379.
(20) Bashir, M. S.; Jensen, P. A.; Frandsen, F.; Wedel, S.; Dam-Johansen, K.; Wadenbäck, J.; Pedersen, S. T.; Ash transformation and deposit build-up during biomass suspension and grate-firing: Full-scale experimental studies. *Fuel Process Technol.* **2012**, 97, 93-106.
(21) Lokare, S. S.; Dunaway, J. D.; Moulten, D.; Rogers, D.; Tree, D. R.; Baxter, L. L. Investigation of ash deposition rates for a suite of biomass fuels and fuel blends. *Energy Fuels* **2006**, 20, 1008-1014.
(22) IFRF Suction Pyrometer, User Information Document, International Flame Research Foundation.
(23) IFRF Handbook, ISSN 1607-9116 www.handbook.ifrf.net/handbook/index.html
(24) Biomass energy centre, www.biomassenergycentre.org.uk (29-09-2011).
(25) Dam-Johansen, K.; Frandsen, F. J.; Jensen, P. A.; Jensen, A.D.; Co-firing of coal with biomass and waste in full-scale suspension-fired boilers. 7th international symposium on coal combustion, Harbin, China, July 17-20, **2011**.

Appendices

A: Boiler drawings

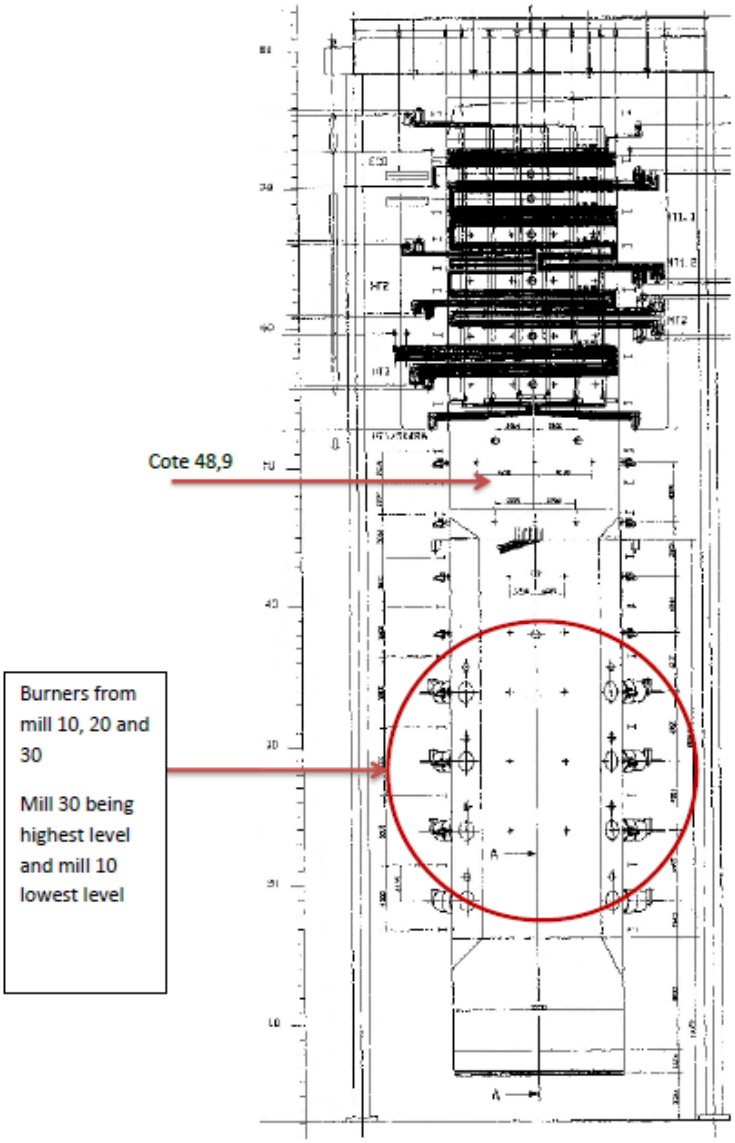

Figure A 1: Drawings of AVV2 boiler with identification of probe measuring position [5].

Appendix B: Flue gas temperature, deposit mass uptake signals, probe heat uptake, boiler operational conditions and ash deposition propensity during each test.

Test 1

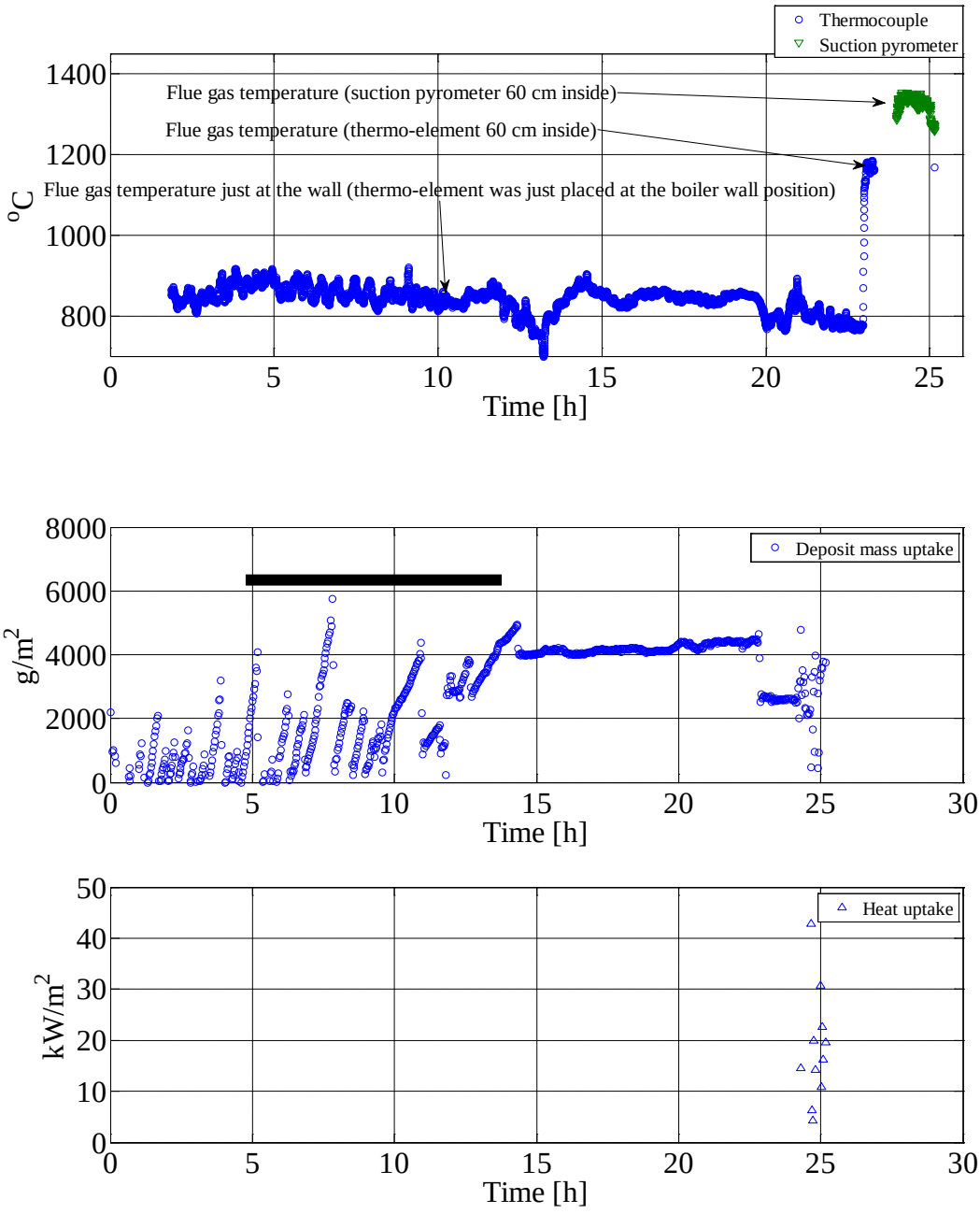

Figure B 1: Flue gas temperature, deposit mass uptake, sootblowing events and probe heat uptake during test 1. The black line in the middle figure shows the time when the surrounding sootblowers were in operation.

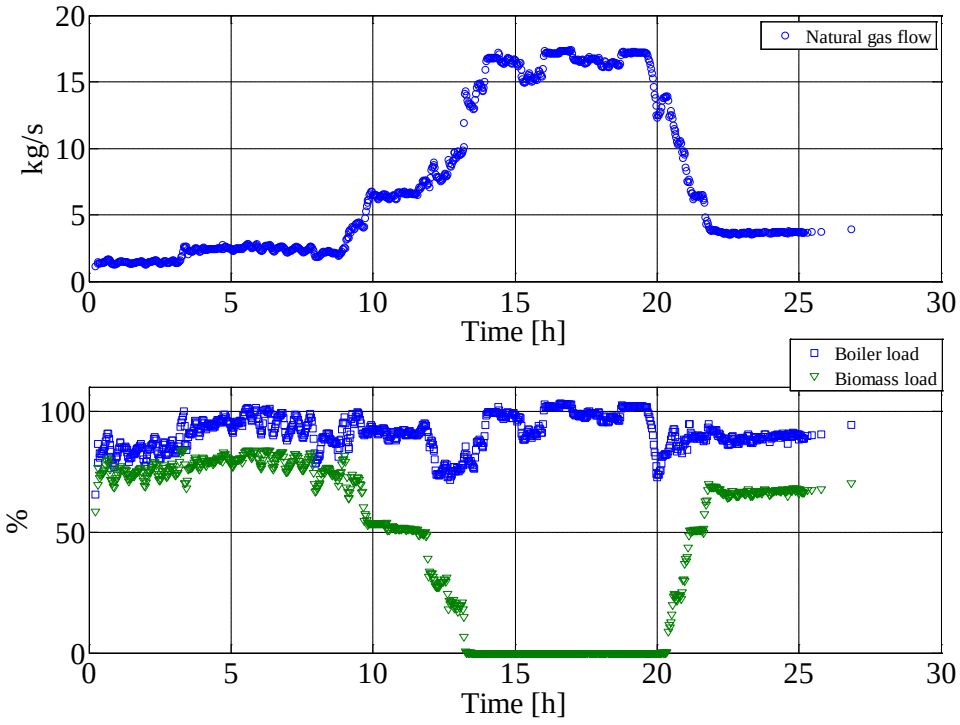

Figure B 2: Natural gas flow, overall boiler load and biomass load during test 1.

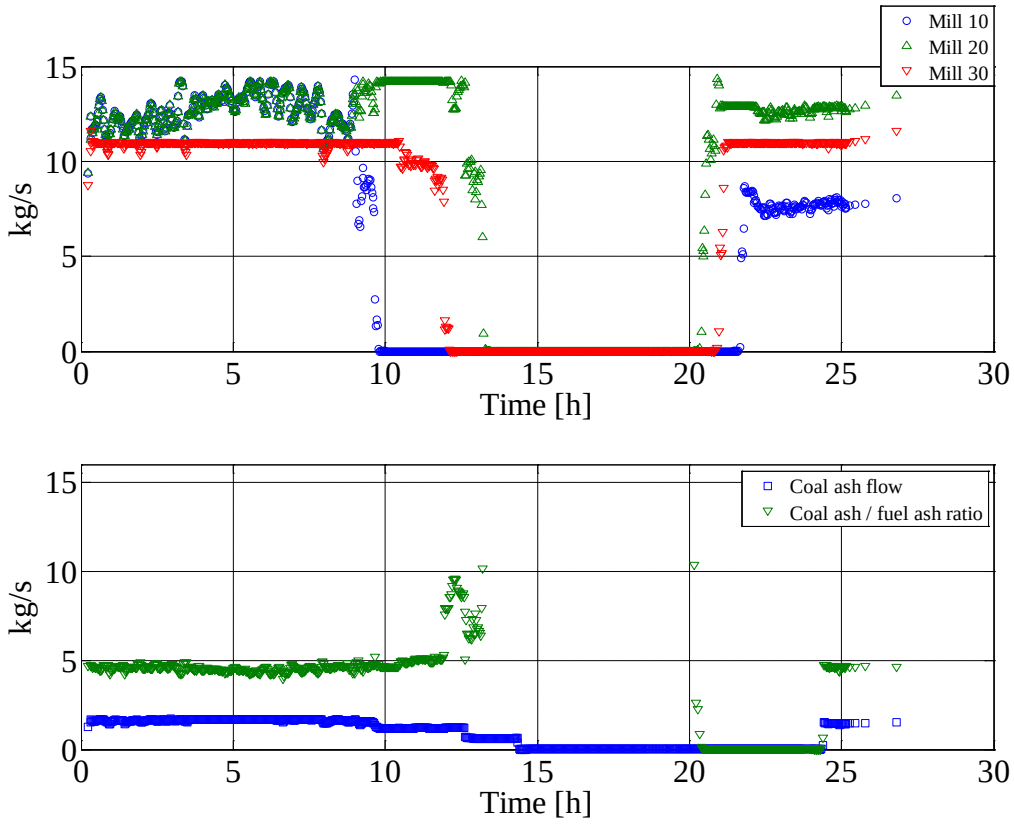

Figure B 3: Fuel flow (wood) through each mill, coal ash flow (kg/s) and ratio between coal ash and wood ash during test 1.

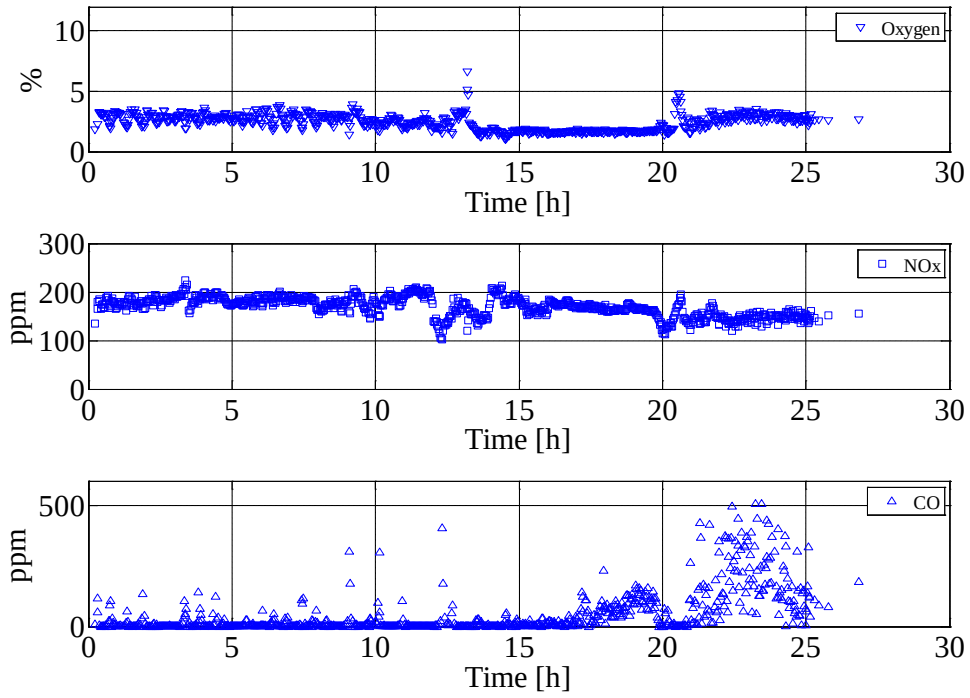

Figure B 4: Oxygen level, NOx level before DeNOx and CO level during test 1.

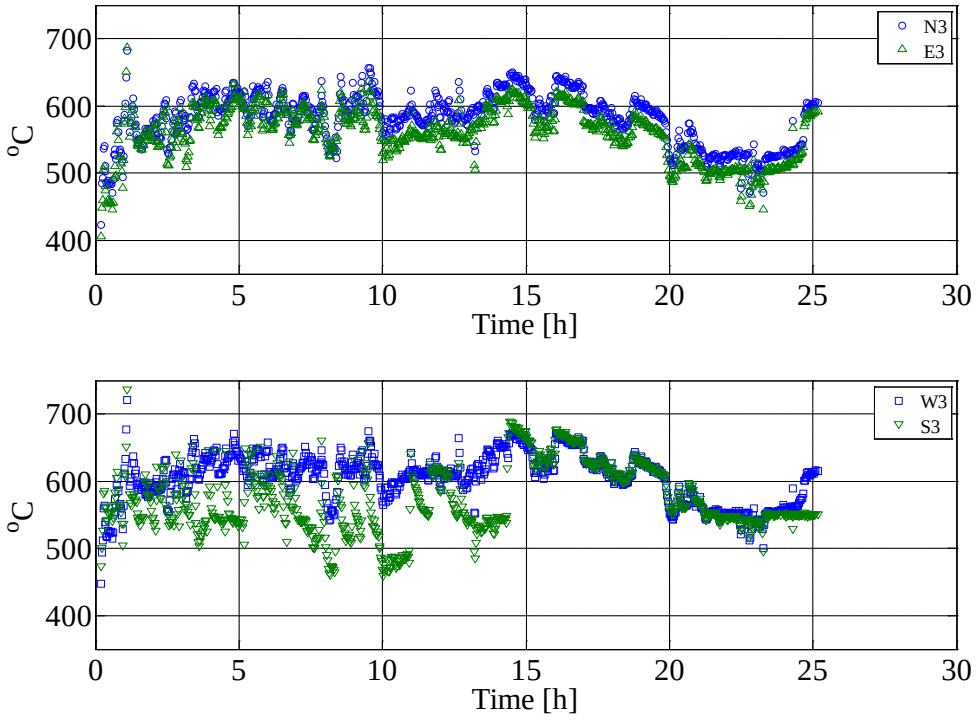

Figure B 5: Measured probe surface temperatures during test 1.

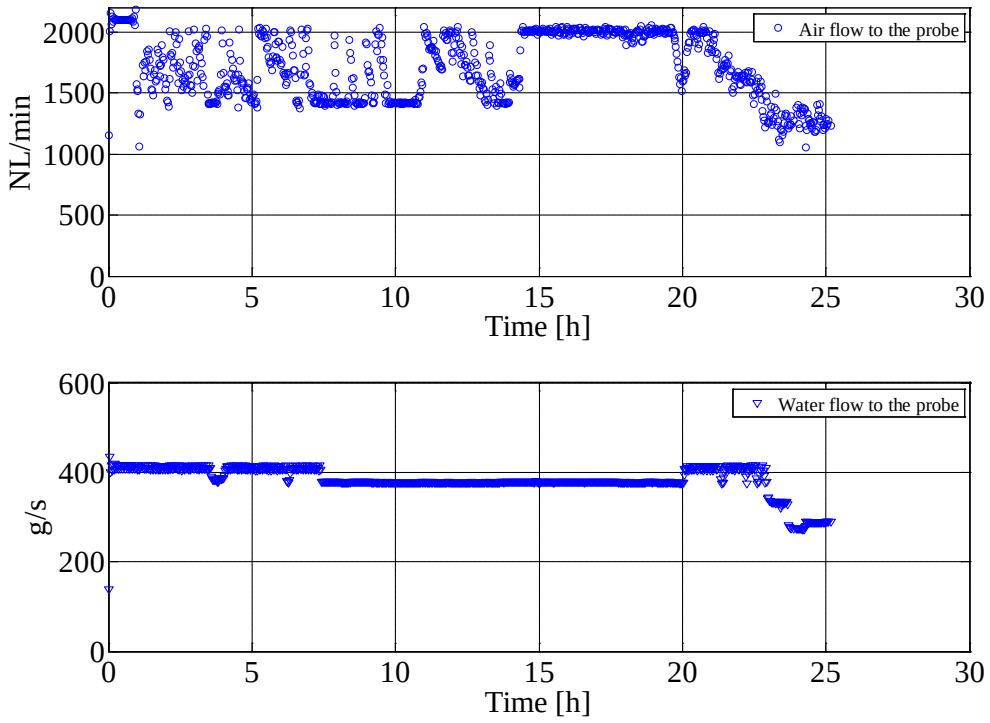

Figure B 6: Water and air flow to the probe measured during test 1.

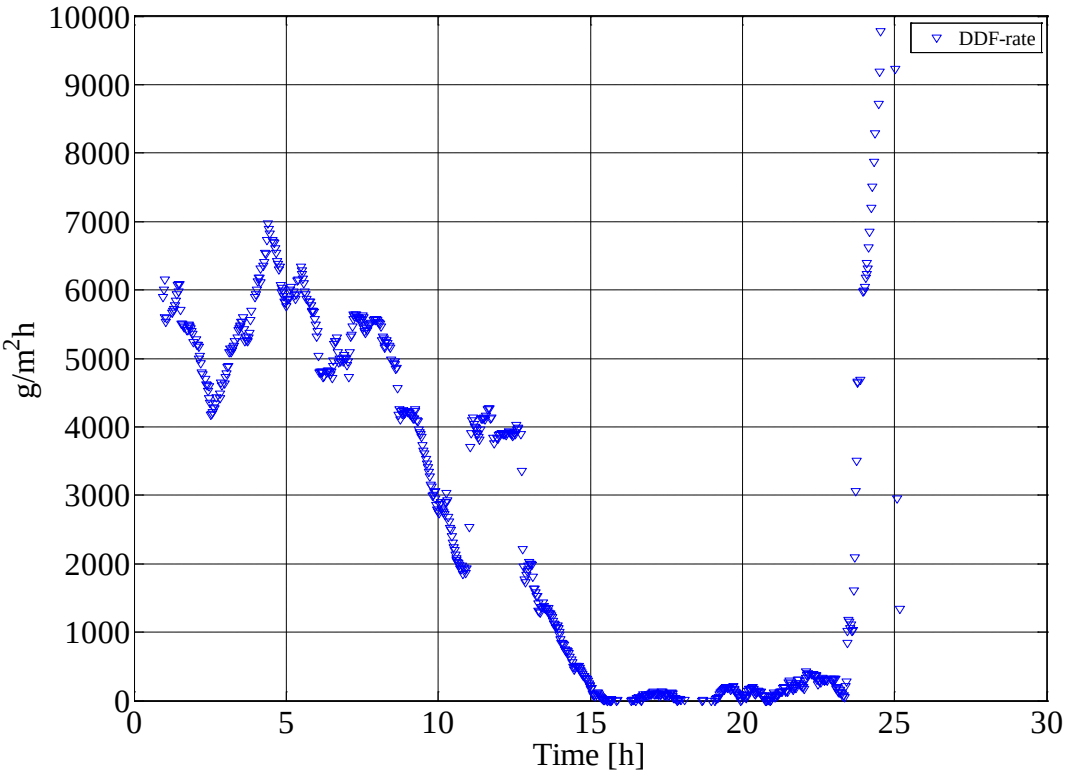

Figure B 7: Calculated Derivative-based Deposit Formation (DDF) rate during test 1.

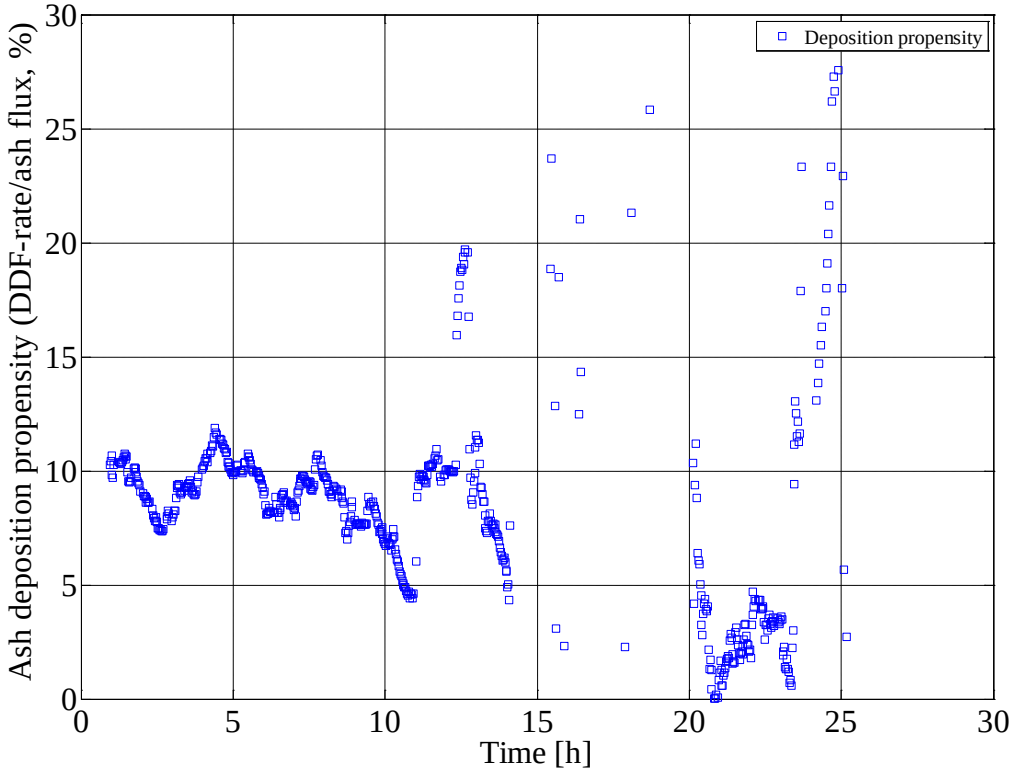

Figure B 8: Calculated ash deposition propensity during test 1.

Test 2

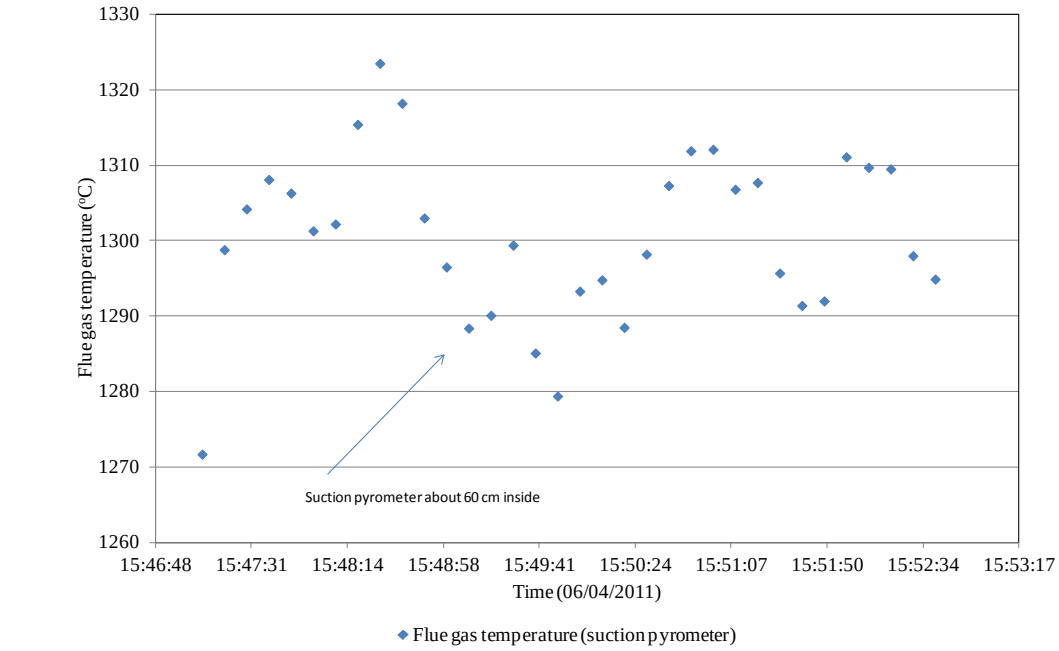

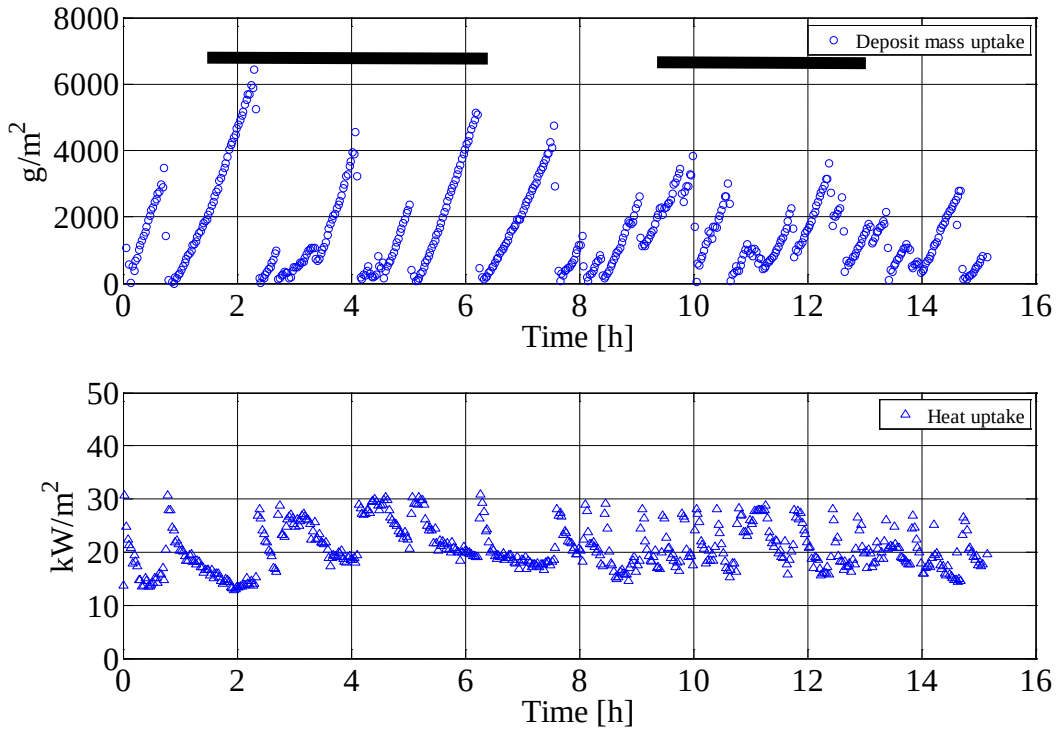

Figure B 9: Flue gas temperature (just after 2-3 hours of test 2) by suction pyrometer, deposit mass uptake, sootblowing events and probe heat uptake during test 2. The black lines in the middle figure show the time when the surrounding sootblowers were in operation.

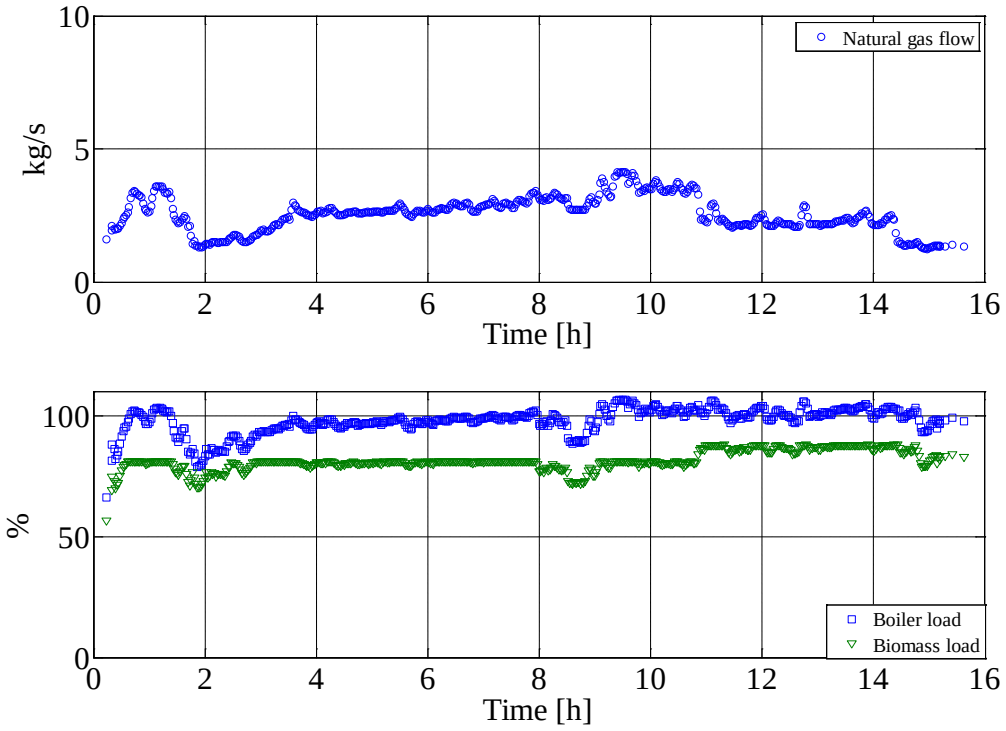

Figure B 10: Natural gas flow, overall boiler load and biomass load during test 2.

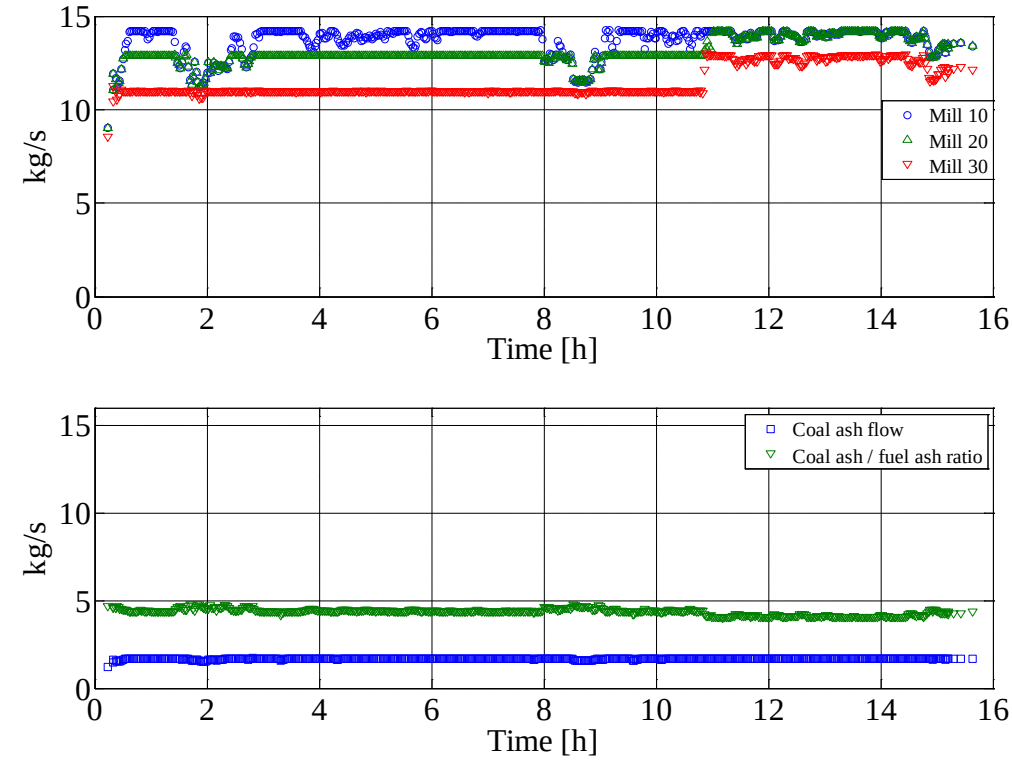

Figure B 11: Fuel flow (wood) through each mill, coal ash flow (kg/s) and ratio between coal ash and wood ash during test 2.

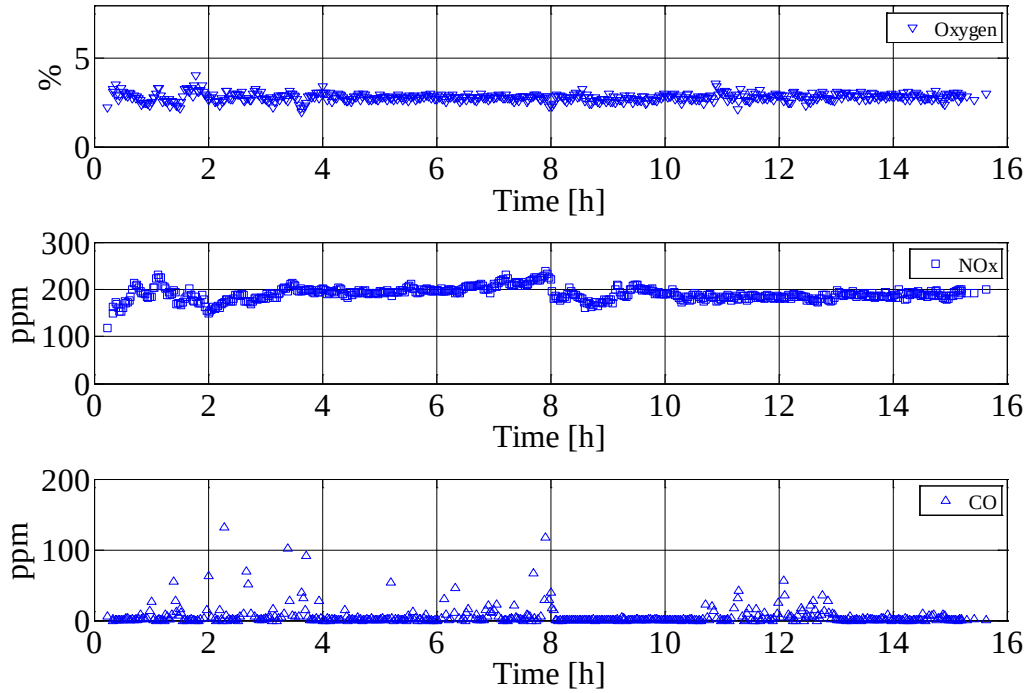

Figure B 12: Oxygen level, NOx level before DeNOx and CO level during test 2.

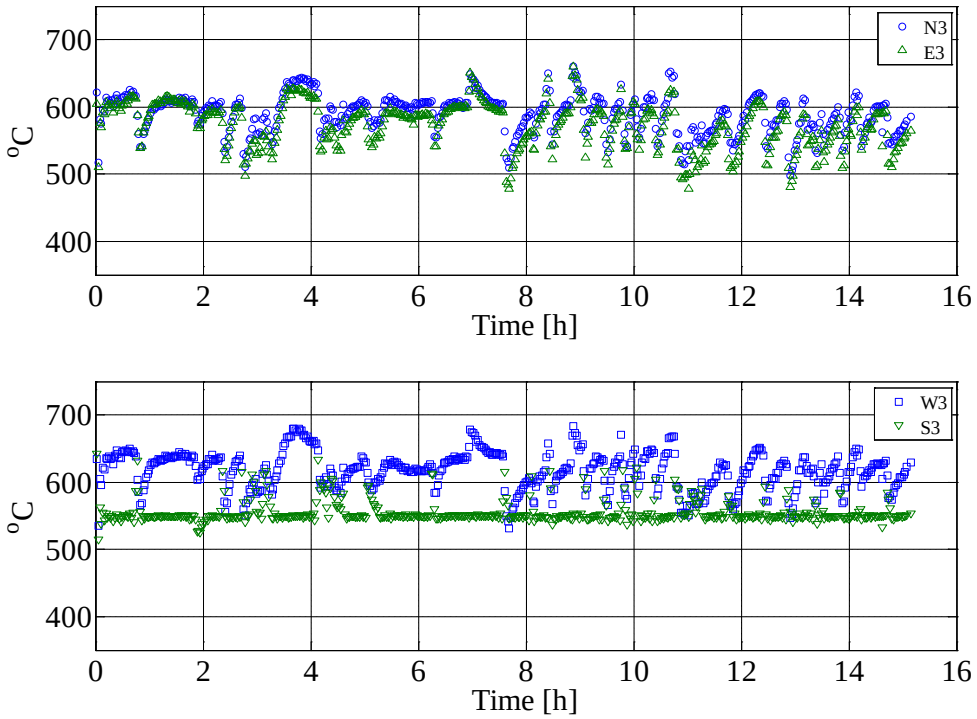

Figure B 13: Measured probe surface temperatures during test 2.

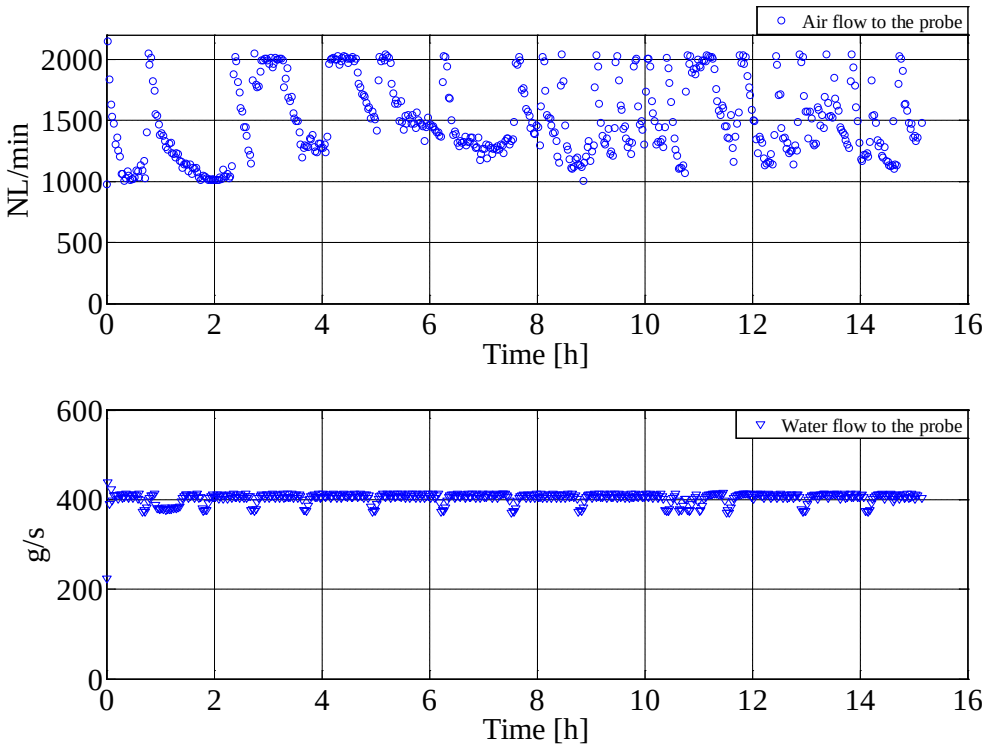

Figure B 14: Water and air flow to the probe measured during test 2.

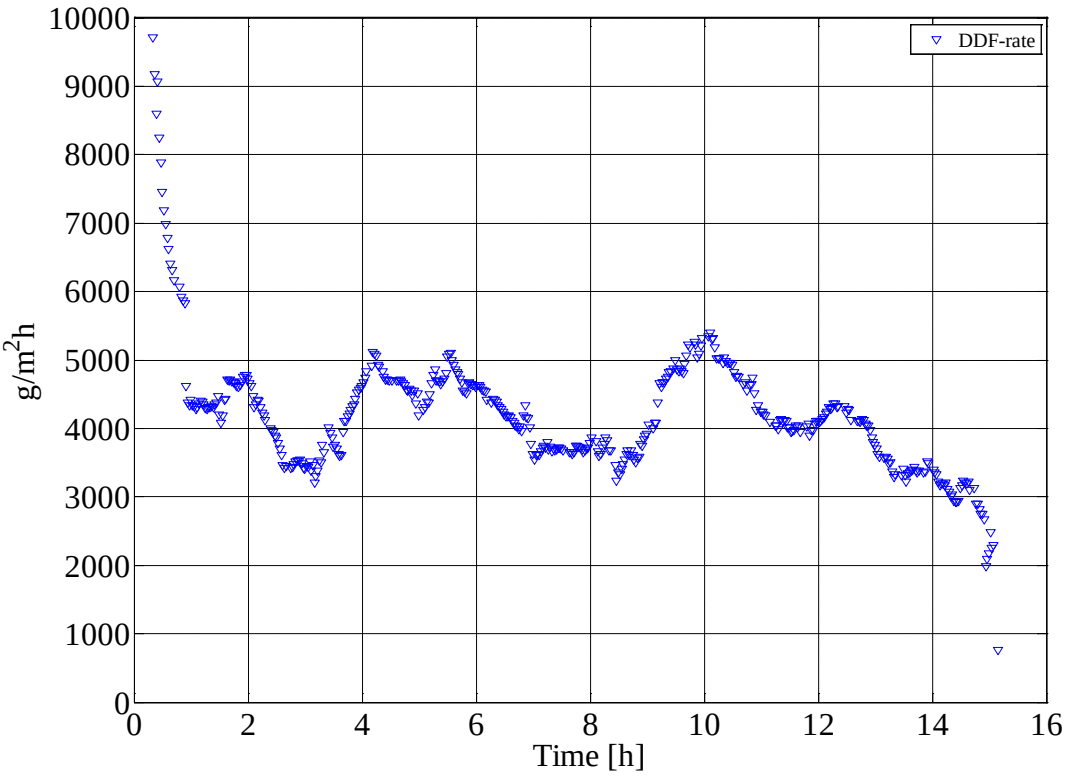

Figure B 15: Calculated Derivative-based Deposit Formation (DDF) rate during test 2.

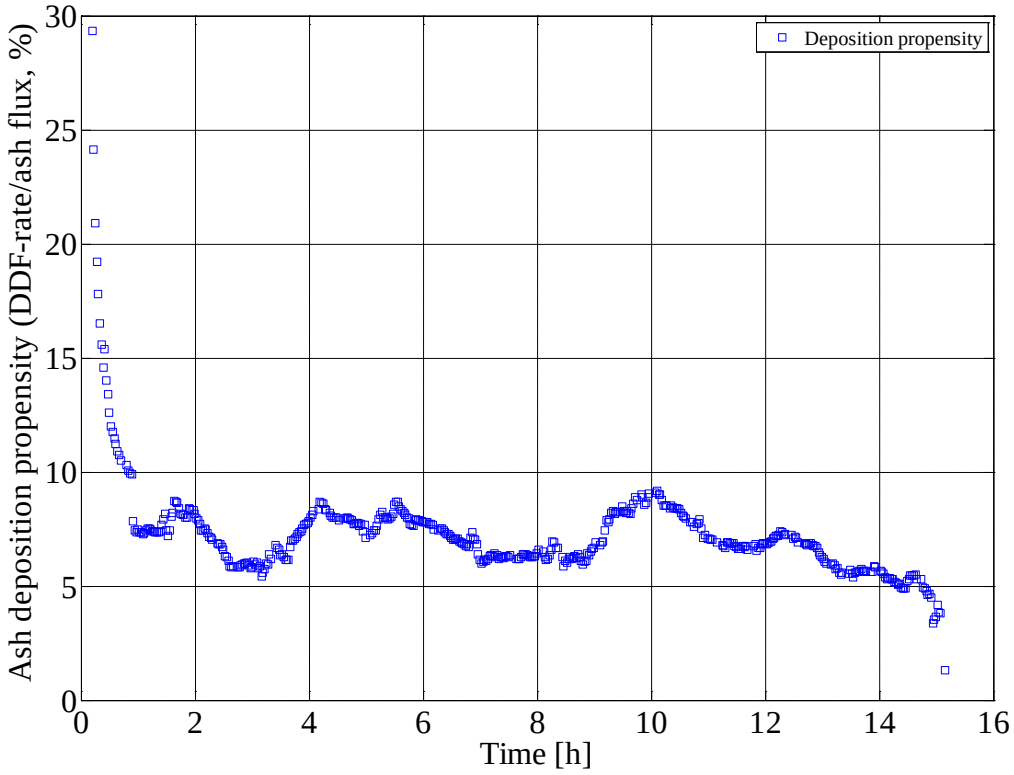

Figure B 16: Calculated ash deposition propensity during test 2.

Test 4

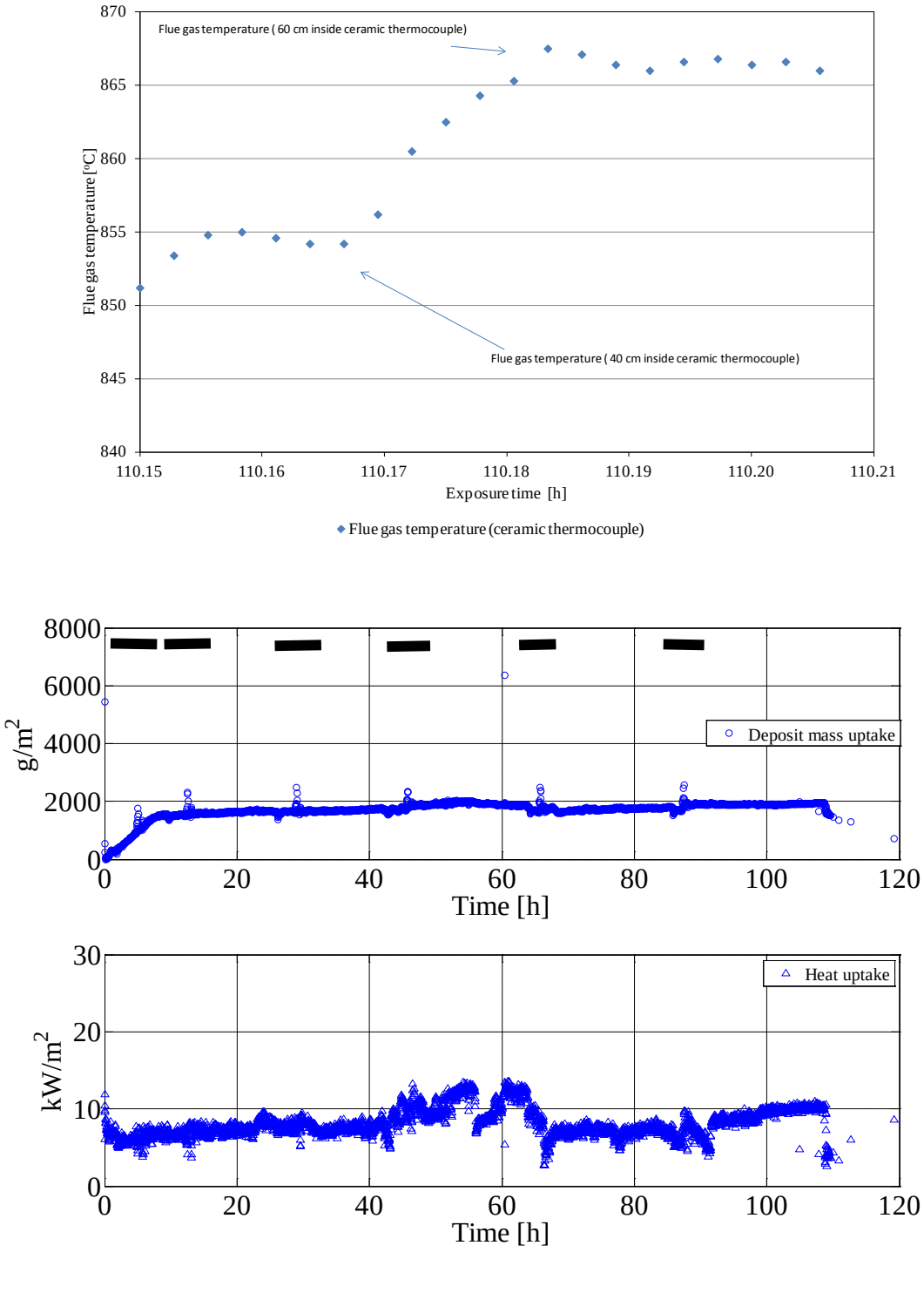

Figure B 17: Flue gas temperature (ceramic thermocouple, at the end of test 4), deposit mass uptake, sootblowing events and probe heat uptake during test 4. The black lines in the middle figure show the time when the surrounding sootblowers were in operation.

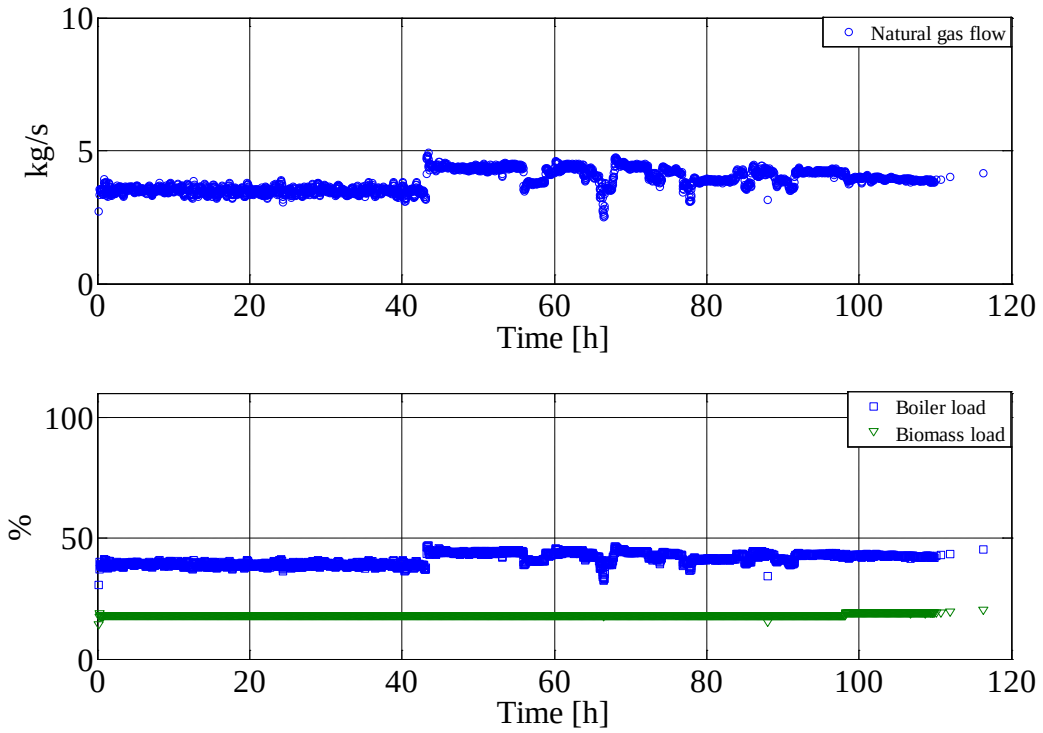

Figure B 18: Natural gas flow, overall boiler load and biomass load during test 4.

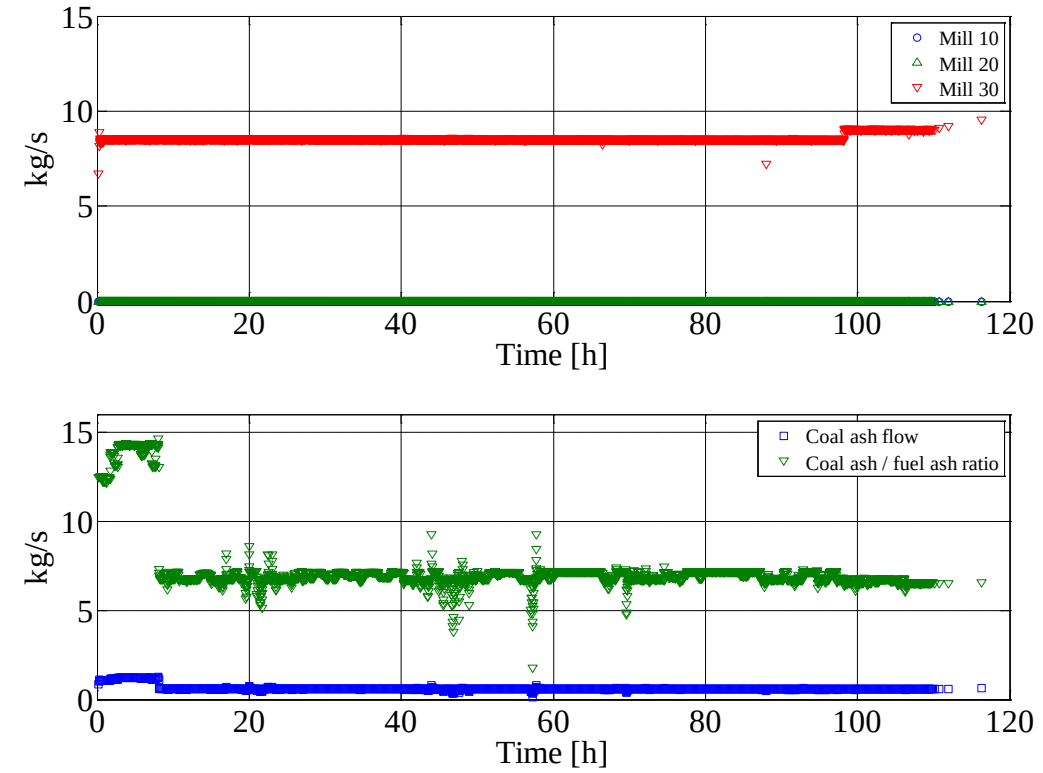

Figure B 19: Fuel flow (wood) through each mill, coal ash flow (kg/s) and ratio between coal ash and wood ash during test 4.

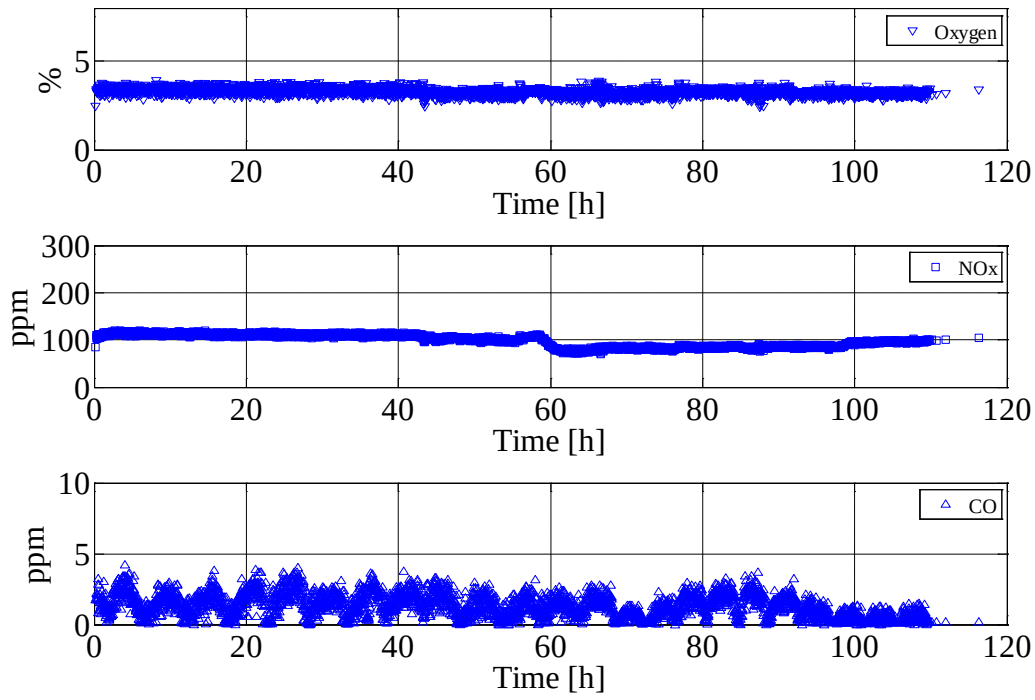

Figure B 20: Oxygen level, NOx level before DeNOx and CO level during test 4.

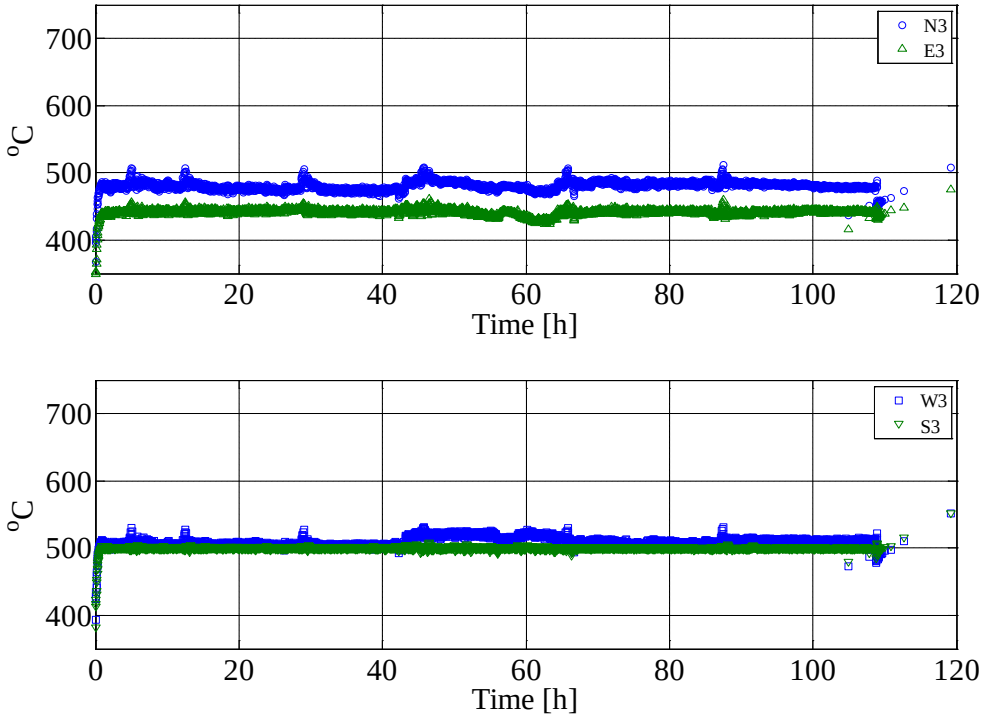

Figure B 21: Measured probe surface temperatures during test 4.

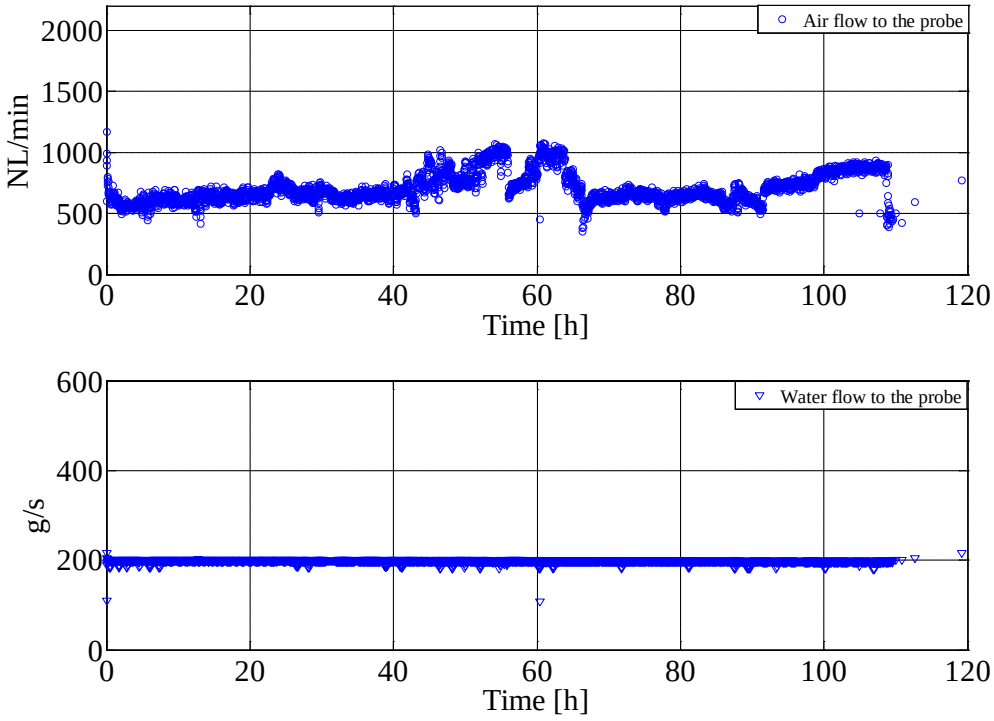

Figure B 22: Water and air flow to the probe measured during test 4.

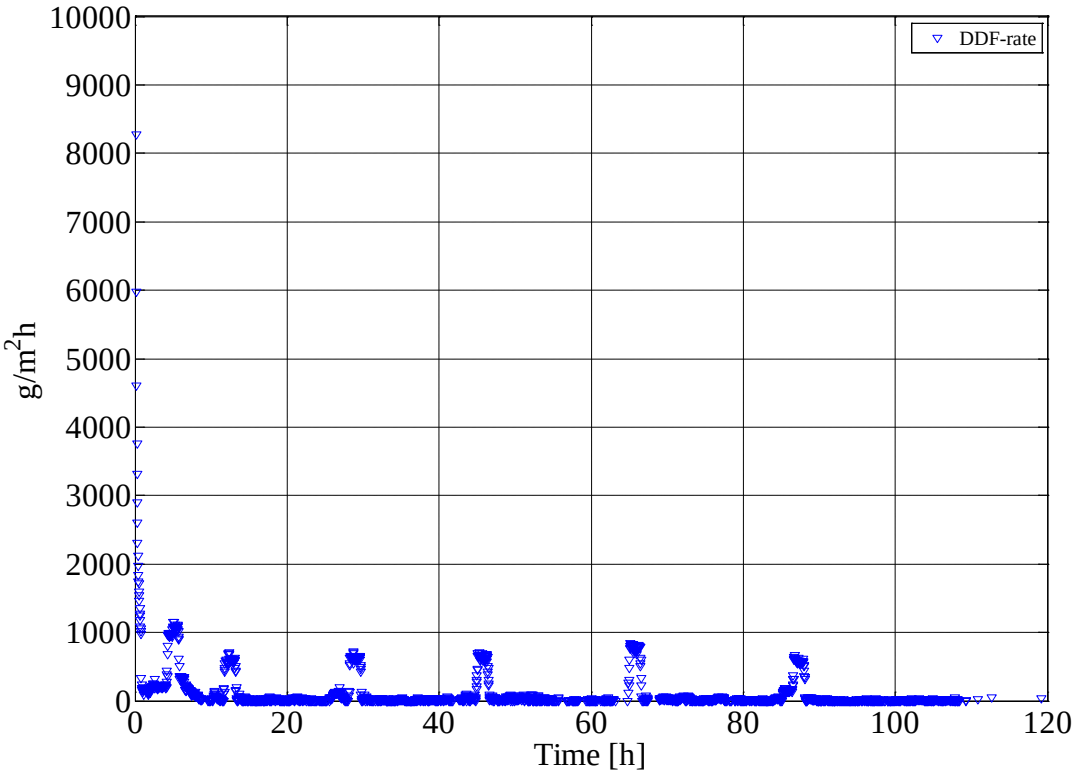

Figure B 23: Calculated Derivative-based Deposit Formation (DDF) rate during test 4.

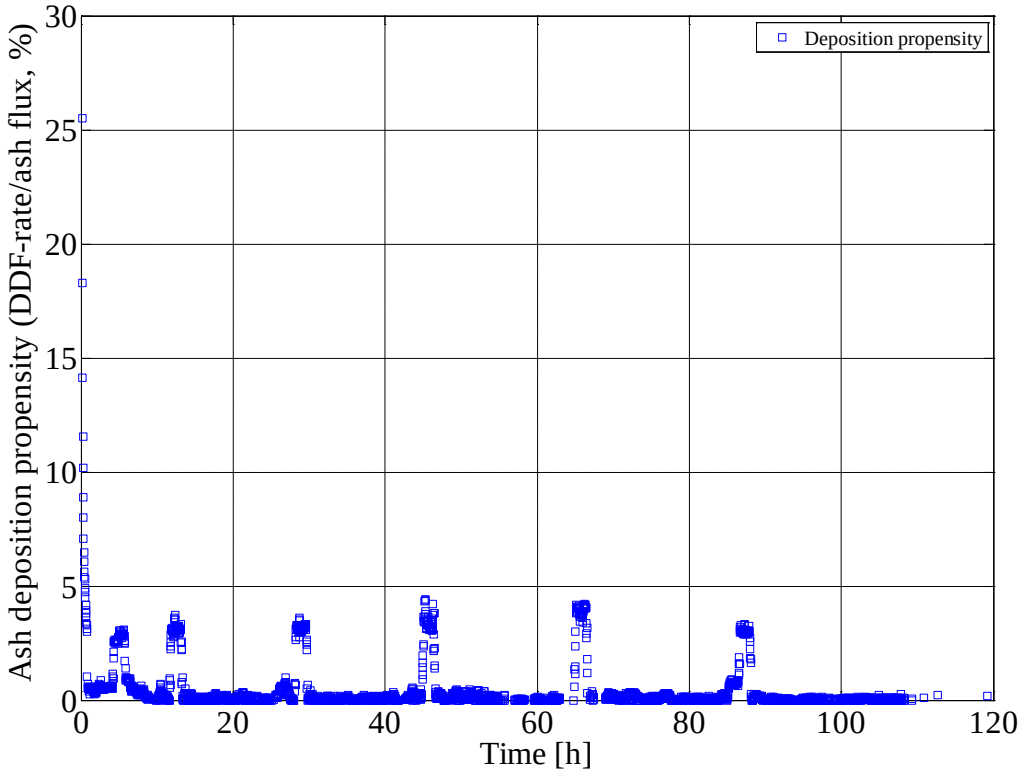

Figure B 24: Calculated ash deposition propensity during test 4.

Test 5

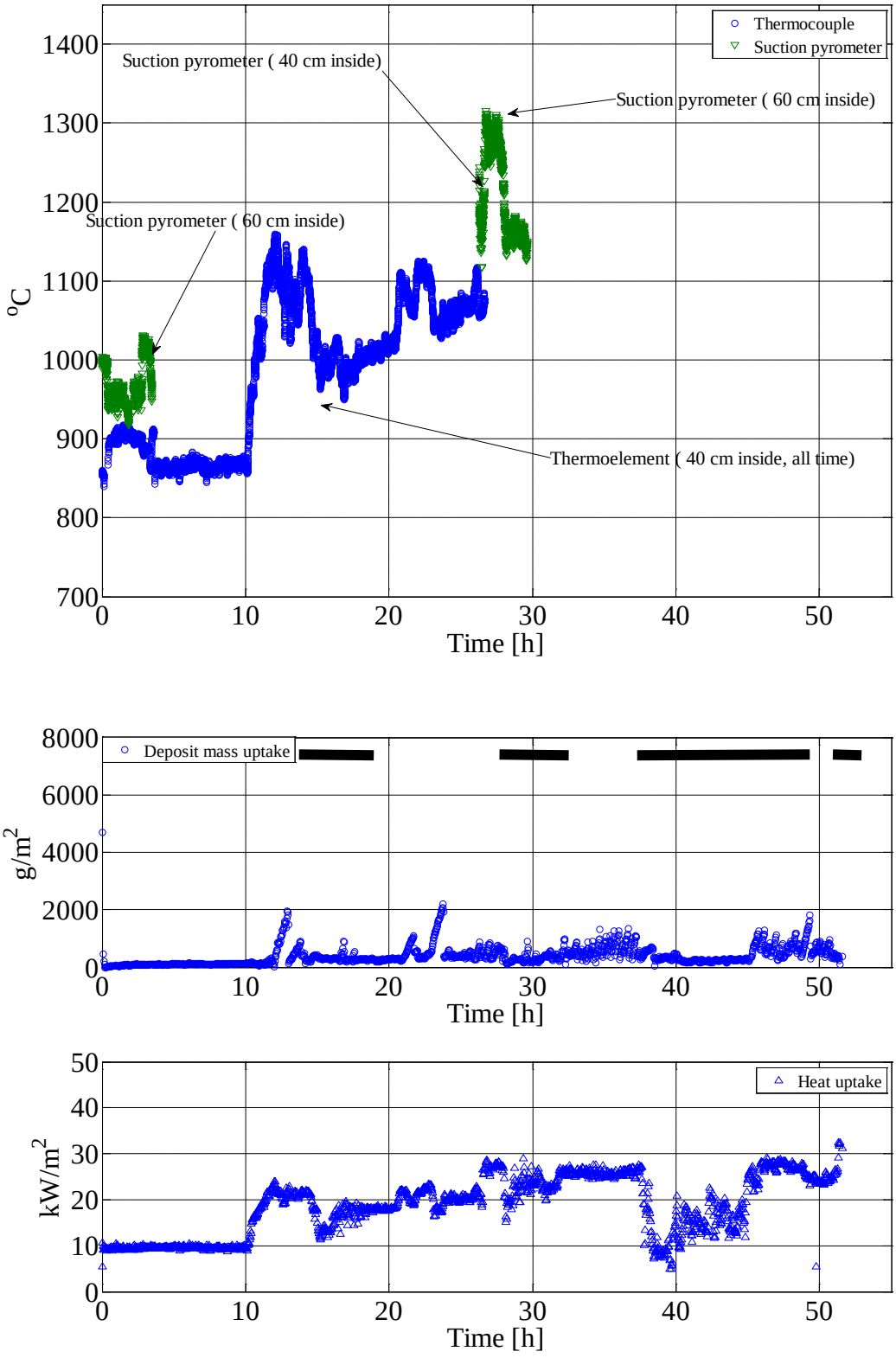

Figure B 25: Flue gas temperature, deposit mass uptake, sootblowing events and probe heat uptake during test 5. The black lines in the middle figure show the time when the surrounding sootblowers were in operation.

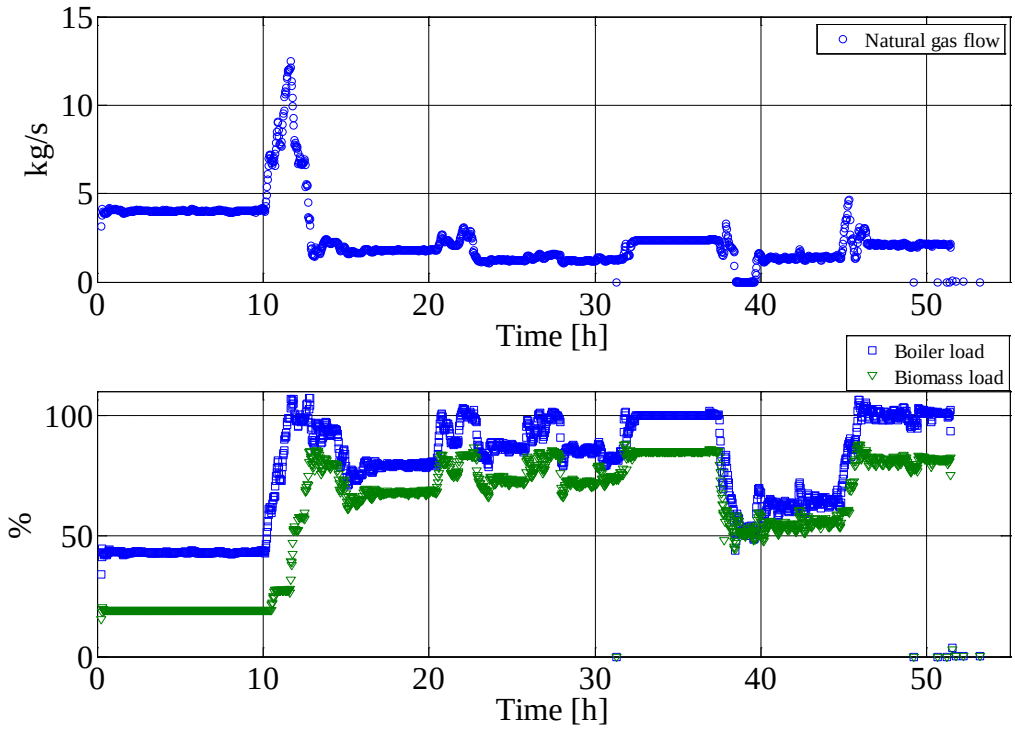

Figure B 26: Natural gas flow, overall boiler load and biomass load during test 5.

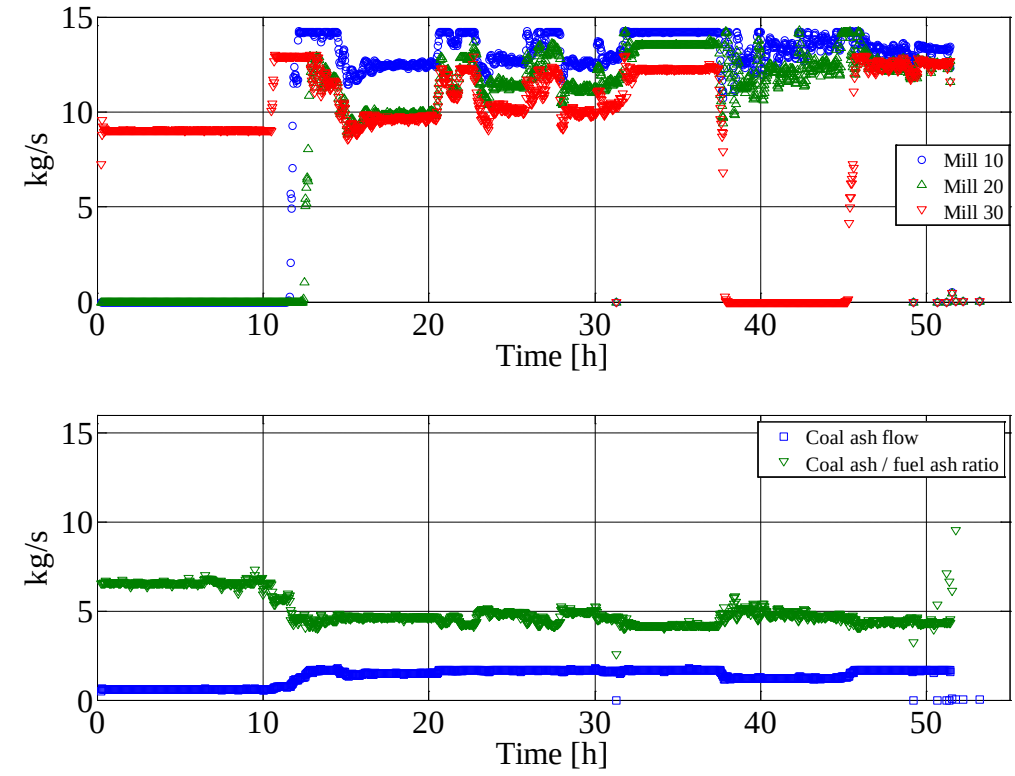

Figure B 27: Fuel flow (wood) through each mill, coal ash flow (kg/s) and ratio between coal ash and wood ash during test 5.

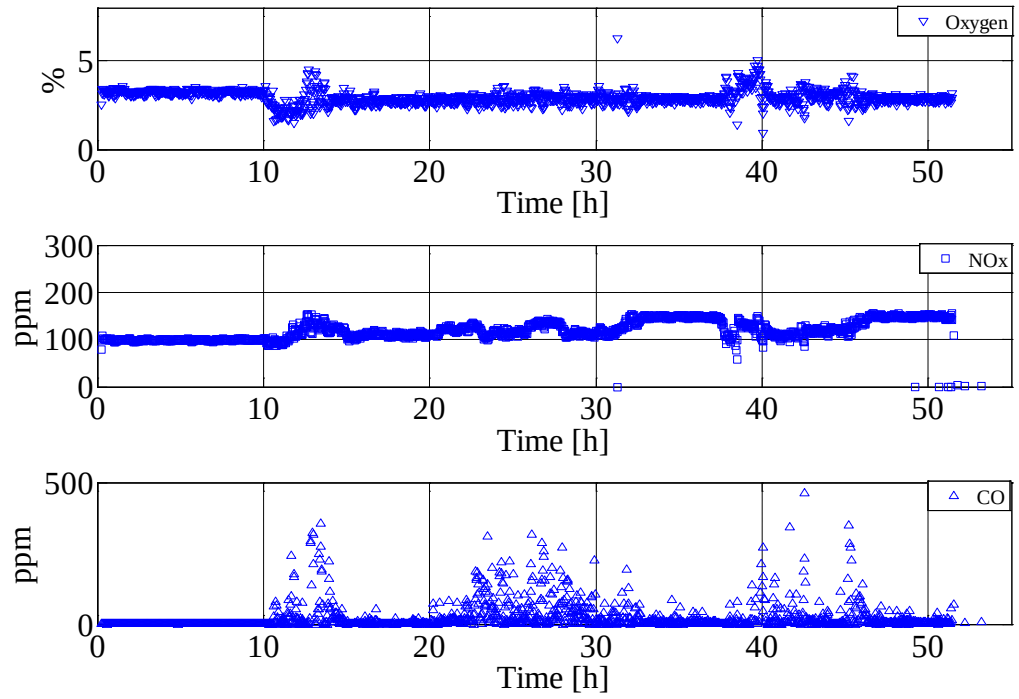

Figure B 28: Oxygen level, NOx level before DeNOx and CO level during test 5.

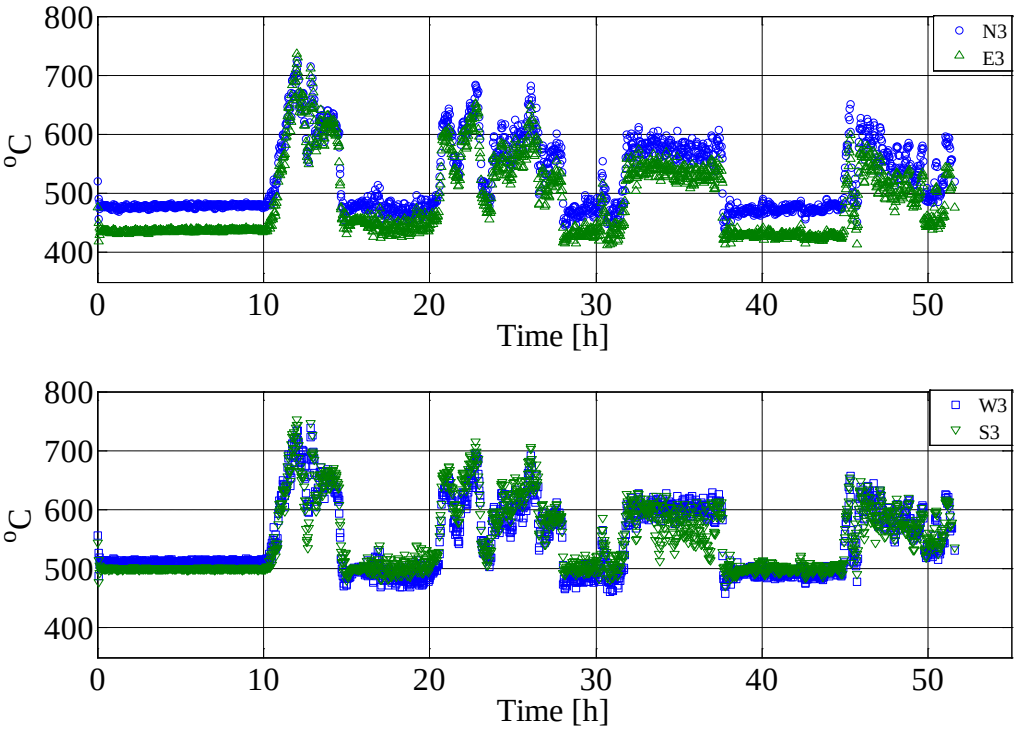

Figure B 29: Measured probe surface temperatures during test 5.

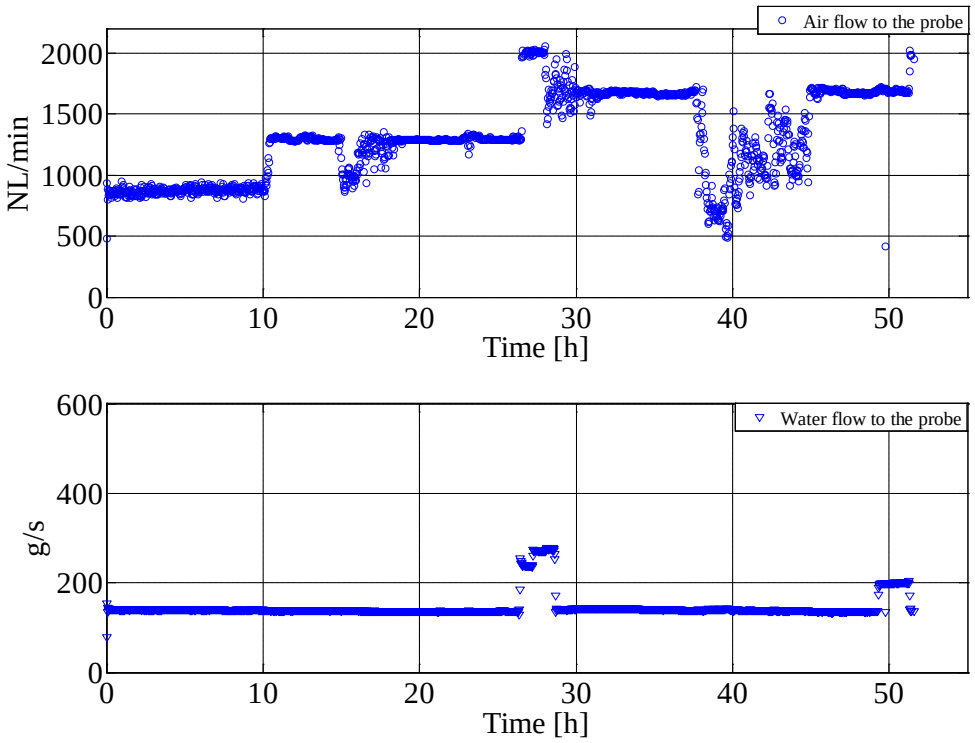

Figure B 30: Water and air flow to the probe measured during test 5.

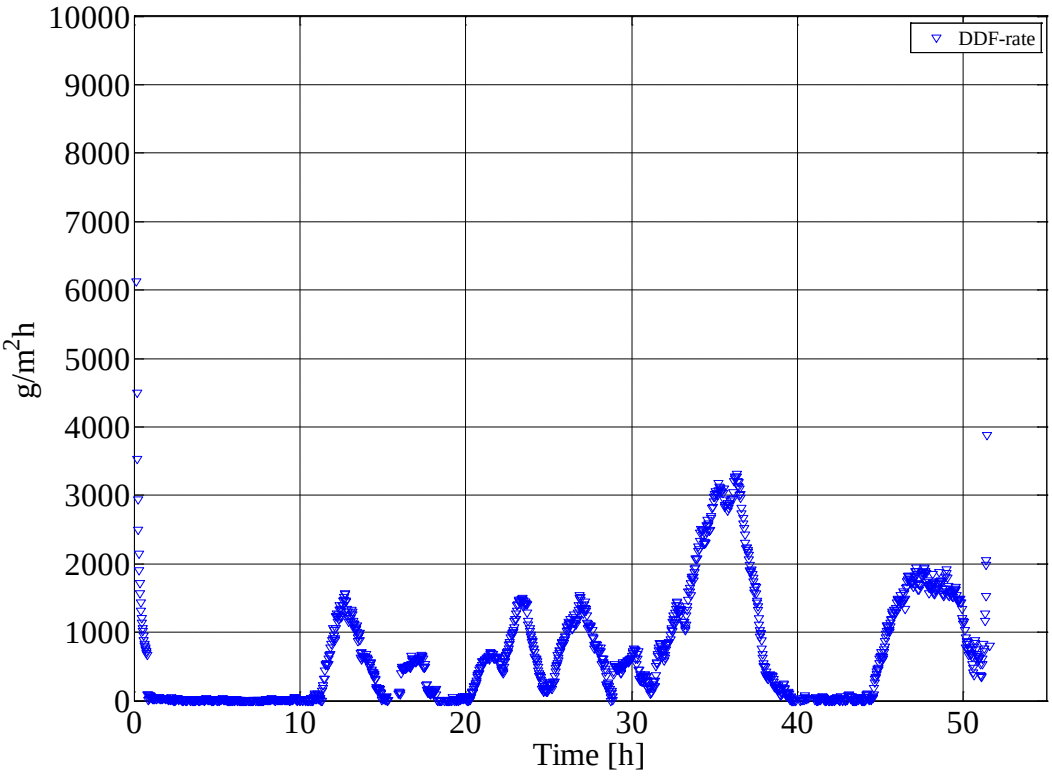

Figure B 31: Calculated Derivative-based Deposit Formation (DDF) rate during test 5.

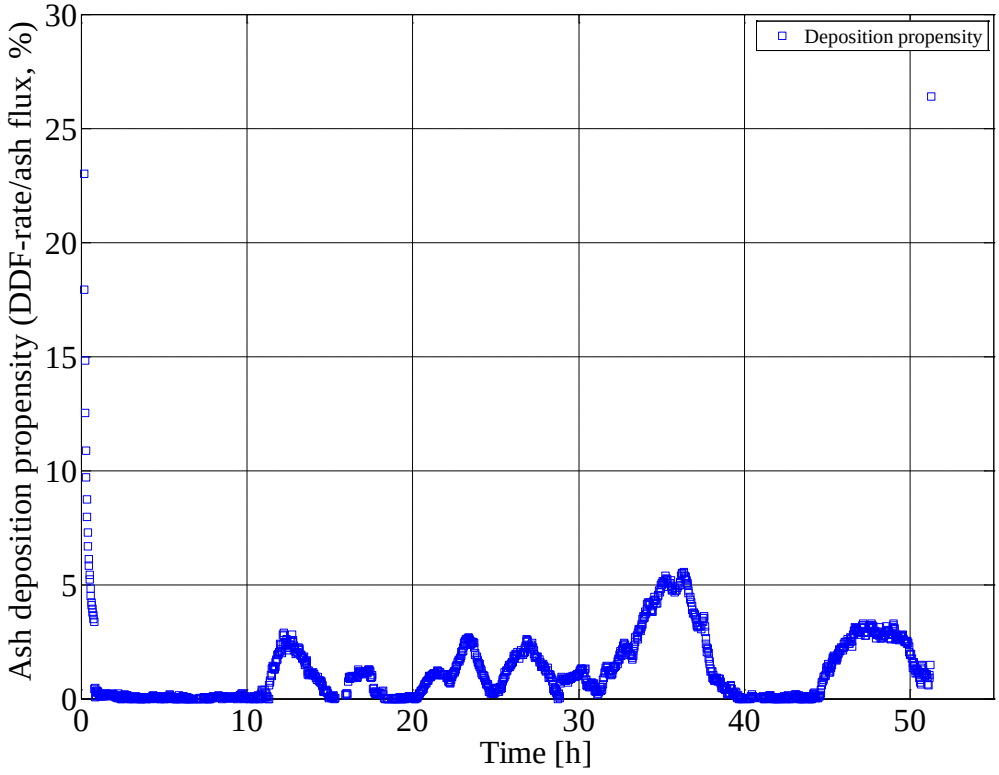

Figure B 32: Calculated ash deposition propensity during test 5.

Appendix C

Method to determine Derivative-based Deposit Formation rate (DDF-rate) (Bashir et al. [18])

The amount of deposit collected on the probe is a function of both the deposit formation process and shedding events. The true deposit formation rate ($g/m^2/h$) cannot be accurately determined, but based on the measured deposit mass increase divided by a given time, the integral deposit formation rate (IDF-rate) or the derivate-based deposit formation rate (DDF-rate), calculated by taking the time derivative of the deposit mass uptake in-between two macro shedding events. However, the DDF-rate should represent a fairly characteristic net-deposition rate for any plant, allowing general features of deposition and its dependence on operating conditions.

The deposit mass uptake signal is influenced by several processes: large shedding events, smaller shedding events (observed as a sudden deposit mass loss on the curve), a relatively slow deposit build-up process and some noise mainly caused by boiler fluctuations. Boiler fluctuations could be mechanical vibrations or large changes in boiler flow dynamics. Some fluctuations are observed when the boiler plant sootblowers were used. Even though the plant sootblowers very near to the probe were shutdown, the rest of the sootblowers to some extent were effective in causing both minor and larger shedding events.

In order to analyze data systematically under these conditions where noise, small and large shedding events are present, a deposit mass uptake signal treatment method is developed. The method allows us to identify shedding events and can quantify the deposit formation rate between major shedding events. The idea is to average out the noise in the deposit mass uptake signals and to identify the larger shedding events.

The steps involved in the deposit mass signal treatment are based on Matlab procedures and are:

Step A: The deposit mass uptake signals are filtered using a 10 point resampling method implemented in Matlab. This effectively smoothes the data over 10 points, returning one resampled data point for further use.

Step B: Slope calculations are done using a moderately low order polynomial (3^{rd} order, current case) that is fitted to the data in a sliding window (5 data points) and finally differentiation of the model is performed.

Step C: Cut off of negative slope values is made to remove major shedding events. The cut off level is adjusted to determine the number of major shedding events accurately while still giving a satisfactory prediction of apparent deposit formation rates. A high cut off level e.g. -200 $g/m^2/h$ may count some noise as shedding events which results in higher deposit formation rate values. A low cut off e.g. -6,000 $g/m^2/h$ will include some shedding in the DDF-rate calculation and results in lower deposit formation rate values. The selected cut off level was -3,800 $g/m^2/h$ for all the tests. This represents a subjective judgment that strikes a balance between determining the most shedding events (a high cut off level is

needed) and not removing selectively a negative noise contribution to the DDF-rate determination (a low cut off level is needed).

Step D: Smoothing of the raw slope calculations is made using a moving average filter over 51 points. Based on the data used in the present study, our choice of 25 data points on each side of the *i*th data point represents a subjective judgment that balances effective smoothing against undesired removal of minor, but significant variations in the deposit formation rate. The result of the smoothed data is the DDF-rate.

This complete procedure was validated. It should be kept in mind that our aim is to treat all data systematically once the subjective judgments of steps C and D have been made, thus avoiding the pitfall of seeing or not seeing trends from case to case based on incomparable criteria. A comparison the approximate manually calculated slopes of the 0-8 h interval during test 1 of these slopes and the calculated DDF-rates using the procedure described above is shown in Figure C 1. It is clear that the DDF-rates calculated by steps A through D are in good agreement with manually calculated average deposition rates.

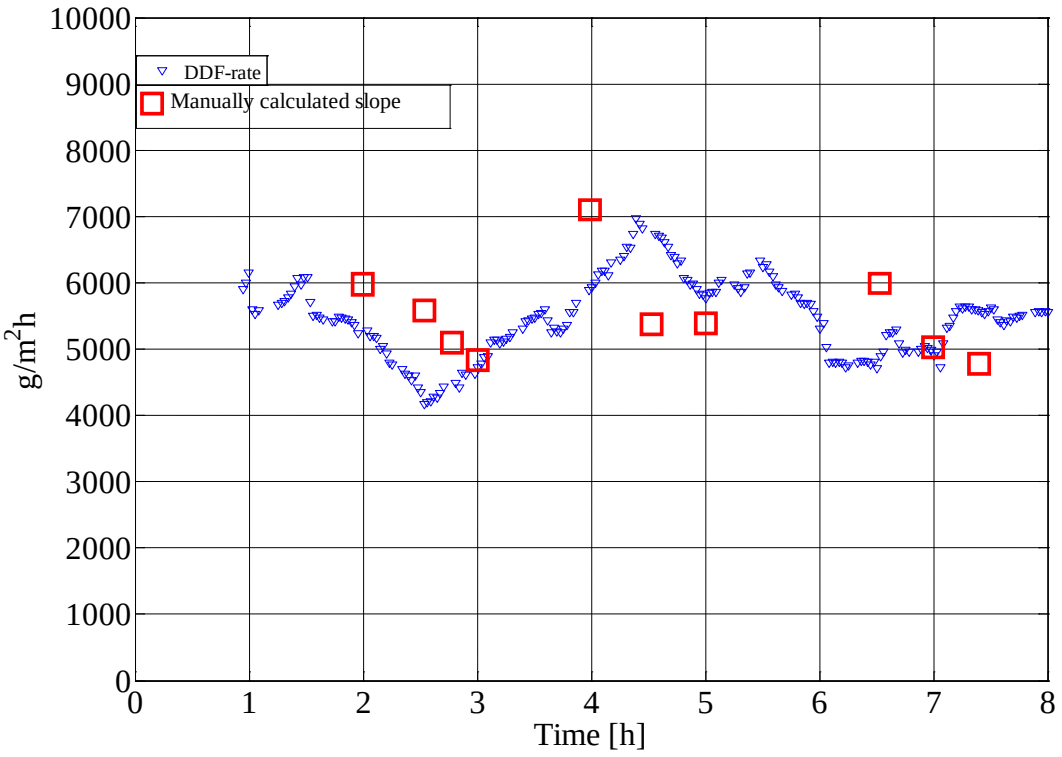

Figure C 1: Comparison of manually calculated slopes and slopes calculated by the mathematical procedure (DDF-rate) for the initial 8 hours of test 1.